

**JANUARY 2024**

**M.Sc. in Civil Engineering**

**HALİL BAL**

**REPUBLIC OF TÜRKİYE  
GAZİANTEP UNIVERSITY  
GRADUATE SCHOOL OF NATURAL & APPLIED SCIENCES**

**GEOTECHNICAL INVESTIGATION OF RECLAIMED  
ASPHALT PAVEMENT AND XANTHAN GUM TREATED  
SILTY SAND**

**M.Sc. THESIS  
IN  
CIVIL ENGINEERING**

**BY  
HALİL BAL  
JANUARY 2024**

**GEOTECHNICAL INVESTIGATION OF RECLAIMED  
ASPHALT PAVEMENT AND XANTHAN GUM TREATED  
SILTY SAND**

**M.Sc. Thesis  
in  
Civil Engineering  
Gaziantep University**

**Supervisor**

**Prof. Dr. Ali Fırat ÇABALAR**

**by**

**Halil BAL**

**January 2024**



©2024[Gaziantep University]

**GEOTECHNICAL INVESTIGATION OF RECLAIMED ASPHALT  
PAVEMENT AND XANTHAN GUM TREATED SILTY SAND**

submitted by **Halil BAL** in partial fulfilment of the requirements for the degree of  
Master of Science in **Civil Engineering, Gaziantep University** is approved by,

Prof. Dr. Çiğdem AYKAÇ  
Director of the Graduate School of Natural and Applied Sciences .....

Prof. Dr Nildem TAYŞI  
Head of the Department of Civil Engineering .....

Prof. Dr Ali Fırat ÇABALAR  
Supervisor, Civil Engineering  
Gaziantep University .....

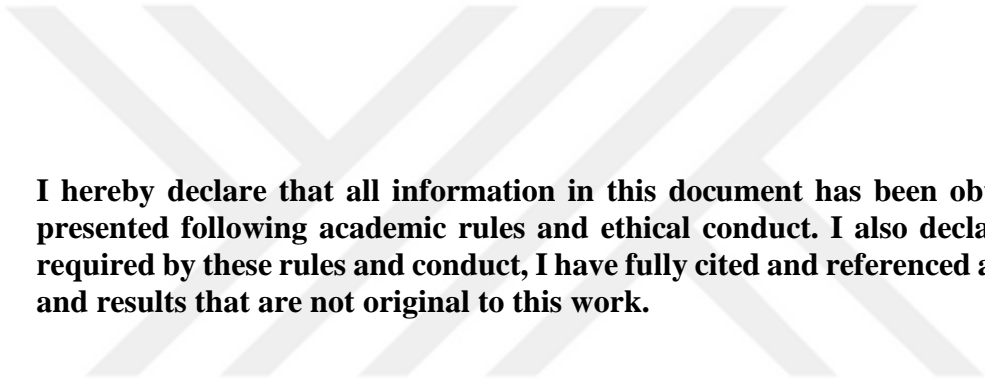
Exam Date: 12 January 2024

**Examining Committee Members:**

Prof. Dr Ali Fırat ÇABALAR  
Gaziantep University .....

Prof. Dr. Nihat ATMACA  
Gaziantep University .....

Assoc. Prof. Dr. Eyyüb KARAKAN  
Kilis 7 Aralık University .....



**I hereby declare that all information in this document has been obtained and presented following academic rules and ethical conduct. I also declare that, as required by these rules and conduct, I have fully cited and referenced all material and results that are not original to this work.**

**Halil BAL**

## **ABSTRACT**

### **GEOTECHNICAL INVESTIGATION OF RECLAIMED ASPHALT PAVEMENT AND XANTHAN GUM TREATED SILTY SAND**

**BAL, Halil**  
**M.Sc. in Civil Engineering**  
**Supervisor: Prof. Dr. Ali Fırat ÇABALAR**  
**January 2024**  
**81 pages**

This thesis conducts a comprehensive investigation into the impact of recycled waste construction material and an eco-friendly biopolymer on the stabilization of local soil. The laboratory-based experimental program focused on silty sand (SM) soil treated with 10% reclaimed asphalt pavement (RAP) and Xanthan gum (XG) concentrations (0%, 0.5%, 1%, and 3% by total dry weight) across curing periods of 0, 7, 28, and 56 days. Results indicate distinct effects on soil properties: RAP reduced liquid limit, plastic limit, and optimum water content (OMC) while increasing maximum dry density (MDD). Conversely, XG elevated these parameters and decreased MDD. In 7-day cured specimens, the inclusion of 10% reclaimed asphalt pavement (RAP) significantly enhanced compressive strength. The initial strength of 2983 kPa for the clean soil rose to 3464.9 kPa with the addition of RAP. Incremental changes were observed at rates of 0.5%, 1%, and 3% XG, resulting in compressive strengths of 4754.9 kPa, 6189.6 kPa, and 7999.1 kPa, respectively. Curing effects on strength were partially positive, peaking at 28 days. The biopolymer positively influenced shear strength but exhibited a paradoxical outcome in consolidation and California bearing capacity tests, increasing consolidation while decreasing bearing capacity. In summary, this study highlights the multifaceted effects of XG on soil behaviour, emphasizing the need for a nuanced exploration of the intricate interplay between XG and water in soil systems.

**Key Words:** Geotechnical Investigation, Silty Sand, Reclaimed Asphalt Pavement, Xanthan Gum

## ÖZET

### GERİ KAZANILMIŞ ASFALT KAPLAMA VE KSANTAN SAKIZI İLE İŞLENMİŞ SİTLİ KUMUN GEOTEKNİK İNCELENMESİ

**BAL, Halil**  
**Yüksek Lisans, İnşaat Mühendisliği**  
**Danışman: Prof. Dr. Ali Fırat ÇABALAR**  
**Ocak 2024**  
**81 sayfa**

Bu tez, geri dönüştürülmüş inşaat atığı malzemenin ve çevre dostu bir biyopolimerin yerel toprağın stabilizasyonu üzerindeki etkisini kapsamlı bir şekilde araştırmaktadır. Laboratuvar tabanlı deneysel program, 0, 7, 28 ve 56 gün kürlenme periyotlarında, %10 geri kazanılmış asfalt kaplama (RAP) ve Ksantan gam (XG) konsantrasyonları (toplam kuru ağırlığa göre sırasıyla %0, %0.5, %1 ve %3) ile işlenmiş siltli kum (SM) zeminine odaklanmıştır. Sonuçlar, toprak özellikleri üzerinde belirgin etkiler göstermektedir: RAP likit limiti, plastik limit ve optimum su muhtevasını (OMC) azaltırken maksimum kuru yoğunluğu (MDD) artırmıştır. Tam tersine, XG bu parametreleri yükseltmiş ve MDD'yi azaltmıştır. 7 gün süreyle iyileşmiş örneklerde, %10 RAP eklenmesi, basınç dayanımını önemli ölçüde artırmıştır. İşlenmemiş toprak için başlangıç dayanımı olan 2983 kPa, RAP eklenmesi ile 3464.9 kPa'ya yükselmiştir. %0.5, %1 ve %3 XG ile gözlemlenen aşamalı değişiklikler, sırasıyla 4754.9 kPa, 6189.6 kPa ve 7999.1 kPa basınç dayanımlarında sonuçlanmıştır. Dayanım üzerindeki iyileşme etkileri kısmen pozitif olup, 28 günle zirveye çıkmaktadır. Biyopolimer, kayma dayanımını olumlu yönde etkilemiş ancak konsolidasyon ve California taşıma kapasitesi testlerinde çelişkili bir sonuç göstermiş, konsolidasyonu artırırken taşıma kapasitesini azaltmıştır. Özetle, bu çalışma, XG'nin toprak davranışı üzerindeki çok yönlü etkilerini vurgulayarak, XG ve su arasındaki karmaşık etkileşimin nüanslı bir şekilde keşfi için bir ihtiyacı vurgular.

**Anahtar Kelimeler:** Geoteknik Analiz, Siltli Kum, Geri Kazanılmış Asfalt Kaplama, Ksantan Sakızı



*“Dedicated to my love, Özlem”*

## ACKNOWLEDGEMENTS

I wish to convey my sincere appreciation to my advisor, Prof. Dr. Ali Fırat ÇABALAR, for his invaluable guidance throughout this arduous process and for generously sharing his extensive knowledge in the field of study. It is truly an honour to have had the opportunity to work with him and to be his student.

My profound gratitude extends to my elder brother, İsa Bal, for his unwavering belief in me and steadfast support from my childhood to the present moment.

I express deep love and appreciation to my family for their enduring support and unwavering well-wishes.

Endless gratitude is extended to my graduate and laboratory colleagues, İlker Kıymık Büşra Özaslan, and Ahmet Kaya. I consider myself fortunate to have faced challenges together, successfully resolving difficulties with minimal external assistance.

Special recognition is due to Research Assistant Süleyman Demir for providing invaluable experience and unwavering support.

I would like to express my thanks to Associate Professor Eyyüb KARAKAN, who graciously permitted the use of laboratory facilities and offered valuable insights and advice throughout this process.

Finally, I dedicate this thesis to my beloved Muazzez Özlem GÜLSEROĞLU, whose presence has been captivating since our initial encounter, and who has consistently believed in me and stood by my side.

## TABLE OF CONTENTS

	<b>Page</b>
<b>ABSTRACT</b> .....	<b>vi</b>
<b>ACKNOWLEDGEMENTS</b> .....	<b>viii</b>
<b>TABLE OF CONTENTS</b> .....	<b>ix</b>
<b>LIST OF TABLES</b> .....	<b>xi</b>
<b>LIST OF FIGURES</b> .....	<b>xii</b>
<b>LIST OF SYMBOLS</b> .....	<b>xiv</b>
<b>LIST OF ABBREVIATIONS</b> .....	<b>xv</b>
<b>CHAPTER 1 INTRODUCTION</b> .....	<b>1</b>
1.1 Introduction .....	1
1.2 Problem Statement .....	2
1.3 Objectives.....	3
1.4 Outline.....	3
<b>CHAPTER 2 LITERATURE REVIEW</b> .....	<b>4</b>
2.1 General .....	4
2.2 The Use of Waste Materials in the Construction and Environmental Field.....	4
2.3 The Use of Reclaimed Asphalt Pavement in Construction Applications.....	7
2.4 The Use of Biopolymers in the Construction Field.....	9
2.5 The Use of Xanthan Gum in the Geotechnical Applications .....	11
<b>CHAPTER 3 MATERIALS AND EXPERIMENTAL METHODOLOGY</b> .....	<b>22</b>
3.1 Introduction .....	22
3.2 Materials .....	23
3.2.1 Soil .....	23
3.2.2 Reclaimed Asphalt Pavement .....	25
3.2.3 Xanthan Gum .....	26
3.3 Sample Preparation.....	29

3.4 Experimental Methodology .....	29
3.4.1 Atterberg' Limit tests .....	29
3.4.2 Standard Compaction Test .....	30
3.4.3 Fall Cone Test .....	31
3.4.4 Vane Shear Test .....	32
3.4.5 Unconfined Compressive Strength Test .....	34
3.4.6 Consolidation Test .....	37
3.4.7 California Bearing Ratio (CBR) Test.....	39
3.4.8 Direct Shear Test.....	42
<b>CHAPTER 4 RESULTS AND DISCUSSION.....</b>	<b>44</b>
4.1 Introduction .....	44
4.2 Atterberg' Limits .....	44
4.3 Standard Compaction Test .....	45
4.4 Fall Cone Test .....	47
4.5 Vane Shear Test.....	50
4.6 Unconfined Compressive Strength Test.....	53
4.7 Consolidation Test.....	59
4.8 California Bearing Ratio (CBR) Test.....	63
4.9 Direct Shear Test .....	65
<b>CHAPTER 5 CONCLUSIONS AND RECOMMENDATIONS .....</b>	<b>68</b>
5.1 General .....	68
5.2 Conclusion.....	68
5.3 Recommendations .....	70
<b>REFERENCES.....</b>	<b>72</b>
<b>CURRICULUM VITAE.....</b>	<b>81</b>

## LIST OF TABLES

	<b>Pages</b>
<b>Table 3.1</b> Description of samples .....	23
<b>Table 3.2</b> Several characteristics of the soil utilized in the experiments.....	24
<b>Table 4.1</b> Optimum water content and maximum dry density .....	46



## LIST OF FIGURES

	<b>Pages</b>
<b>Figure 2.1</b> The effect of curing time on UCS values at 3% XG (Cabalar et al., 2018) .....	13
<b>Figure 3.1.</b> The soil material used in experiments .....	24
<b>Figure 3.2.</b> Particle size distribution of the silty sand, reclaimed asphalt pavement and 90% silty sand-10% reclaimed asphalt pavement.....	25
<b>Figure 3.3.</b> The reclaimed asphalt pavement (RAP) used during experiments.....	26
<b>Figure 3.4.</b> Xanthan gum utilized in the experiments .....	27
<b>Figure 3.5.</b> Scanning Electron Microscope images of (a) SM, (b) RAP, and (c) XG .....	28
<b>Figure 3.6.</b> Casagrande Device .....	30
<b>Figure 3.7.</b> Standard Compaction Test Apparatus .....	31
<b>Figure 3.8.</b> Fall Cone Test Device.....	32
<b>Figure 3.9.</b> Device used in the Laboratory Vane Shear Test.....	33
<b>Figure 3.10.</b> Modified Compaction Apparatus of UCS .....	35
<b>Figure 3.11.</b> Cured Specimens of UCS .....	35
<b>Figure 3.12.</b> The unconfined compression testing device.....	36
<b>Figure 3.13.</b> (a) brittle specimen (b) ductile specimen after the test.....	37
<b>Figure 3.14.</b> Oedometer device .....	38
<b>Figure 3.15.</b> One-dimensional consolidation testing apparatus .....	39
<b>Figure 3.16.</b> Compaction and sample preparation equipment for CBR test .....	40
<b>Figure 3.17.</b> The cured CBR specimen .....	41
<b>Figure 3.18.</b> CBR loading machine.....	42
<b>Figure 3.19.</b> Direct shear test device .....	43
<b>Figure 4.1.</b> Liquid Limit (LL) of silty sand from Casagrande Test .....	45
<b>Figure 4.2.</b> Compaction curve from the standard compaction test.....	47
<b>Figure 4.3.</b> Liquid Limit (LL) and Plastic Limit (PL) from the fall cone test.....	49
<b>Figure 4.4.</b> The water content versus undrained shear strength ( $S_u$ ) graph of the fall cone test .....	50

<b>Figure 4.5.</b> The water content versus $S_u$ graph of the vane shear test .....	51
<b>Figure 4.6.</b> Comparison of the undrained shear strength of the fall cone and vane shear .....	52
<b>Figure 4.7.</b> Correlation between undrained shear strength ( $S_u$ ) from Fall Cone Test (FCT) and Vane Shear Test (VST) .....	53
<b>Figure 4.8.</b> Stress-strain graph at (a) 7 days, (b) 28 days and (c) 56 days curing .....	54
<b>Figure 4.9.</b> Stress-strain graph of a 1% XG-cured UCS sample at variable curing periods.....	56
<b>Figure 4.10.</b> Maximum compressive stresses for all the mixtures at different curing periods.....	57
<b>Figure 4.11.</b> Energy absorption levels of all the mixtures at different curing periods .....	58
<b>Figure 4.12.</b> Modulus of Elasticity.....	58
<b>Figure 4.13.</b> Void Ratio-Log Graphic .....	60
<b>Figure 4.14.</b> Compression index ( $C_c$ ) and recompression index ( $C_r$ ) of all the mixtures .....	60
<b>Figure 4.15.</b> Variation of the consolidation ratio .....	62
<b>Figure 4.16.</b> The coefficient of permeability for all the mixtures .....	62
<b>Figure 4.17.</b> Load-penetration of all the mixtures.....	64
<b>Figure 4.18</b> CBR values at different penetrations .....	64
<b>Figure 4.19:</b> CBR values at 2.5 mm.....	65
<b>Figure 4.20.</b> Stress-strain from the direct shear test at 150 kPa normal pressure .....	66
<b>Figure 4.21:</b> Cohesion and internal friction angle bar graph .....	67

## LIST OF SYMBOLS

<b>k</b>	A Constant Related to Angle of the Cone
<b>c</b>	Cohesion
<b>c<sub>c</sub></b>	Compression Index
<b>γ<sub>d</sub></b>	Dry Unit Weight
<b>F</b>	Force (N)
<b>d</b>	Gauge Reading (mm)
<b>g</b>	Gravitational Acceleration
<b>e<sub>0</sub></b>	Initial Void Ratio
<b>φ</b>	Internal Friction Angle (°)
<b>m</b>	Mass of the Cone
<b>γ<sub>drymax</sub></b>	Maximum Dry Unit Weight (kN/m <sup>3</sup> )
<b>γ<sub>m</sub></b>	Moist Unit Weight
<b>σ</b>	Normal Stress (Vertical)
<b>w<sub>opt</sub></b>	Optimum Water Content (%)
<b>c<sub>r</sub></b>	Recompression Index
<b>τ</b>	Shear Strength
<b>τ</b>	Shear Strength (kPa)
<b>G<sub>s</sub></b>	Specific Gravity
<b>A</b>	Surface Area of Shear Plane (mm <sup>2</sup> )
<b>T</b>	Torque (N*m)
<b>K</b>	Vane Blade Constant (N*m)

## LIST OF ABBREVIATIONS

<b>ASTM</b>	American Society for Testing and Materials
<b>CBR</b>	California Bearing Ratio
<b>LL</b>	Liquid Limit (%)
<b>MDD</b>	Maximum Dry Density (kN/m <sup>3</sup> )
<b>OMC</b>	Optimum Moisture Content (%)
<b>PL</b>	Plastic Limit (%)
<b>PI</b>	Plasticity Index (%)
<b>RAP</b>	Reclaimed Asphalt Pavement
<b>UCS</b>	Unconfined Compressive Strength
<b>wc</b>	Water Content
<b>XG</b>	Xanthan Gum

# CHAPTER 1 INTRODUCTION

## 1.1 Introduction

There is a fundamental concern in the world regarding sustainability. Sustainability is used in almost every aspect of modern life and has a wide range of meanings. In this context, the term is mainly used to refer to the environmental future of the earth. The industrialized world within the last century has been producing a large amount of waste material during the production process. According to the United States Environmental Protection Agency (EPA) 600 million tons of construction and demolition debris were generated in the USA in 2018. A majority of the waste is composed of concrete, with 405 million tons (67.5%), and asphalt, with 107 million tons (17.8%), most of which is generated during demolition, with concrete representing 94% and asphalt representing 100%, respectively. The same report also presents that 456 million tons of debris were recycled for various purposes, like landfills (24%), manufactured products (22%), and aggregates (52%). Moreover, 92% of asphalt waste is used for manufactured products, and aggregate, where manufactured products include recycling road pavements. Asphalt debris, which is obtained by trimming the pavement of roads that are from roads that have reached the end of their service life, is called reclaimed asphalt pavement (RAP). Adhikari et al., (2020) used RAP in rehabilitating deteriorated pavement techniques such as cold in-place (CIP) and hot in-place recycling (HIP) and also used in geotechnical applications such as subbase and subgrade of road construction and the foundation of infrastructures and superstructures since the second half of the 20th century (Khay et al., 2015), because of both trending environmental concerns and the increased cost of using new construction materials (Suebsuk & Suksan, 2014). Using asphalt aggregates as subbase or subgrade material is classified in the literature as a ground improvement technique that is a method to improve the geotechnical properties of weak grounds in several ways, reducing permeability and compressibility and increasing strength by using different methods such as chemical, mechanical, and biological (Biju & Arnepalli, 2020; Fattah et al., 2012; Rajabi & Hosseini, 2022).

Moreover, soil improvement techniques are common terminology used to define all the methods for stabilizing the engineering properties of the working site before, during, or after construction. The methods can basically be classified based on their process; for example, chemical soil stabilization is a method in which some chemicals are added to soils to achieve better performance from the soil. Chemical soil stabilization has a history dating back to the early 20th century (Winterkorn & Pamukcu, 1991) and a lot of research has been carried out since then. These studies show that most of the chemicals used are calcium-based materials (Kota et al., 1996).

## **1.2 Problem Statement**

Materials used in soil improvements like cement and lime have been called traditional stabilizers since serious studies are being carried out to alternate these materials that are considered hazardous and generate great amounts of poison gases (CO, CO<sub>2</sub>, SiO<sub>2</sub>) during production (Worrell et al., 2001). To reduce the environmental pollution of these materials, eco-friendly chemical and biological materials such as biopolymers, resins, and enzymes have been studied and used recently (Naeini & Masoud, 2010; Khatami & O'Kelly, 2013). Biopolymers are popular for use in replacing cement in soil stabilization as a binder lately (Jang, 2020). Guar gum, xanthan gum, and agar gum are the most commonly used biopolymers for treating soils. These gums have been used for investigating geotechnical parameters like compressibility, strength, and permeability on both fine and coarse-grained soils, with different conditions such as wet-dry and cured-noncured, by performing a very wide range of testing programs previously (Chang, Prasadhi, et al., 2015; Acharya et al., 2017; Biju & Arnepalli, 2020). In addition, waste management has been a critical problem for many years, so recycled materials are also being used in soil stabilization to reduce the effect of disposal on the environment and to avoid the high cost of using new materials. Waste concrete, brick, stone powder, and asphalt pavement can be given as examples of disposals generated from producing construction materials, construction, and demolition of any type of structure (Pappu et al., 2007). Although there are many applications for the use of reclaimed asphalt pavement (RAP), such as subbase-subgrade in highway and roadway construction and filling material for embankments (Plati & Cliatt, 2019; Rahman et al., 2015), not so many good-quality studies about using RAP as a stabilizer of soils were observed in the past.

### **1.3 Objectives**

This study aimed to assess the potential of reclaimed asphalt pavement (RAP) and powdery xanthan gum (XG) biopolymer as environmentally friendly soil stabilizers in geotechnical engineering. Driven by a commitment to reduce waste material impact and explore sustainable alternatives, the research delved into the intricate interactions between RAP and XG. Focusing on silty soil from Gaziantep province, extensive laboratory experiments were conducted to understand the influence of RAP and XG on engineering properties. The investigation also aimed to elucidate the performance dependency of XG in varying water conditions. This thesis contributes valuable insights to geotechnical engineering, offering solutions for sustainable soil stabilization practices and minimizing the environmental footprint of infrastructure projects.

### **1.4 Outline**

This thesis contains 5 chapters. The first chapter is an introduction to the studied topic, gives general information about the background of the topic, states the main reasons for conducting this research, and briefly mentions the objectives. Chapter 2 is mainly about past research related to this topic. The used materials and experimental methodology are summarized in the third chapter, and the results and discussion of the experiments are presented in chapter 4. Lastly, the conclusion of this thesis is given in Chapter 5.

## **CHAPTER 2 LITERATURE REVIEW**

### **2.1 General**

In this chapter, the literature review regarding the materials used in this study is presented. Initially, the studies related to recycling and reusing waste materials from construction and demolition are summarized, and then the use of reclaimed asphalt pavement in construction and geotechnical applications is reviewed. Moreover, many studies carried out about utilizing biopolymers in construction areas were also investigated. Studies on the applicability of XG—which is the main factor in this study—in geotechnical applications were examined and presented in the form of a summary.

### **2.2 The Use of Waste Materials in the Construction and Environmental Field**

Most of the waste materials produced from demolitions are concrete, and to reduce the harmful impact of the intense amount of concrete, the material has been recycled and used for various engineering purposes (Rahman et al., 2015; Tavakol et al., 2020). Corinaldesi (2010) studied the potential of using recycled concrete aggregates (RCA) in producing concrete. Slump and compression tests were carried out on concrete samples prepared with a 0.40 to 0.60 water/cement ratio and different contents of pure virgin aggregates, replacing 30% of fine or coarse aggregates with recycled aggregates. The compression results indicate that the strength of C32/40 concrete can be reached by using 30% RCA instead of using new aggregates. Another perspective on replacing natural aggregate with RCA is the effect of RCA on concrete bond strength with reinforcing steel, as investigated by Butler et al. (2011). In the study, two different RCAs were used to replace the natural aggregates by 100%. The study shows that concrete prepared with both RCA types has a higher compression strength compared to the one with natural aggregate, and the correlation between bonding strength and RCA is based on the average crushing value of the RCA, which is lower than the strength with natural aggregates.

Besides being used in concrete production, recycled concrete aggregates (RCA) are also used in soil stabilization. For example, in the study of Kianimehr et al. (2019), different proportions (5%, 10%, and 15%) of RCA were used to stabilize clay soil, and the testing results show some improvement in several parameters of clay, such as reducing dry density, increasing optimum water content, increasing compression strength, reducing settlement, and increasing shear strength parameters (cohesion ( $c$ ) and internal friction angle ( $\phi$ ), but the RCA also leads to a brittle behaviour in clay. During the process of manufacturing construction materials, some unnecessary by-products can occur. Rock powder is one of these products, and rock powder tends to be reused in several ways. Cabalar and Alosman (2021) found that in their study, rock powder was used with different concentrations (10%, 20%, 35%, and 50% by dry weight) to stabilize organic soil. Several testing procedures were conducted, and the results showed that dry density increased and optimum water content decreased. Besides, the UCS results prove that soil becomes more brittle when rock powder is added, and the consolidation was enhanced with rock powder addition. Similar to rock powder, limestone powder is also used for improving soils. For instance, Pastor et al. (2019) used limestone powder in an experimental study to improve the geotechnical properties of clayey soil. The test results show the addition of limestone powder causes a great reduction in the liquid and plastic limits of clay, similar to past research. The reason for this is that limestone is less plastic than clay, and this also decreases the compressibility of clay soil. The limestone caused a reduction in the free swelling index by 61% at 15% limestone powder, but a much higher strength was achieved from UCS tests. Moreover, granite powder is used as a stabilizer by Eltwati et al. (2020) at 4%, 8%, 12%, 16%, and 20% concentrations to improve the properties of A-6 clay soil. Compactor tests, California bearing capacity (CBR) tests, and direct shear tests were performed to investigate the effect of granite dust on clay. The test results pointed out that granite dust increases the dry density of the soil while CBR values increase greatly, especially in 9% granite dust, where the bearing capacity reaches its peak. The direct shear test results show the difference between the untreated soil and soil treated with 8% granite dust, and treated soil samples have much greater strength compared to non-treated soil. One of the other construction and demolition (C&D) debris used as a base or subbase material for geotechnical purposes is brick. A laboratory study was performed by Arulrajah et al. (2011) to evaluate the performance of recycled crushed brick (RCB) by applying some laboratory tests like California

bearing ratio and triaxial tests. The results of the testing program show that the RCB can be useful compared to road design standards with both compaction and California bearing capacity, but the authors suggest the use of RCB with other recycled aggregates since the results of the triaxial tests show the RCB can be effective at moisture content up to 65%; at higher water content, the strength values are decreasing. Milled brick is used as a cementing agent for stabilizing two soil types, clay and silty clay, by Hidalgo et al. (2019). Compaction test results reveal distinct effects on both silty and clayey soils. Specifically, the incorporation of brick dust led to a reduction in dry density and an increase in water content for the silty soil. In contrast, for the clayey soil, there was an observed increase in dry density accompanied by a decrease in the optimum water content. This discrepancy can be attributed to the inherent differences in particle size, as clay particles are finer than brick dust, while silty soil particles are coarser than brick dust.

Waste materials can be used together, apart from being used alone. Examples of this situation have been explored in past studies. As an illustration, Rahmani et al. (2015) conducted a study about utilizing reclaimed asphalt pavement (RAP) and recycled concrete aggregates (RCA) in road pavement applications. Several laboratory tests and field-testing programs were carried out to comprehend the usability of the RCA mixture with 100, 50, 30, and 15% of RAP. The stain and resilient modulus at 15% RAP are acceptable, but the CBR test results show that the more RAP/RCA increased, the less CBR was achieved. This means that for any of the RAP/RCA ratios, the requirements could not match. Another study related to stabilizing waste material and its use for road construction as a base or subbase material was done by Mohammadinia et al. (2017). The researchers are focused on comparing two different wastes, reclaimed asphalt pavement (RAP) and crushed brick (CB), using another disposal material, fly ash, with several proportions (0, 5, 10, 15, 20, 25, and 30% by dry weight) at different temperatures (20° and 40° Celsius). The results of UCS tests show that the compression strength for both RAP and CB increases by up to 15% of fly ash, but a higher concentration of fly ash causes a reduction in strength because the FA changes the microstructural structure of RAP and CB, and for all fly ash ratios, the strength is greater at 40°C compared to 20°C. An interesting study related to comparing five waste materials—reclaimed asphalt pavement (RAP), recycled concrete aggregates (RCA), crushed brick (CB), waste rock (WR), and fine recycled glass (FRG)—in terms

of reuse in a geotechnical manner was done by Arulrajah et al. (2013) Many laboratory experiments were conducted, and the results pointed out that FRG is less susceptible to water absorption compared to other wastes, and the hydraulic conductivity is found to be lower for CB and RCA than the others. Maximum dry density (MDD) was highest and lowest for WR and FRG, respectively, and the cohesion values of the materials are similar, whereas FRG shows no cohesion and RAP shows the highest. Concerning permanent strain, RCA and WR show great potential for meeting requirements, contrary to FRG and RAP.

### **2.3 The Use of Reclaimed Asphalt Pavement in Construction Applications**

Asphalt pavement is one of the most frequently generated waste materials due to construction and demolition events. It is very important to reutilize asphalt pavements since this waste material does not disappear in nature over time, the production of new aggregates is harmful to the environment and is expensive, and the aggregate of this waste has many advantages in terms of engineering. There have been many studies on this subject in the past, and important studies related to this thesis will be summarized. Stabilization of the reclaimed asphalt pavement (RAP) by mixing with virgin aggregates and adding a binder is a common technique. Khay et al. (2015) used cement to stabilize RAP-mixed crushed aggregates. The experimental program was applied to crushed aggregates and various percentages of RAP (0, 25, 50, 75, and 100%) by total weight. The compression strength, indirect tensile strength, flexure strength, and elastic modulus were worsened with the addition of RAP since, contrary to crushed aggregates, RAP aggregates are coated with bitumen material and thus prevent the interlocking ability of particles against any type of stress. The design requirements of road pavements are achieved at 60% RAP, according to the testing program. The RAP-Lateric soil mixture was stabilized with 0, 0.5, 1, 1.5, and 2% cement ratios by Edeh et al. (2012). The gradation of the RAP became finer than the initial, and the plasticity index increased with soil and cement. Compaction and CBR tests were conducted on samples, and the results show that the maximum dry density increased with cement content while the soil was kept constant and decreased with increased soil amounts in the mixtures. The optimum moisture content increased parallelly with decreasing RAP and increasing cement at constant soil. The bearing capacity CBR test was calculated at 180% for the soaked condition (55% at 40% soil and 2% cement), and these values

meet the minimum for road design. Modified compaction tests and triaxial tests were conducted on 100% reclaimed asphalt pavement (RAP) aggregates, 50–50% RAP-VA (virgin aggregates), and 100% VA specimens in the study of Plati and Cliatt (2019) to evaluate the resilient modulus ( $M_r$ ) characteristic of RAP as a base or subbase material. The optimum water content (OMC) increases slightly from 4.1% to 5.9% for 100% RAP and 50–50% RAP-VA, then it reduces to 5.5% for only VA, and the maximum dry density was found to be 2.079, 2.225, and 2.245 kg/m<sup>3</sup> for RAP, 50–50% RAP-VA, and VA, respectively. The close values of OMC point out that the bitumen material did not coat the RAP aggregates, but in the aspect of MDD, the VA is more compactible compared to RAP. VA has the highest confining stress compared to RAP-containing tested samples, which are supported by a lower  $M_r$  of RAP and 50–50% samples. Suebsuk et al. (2019) also researched the effect of the soil-water/cement ratio on improving the engineering properties of RAP by conducting laboratory experiments on soil- and cement-treated RAP. Lateritic soil was classified as clayey sand (SC) according to USCS and well-graded clean gravel (GW) during the experimental program. According to testing results, the maximum dry density (MDD) increases as the soil ratio increases, but surprisingly, the optimum water content of samples does not change dramatically. The compression stress increases greatly with higher soil concentration at 28 days of curing, and the cement content also increases the strength, but it decreases the ductility of the samples. Water content is also effective for strength; as the WC increases, the peak stresses decrease. When the soil-water/cement ratio increases, the unconfined compressive strength decreases.

Besides cement, another cementing material, lime, is used for utilizing RAP in pavement design. For example, Alizadeh and Modarres (2019) carried out a study regarding stabilizing RAP with various low-plasticity clay (CL) soil contents, bitumen emulsion, and lime. The macroscale tests were conducted on RAP mixed with different clay ratios (5, 10, 15, and 20% by dry weight), different bitumen emulsion content (3, 4, 5, 6, 7, 8, and 9% by dry weight), and a constant ratio of lime determined according to previous studies considering economic and environmental concerns. Indirect tensile strength test results for unconditioned specimens show an increment with increasing clay content up to 15%, then it slightly decreases. However, in conditioned specimens, it is found that the peak strength is achieved at 10% clay. The reduction in tensile strength of specimens containing a higher clay ratio, such as 15%, can be referred to

as the effect of lime during the process, increasing the durability with cementing chemicals interreacting with clay minerals, but the excessive amount of clay could not be consumed since the lime content was limited. Also, the tensile strength ratio (TSR) was maximum at 10% clay since the curve is a classic parabola that first increases, then decreases. At 15% clay, the Mr was highest, and the effect of bitumen emulsion was not clearly observed. The authors recommend further investigation related to the possibility of bitumen emulsion delaying the lime-clay mineral reactions. Alternatives to chemical stabilizers, fly ash-based geopolymers (Class F FA) and RAP are used to stabilize two types of soils: lean clay (CL) and elastic silt (MH) by Adhikari et al. (2020). Different variations of materials (0-0, 15-10, and 25-25% Geopolymer-RAP percentages by the total weight) were used during the experimental program, and ordinary portland cement (OPC) was used by 5 and 10% of the soil weight for comparison with Geopolymer-RAP. According to testing results, the UCS values increase with FA and RAP at every percentage compared to the control. In a comparison of CL and MH soils, low-plasticity clay has more strength compared to high-plasticity silt. RAP increases the elastic modulus and density of the mixture, but FA both increases and decreases these parameters depending on sodium silicate content. The maximum UCS values were achieved at 25–25% FA–RAP mixtures, whereas the proper amount of sodium silicate shows variation with CL and MH. Compared to cement addition, geopolymer-added mixtures show higher resilient modulus (Mr) and dynamic modulus. The durability of the FA-RAP-treated CL matches the 10% cement-treated soil, contrary to the 5% cement, which was not sufficient for durability. Geopolymer-RAP is found to be effective for stabilizing two types of plasticity in soil by enhancing its strength, durability, and mechanical properties to meet the minimum requirements of pavement design.

#### **2.4 The Use of Biopolymers in the Construction Field**

In recent decades, there has been a global shift towards a more environmentally conscious worldview, particularly evident since the turn of the millennium. This shift emphasizes the protection of nature through increased use of renewable energy, strict controls on harmful waste, and efforts to conserve water and energy to combat the climate crisis. This rationalized behaviour extends to engineering disciplines, prompting studies to address environmental concerns. One notable concern is the

environmental impact of materials like cement and lime used in structural and geotechnical engineering for soil improvement. In response, there has been a concerted effort to identify environmentally friendly alternatives. Biopolymers, derived from biological sources and known for their eco-friendly characteristics, have gained popularity for improving soil parameters. This section provides a concise summary of studies on the use of biopolymers for soil improvement, with a focus on geotechnical applications, offering insights into sustainable engineering practices. Dehghan et al. (2019) conducted a study to obtain information about the effectiveness of two biopolymers, guar gum and xanthan gum, on stabilizing collapsible soil. A series of laboratory experiments were performed, including compaction, triaxial, permeability, and consolidation tests on samples prepared by soil and different percentages of xanthan gum and guar gum (0, 0.5, 1, 2), and various curing periods (0, 1, 7, and 28 days). The local soil with 2.65 specific gravity used during experiments is classified as silty clay with low plasticity, which is very similar to the soil used in this presented study, and the biopolymers were provided by the industry. The testing program started with a modified Proctor compaction test, and the graphic of maximum dry unit weight and optimum water content versus biopolymer shows that the unit weight of soil reduces when both guar gum and xanthan gum are added. In contrast to unit weight, the optimum water content shows the opposite trend; it increases with biopolymer content. The reduction in unit weight is similar for both guar and xanthan gum, but it is always smaller for guar gum, especially at 1% biopolymer content. The xanthan gum reduces the unit weight sharply compared to guar gum and other biopolymer contents. Although xanthan gum decreases the unit weight of soil more compared to guar gum, xanthan gum increases the optimum water content more than guar gum does. This general behaviour is explained by the author by the fact that the water is absorbed by the biopolymer particles and interacts with the fine soil particles, and because this formation fills the pores in the soil, a structure that is large in volume but relatively lighter in mass occurs. The absorption of this water thus explains the increase in the optimum water content. The permeability tests were applied to two different dry unit weights of soil ( $14 \text{ kN/m}^3$  and  $15 \text{ kN/m}^3$ ). The results at both unit weights show that xanthan gum is more effective in reducing the permeability of soil, though both guar gum and xanthan gum reduce the permeability. Additionally, specimens containing biopolymer have higher permeability at a longer curing time (28 days) than at a shorter curing time (7 days), which is attributed to the effect of dehydration over time. The

strength data received from the triaxial test at unconsolidated, undrained conditions shows that the increased biopolymer in the sample leads to an improvement in strength. Changing confining pressure did not affect the deviator stress seriously, but the deviator stresses were slightly higher at 200 kPa confining pressure compared to 50 and 100 kPa. In addition, the curing effect was as expected; the stress strength of the samples increased in parallel with the curing time. For example, 272 and 464 kPa pressures were obtained for 1-day and 28-day curing at 100 kPa confining pressure, respectively. Furthermore, higher deviator stress was achieved when the density of the sample increased, and the comparison of xanthan gum and guar gum on strengthening was evaluated by performing tests on the exact same condition, and the results show that xanthan gum is more effective at improving the strength of the soil at 2% concentration and 14 kN/m<sup>3</sup> unit weight. Generally, although both guar gum and xanthan gum are effective at enhancing the engineering properties of soil, xanthan gum was found to be more effective than guar gum. The curing effect, variation of density, and many different biopolymer concentrations were investigated, and in conclusion, both guar gum and xanthan gum play a big role in reducing the collapsibility of soils.

## **2.5 The Use of Xanthan Gum in the Geotechnical Applications**

Xanthan gum has been a popular organic stabilizer used for soil stabilization in geotechnical applications due to its many advantages compared to other stabilizers. Many studies have been carried out to put this popularity on a scientific basis (Lee et al., 2017; Chen et al., 2019; Elkafoury & Azzam, 2020; M. Hamza et al., 2022;). One of these studies, carried out by Chang et al. (2015), investigated the effect of xanthan gum (XG) on stabilizing different soil types: sand (SP), natural soil (SM), red-yellow soil (CL), and clay (CH) in many aspects, including the chemical and mechanical interaction of XG and soil particles, soil type effect, long-term durability, the effectiveness of XG concentration, and mixing methods, by performing micro- and macro-scale testing programs. The unconfined compression test (UCS) conducted on mixtures contains four different soils, various XG content (0, 0.5, 1, and 1.5%), 10% cement on different curing periods (3, 7, 12, 21, 28, 63, and 750 days), and different water contents. Soil-type effectiveness in strengthening is based on the gradation of the soil. The UCS results indicated that the XG is more susceptible to enhancing strength in fine-grained soils compared to coarser-grained soils due to the interaction

of the XG with clay particles. The peak stress was achieved at 1.5% XG-treated red-yellow soil, and the minimum stress values were at 0.5% XG-treated sand. The strength gained in XG-treated sand is greater in percentage than that gained in CH. The cured specimens show a great increment in strength, even in the long-cured specimens, but when the water content of the specimens increases, the strength decreases. The strength gain mechanism is mainly based on the bond firming between clay minerals (XG) for fine-grained soils, but for coarse-grained soils like sand, the strength comes from the matrixes formed between soil particles. For this reason, the authors advised that adding a small amount of fine soil to coarse soils will be effective on the performance of XG. Although the strength of soils increases with increasing XG content, 1.5% was found to be optimal due to the high cost and workability of using a high amount of XG, and generally, XG was proven to be effective in improving the geotechnical properties of soil, especially in dry conditions.

Cabalar et al. (2018) have done experimental research related to improving the engineering properties of clay with xanthan gum. Laboratory experiments were conducted on samples prepared by mixing clay classified as CL and XG at different contents (0, 0.5, 1, 1.5, 2, and 3%) over various curing periods (0, 7, 28, and 56 days). Firstly, a reduction in maximum dry density (MDD) and an increment in optimum water content (OMC) were observed from the standard proctor test. As XG concentration increased, the amount of water that could be absorbed increased, but the compressibility of the soil decreased since the XG interacted with water to form a hydrogel. Moreover, the results of the unconfined compressive strength tests show a linear reduction in measured stresses as XG increased at specimens tested immediately, but at cured specimens, the strength values increased remarkably as XG content increased. Even if the maximum stress was measured at a soil sample 56 days cured and treated with 3% of XG, the stresses at 28 days and 56 days curing are so close, as can be seen in Figure 2.1 below. Similarly, to compressive strength, the energy absorption of samples calculated from UCS values increases parallel to XG in the cured condition, but it shows no reasonable trend in the non-cured condition.

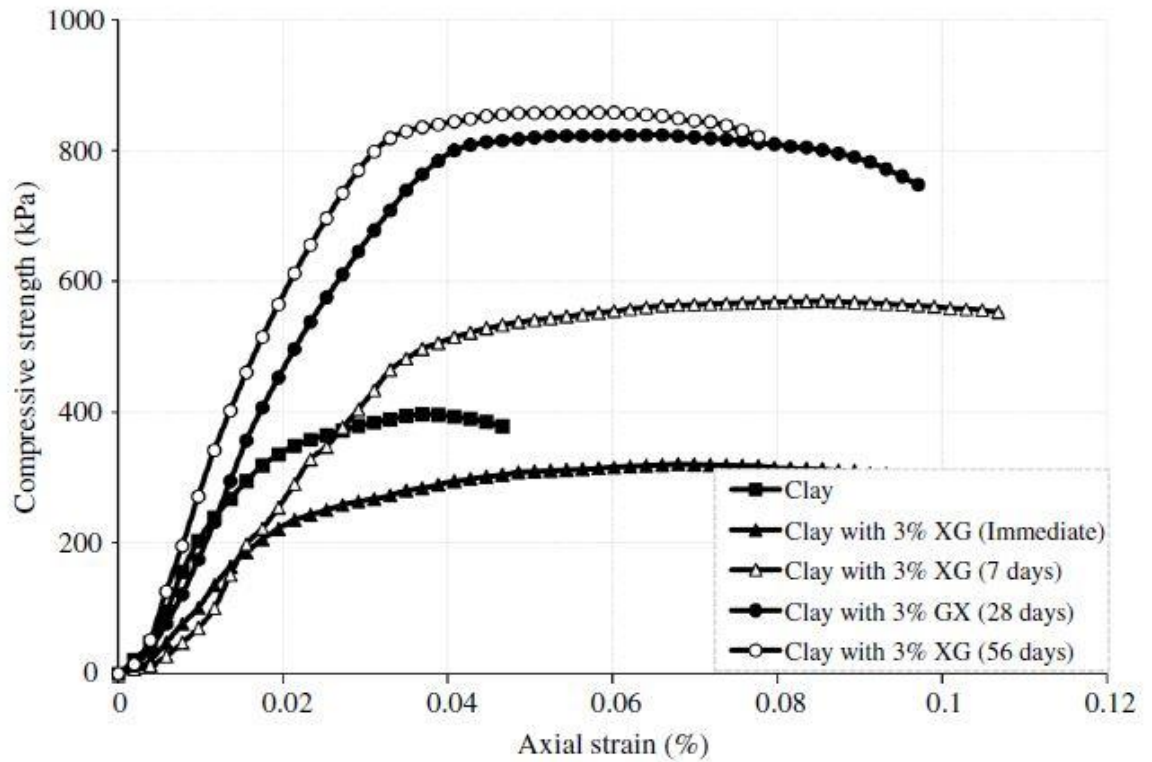


**Figure 2.1** The effect of curing time on UCS values at 3% XG (Cabalar et al., 2018)

The cohesion of the soil from the direct shear test increased not only with the XG but also with curing time. The cohesion of the sample with 3% XG increased by nearly 30% at 56 days of curing compared to non-stabilized soil and increased by 25% at 56 days of curing compared to non-cured soil. However, the internal friction angle values show a considerable linear reduction while XG increases, and as the curing time extends, the internal friction angle slightly increases. Although the undrained shear strength ( $s_u$ ) increases with XG content for fall cone and laboratory vane shear and test results show similar trends in reacting with XG in both tests, the undrained shear strength values have major differences. Undrained shear strength from the laboratory is higher than strength from the fall cone test, and an equation was built to show the correlation between the two test values. Additionally, 1-dimensional consolidation tests were carried out using an oedometer apparatus, and from the results, both compression ( $C_c$ ) and expansion indexes ( $C_e$ ) increased with increasing XG content. According to the  $C_c$  trend, the soil became more susceptible to compressibility, but  $C_e$  shows the volumetric deformation is mainly elastic. The increasing swelling ratio up to 1.5% XG supports this idea. Xanthan gum was very effective in reducing the

permeability of the soil as well. Overall, xanthan gum at a low ratio was sufficient for improving the engineering properties of low-plasticity clay soil.

The main working mechanism of xanthan gum is its interactions with water and fine-grained soil particles. For this reason, Nugent et al. (2009) have decided to investigate the interaction of two different biopolymers, xanthan gum and guar gum, with high plasticity clay (CH) in their study by focusing on the liquid limit. Different proportions of xanthan gum (0.25–10%), guar gum (0.25–3%), CH, and some salts (0.1 M  $\text{Ca}(\text{NO}_3)_2$ , 0.01 M KCl, and 0.01 M NaCl) were used to achieve a biopolymer solution for observation of the fluence of several cations ( $\text{Ca}^{2+}$ ,  $\text{Na}^+$ , or  $\text{K}^+$ ). The mixtures were subjected to liquid limit tests using the Casagrande apparatus by following the related ASTM standard, and the results of the experiments point out that the increasing biopolymer content leads to an increasing liquid limit, especially with guar gum, due to the more hydrogel-formed. Moreover, the cations caused a reduction in the liquid limit by absorption of the biopolymer molecules.

Another comparison of guar gum and xanthan gum on soil stabilization was covered by Mugada et al. (2017). In this study, soil containing 20% kaolin, 70% sand, and 10% gravel was stabilized by various contents (0, 0.5, 1, 1.5, 2, and 3% by dry weight) of guar gum and xanthan gum at 7- and 28-day curing periods. Both xanthan gum and guar gum increase the compression strength from unconfined compressive strength tests for all curing periods. At 7 days, the curing sample contains 3% XG, which reaches the maximum UCS value, but generally, at the same concentration, for guar gum and xanthan gum, the strength values are very close for both 7 and 28 days. Air-dried samples' strengths were compared to the maximum strengths of 7 and 28-day-cured cement-stabilized soil and non-treated samples. Specimens with biopolymer are always higher than the non-treated sample, and the strength of the sample treated with guar gum at 1.5% or a higher percentage and cured for 28 days passes the strength values of cement-treated samples for both 7 and 28 days. However, the 7-day-cured guar gum-treated samples' strength can only pass the cement-treated soil strength. For the xanthan gum, the strength of samples treated with 1.5% biopolymer content and cured for both 7 and 28 days stays between the strength of the 7-day cured cement-treated sample and the 28-day cured ones. At higher concentrations, it is much higher than cement-treated samples. Generally, guar gum is found to be more effective at

strengthening the soil compared to xanthan gum, but both biopolymers are sufficient to be used in soil stabilization.

Most of the waste materials produced from demolitions are concrete, and to reduce the harmful impact of the intense amount of concrete, the material has been recycled and used for various engineering purposes (Rahman et al., 2015; Tavakol et al., 2020). Corinaldesi (2010) studied the potential of using recycled concrete aggregates (RCA) in producing concrete. Slump and compression tests were carried out on concrete samples prepared with a 0.40 to 0.60 water/cement ratio and different contents of pure virgin aggregates, replacing 30% of fine or coarse aggregates with recycled aggregates. The compression results indicate that the strength of C32/40 concrete can be reached by using 30% RCA instead of using new aggregates. Another perspective on replacing natural aggregate with RCA is the effect of RCA on concrete bond strength with reinforcing steel, as investigated by Butler et al. (2011). In the study, two different RCAs were used to replace the natural aggregates by 100%. The study shows that concrete prepared with both RCA types has a higher compression strength compared to the one with natural aggregate, and the correlation between bonding strength and RCA is based on the average crushing value of the RCA, which is lower than the strength with natural aggregates.

Two different biopolymers, xanthan gum (XG) and  $\epsilon$ -Polylysine (EPL) are used to stabilize the engineering properties of soft marina soil classified as high plasticity clay (CH) by Kwon et al. (2019). A series of laboratory experiments were conducted on specimens prepared by mixing soil with XG (0, 0.5, 1, and 2% by weight of dry soil) and on specimens prepared by mixing soil with EPL (0, 0.1, 0.25, 0.5, 1, and 2% by weight of water content). Experiments including consistency tests fall cone tests, laboratory vane shear tests, consolidation tests, laboratory sedimentation tests, and unconfined compression tests were performed, and the first data from the Atterberg limit tests shows that both liquid and plastic limits increase with increasing XG content in the mixture. The reason for this situation was attributed to the fact that XG interacts with water and forms hydrogels. Findings from the fall cone and laboratory vane shear tests indicated that XG significantly increases the shear strength at the same water content; this reason was not different from the reason for the increment in the LL and PL. Moreover, in consolidation, a single XG content (0.5%) was used for comparison

with untreated soil rather than using several XG contents. The testing results were determined according to the vertical stress magnitude, and at low vertical stress (shallow depths), the specimen including XG showed less compressibility compared to untreated soil. Contrary to low (<50 kPa) vertical stress, higher vertical stress causes much more reduction in the void ratio. When XG increases, the coefficient of consolidation decreases, and parallelly, the permeability of the soil also decreases, which means that the time for the consolidation to take place increases. The settling rate increases with increasing EPL ratios, and the final void ratio decreases with increasing EPL content, so EPL accelerates sedimentation. Untreated, treated with 1% EPL, and 1% XG-treated specimens subjected to 48 and 168 hours of curing were introduced into the UCS experiment. The compressive strength of soft marina soil increases dramatically when the curing period is long (168 hours), compared to 48 hours of curing regardless of the type of biopolymer. EPL shows no significant improvement in strength compared to non-treated soil, but XG increases the UCS values of soil for both curing periods. In general, both EPL and XG can be used as stabilizers to improve the geotechnical properties of soft marine soil.

Another important study related to the usage of xanthan gum in geotechnical soil improvement was carried out by Chang et al. (2021). The study was focused on the undrained shear strength of two types of clay (kaolinite and montmorillonite) treated with xanthan gum (0, 0.1, 0.5, 1, and 2% DI water solution), brine, and kerosene. Two types of tests were performed (the fall cone test and the laboratory vane shear test) to evaluate the undrained shear strength of specimens. The testing results show that the effect of xanthan gum on undrained strength is visible. As a result of compression, clays with DI water's test results were observed, and kaolinite with DI water was found to reach maximum undrained shear strength with 0.5% XG, while higher XG concentrations caused a reduction in  $s_u$ . The reduction in shear strength at high XG-soil ratios was attributed to However,  $s_u$  values drop gradually parallel to the increase in XG content of montmorillonite, which contains DI water solution, where the highest shear strength was reached at 0% XG. Furthermore, the  $s_u$  value of montmorillonite is higher compared to kaolinite with DI water at the same water content. Montmorillonite has a greater capability of holding water compared to kaolinite since its specific surface area is greater than kaolinite's. The  $s_u$  was measured higher at montmorillonite than kaolinite, though brine and kerosene dropped the undrained shear strength of

mixtures. Ni et al. (2020) have carried out a study approaching biopolymer-treated soil with a particular aspect. The study was focused on two major considerations, one of which is the effect of variable initial water content on soil stabilization by using xanthan gum biopolymer, and the other is the evaluation of the fatigue of xanthan gum-treated soil under constant-amplitude and stepping-amplitude fatigue loading tests at optimum water content. The stabilized soil was collected from a construction field and classified as sand-lean clay, which has  $17.3 \text{ kN/m}^3$  unit weight and 2.73 specific gravity. Mixtures prepared by mixing clay and xanthan at a ratio of 0, 1.0, 2.0, 3.0, 4.0, and 5.0 XG/Clay in dry conditions were subjected to a series of laboratory experiments, including standard compaction tests, Atterberg limits tests, unconfined compression tests, and fatigue loading tests according to related ASTM standards. Initially, based on the testing results, the XG affected the optimum moisture content (OMC) and maximum dry density (MDD) in the opposite way. It was observed that the liquid limit (LL) and plastic limit (PL) increased gradually in parallel with the biopolymer/dirt ratio. The challenging effect of XG was observed by applying unconfined compression tests to different biopolymer/soil ratios (0%–5.0%) under several initial moisture contents (16.5, 20, 23, 26, 30%). According to testing results, the XG improves the compression strength of the soil compared to non-treated soil by increasing the peak stresses and strain tolerance of the soil. The UCS value of untreated soil increased gradually and reached its peak point at 23% initial moisture content; at any further moisture content, the strength decreased compared to the previous water content. However, the XG-treated soils show higher compression strength at higher initial water content. Additionally, the fatigue loading tests were applied to the prepared sample, and the results pointed out that the increase in XG content in the mixture leads to an improvement in the fatigue life of the sample against loading cycles at each maximum stress to unconfined compression strength ratio.

Cabalar et al. (2017) investigated the application of xanthan gum (XG) as an environmentally friendly biopolymer in geotechnical engineering. The study focused on evaluating its impact on key geotechnical parameters (compressibility, permeability, strength, and stiffness) under varying concentrations (0%, 0.5%, 1%, and 1.5%). The research utilized constant head permeability tests, oedometer tests, unconfined compression tests, and triaxial tests. A specific gravity of 2.68 sand samples, ranging from 0.075 to 1.0 mm in particle size, was used. XG, an organic biopolymer, served as a stabilizer. Results indicated a reduction in permeability with

increasing XG concentration, attributed to the formation of highly viscous gels impeding water flow through soil pores. Oedometer tests demonstrated XG's impact on compressibility, with increased XG ratios leading to heightened compressibility due to reduced friction between sand particles. Unconfined compression tests revealed increased strength with higher XG ratios and curing times, reaching a maximum of 2.71 MPa at 1.5% XG after 28 days. Triaxial tests under consolidated-drained conditions showed that XG increased deviatoric stress resistance at both 100 kPa and 250 kPa confining pressures. However, brittleness and ductility varied: XG enhanced ductility at 250 kPa but induced a more brittle behaviour at 100 kPa. Cohesion ( $c$ ) increased linearly with higher XG content, while the internal friction angle ( $\phi$ ) showed no significant change, decreasing from  $33^\circ$  to  $29^\circ$  for clean sand and 1.5% XG-added samples.

In summary, the study underscores xanthan gum's potential for enhancing geotechnical properties, including compressive strength, permeability, compressibility, and shear strength in sandy soils.

One of the most important studies about biopolymers in geotechnical use was conducted by Chang et al. (2015). The focus of the study was investigating several perspectives such as soil type effect, durability, biopolymer content effect, and mixing method effect of the xanthan gum-treated four different soil types: sand (SP), natural soil (SP-SM), red-yellow soil (CL), and clay (Kaolinite, CH) at various curing periods (3, 7, 12, 14, 21, 28, 63, and 750 days). The testing results showed that xanthan gum generally improves strength through interaction with fine particles of soil like clay, as the cementation and bonding agents can be clearly seen in scanning electron microscopy images. The compressive strength values of 1% XG-treated specimens were variable for different soil types. The maximum strength was measured in a specimen with red-yellow soil, while the minimum strength was measured in sand. The reason for the strength difference between red, yellow, and sandy soils was the interaction of XG with fine particles, which are relatively less in sandy soil. The stiffness of the soils was evaluated by calculating the elastic modulus, where the stiffest soil was natural soil. Additionally, 10% cement-added red-yellow soil was tested to compare the 1% XG effect strength gain, and the red-yellow soil contains 1% XG, which is higher than the specimen with cement, and its elastic modulus is lower

than that of cement-treated soil. Moreover, the durability aspect of XG treatment was emphasized by conducting compressive strength tests on specimens subjected to various curing periods. The compressive strength of both clay and sandy soil increased with increasing curing time. Dehydration was the main factor leading to strength improvement, and strength and stiffness were not observed even after a 750-day period. In general, the compressive strength increased with increasing XG content for sand, natural soil, and red-yellow soil. The findings were that it increases with higher XG concentrations, but the most effective XG content was found to be between 1% and 1.5% because workability becomes a problem at high XG concentrations. Although the factors were different, the strength of all soils can be improved by XG treatment.

Biopolymers are also effective in treating soils that are collapsible, low-shear, or expansive. Xanthan gum was used to check the possibility of reducing the effect of weak engineering properties of soils on construction use by Singh and Das (2020). The study contains many experiments, such as consistency limit tests, proctor tests, compressibility tests, and hydraulic conductivity tests on mixtures of high plastic silt (CH) and xanthan gum (XG) by 0, 0.2, 0.5, 0.8, and 1.0% weight of the total. The liquid limit increases with XG up to 0.8% concentration, then decreases to a certain level. But contrary to the liquid limit, the plastic limit shows no decrement; it shows a continual increment. For this reason, the plastic index increases up to 0.5% XG content, then starts to decrease. Additionally, linear shrinkage increases and the shrinkage limit decreases while the amount of XG in samples increases. A classical unit weight-moisture content curve was observed from light compaction tests. The dry unit weight of samples increases up to a specific water content (21%), then starts to decrease. However, the difference in XG content does not show a reliable change in dry unit weight. For moisture content, XG increases the optimum water content by having the capability of absorbing a large amount of water. The curing effect was also investigated during strength tests. At both curing times, the XG was found to be effective in improving the maximum compression strength achieved.

Two different soils: bentonite and kaolinite which are considered as problematic soils due to their insufficient engineering properties such as shear strength and compressibility were tested with and without treatment of xanthan gum by Latifi et al.

(2016). The laboratory testing program includes compression tests, direct shear tests, and consolidation on specimens prepared with different xanthan gum contents and cured at different time intervals. The UCS results showed that strength of the both soils increased with increased XG content and curing time. The majority of the strengthening took place during the first 28 days, so there was only a small difference between 28 and 90 days of curing. The compressive strength increased greatly up to 1% and 1.5% XG content for bentonite and kaolinite respectively which are considered optimum ratios since after these points the increment magnitude was lower. The growth in strength was attributed to the formation of cementitious products and electro-static reaction between XG monomers and clay particles. Direct shear tests were performed on specimens with 1% XG for bentonite and 1.5% XG for kaolinite at different curing periods (7, 28, and 90 days). The cohesion of both treated bentonite and kaolinite increased over time, and the internal friction angle varied slightly at the optimum XG contents. The cohesion of 1% XG treated bentonite was found to be 454 kPa which is five-times of the value of untreated soil (95 kPa) and the internal friction angle increased from 21 to 24 degrees at 7 and 28 days curing respectively. The oedometer test results generally the compressibility of the soil decreased with curing time, besides, during the testing, the XG content was kept constant so the effect of variability of the XG was not aimed to be observed. When the curing period increased, the void ratio-pressure curves closed in, and specimens with 90 days of curing showed the least strain. Additionally, compression indices and swelling indices dropped remarkably up to 30 days after that reduction was slight. After all, XG was proved to be effective in increasing compressive strength, increasing cohesion, and reducing compressibility and swelling of both bentonite kaolinite, additionally, the curing showed great impact on the engineering properties of the soils.

Kwon et al. (2023) conducted an insightful exploration into the impact of xanthan gum on the consolidation and swelling behaviour of kaolinite clay. The study unveiled noteworthy alterations in the material's characteristics following the introduction of xanthan gum into the clay matrix. Specifically, the research elucidated that the inclusion of xanthan gum precipitated discernible reductions in both the consolidation degree and swelling propensity of the clay. The observed effects were explicated by the remarkable capacity of xanthan gum to establish a thin, continuous film on the clay surface. This film, in turn, serves to mitigate the aggregation of clay particles, thereby

impeding the unrestricted diffusion of water into the clay structure. A comprehensive analysis was conducted, encompassing three distinct concentrations of xanthan gum (0.1%, 0.2%, and 0.3%), alongside control samples devoid of xanthan gum. The obtained results illuminated a compelling trend, indicating that the incorporation of xanthan gum engendered diminished values for both the void ratio and swelling ratio in comparison to the control samples. This outcome suggests a profound influence of xanthan gum on the clay matrix, manifesting in a more compacted and less-swellable structural configuration. The discerned impact underscores the potential of xanthan gum as a modulating agent in tailoring the geotechnical properties of clay, presenting avenues for enhancing the material's stability and reducing its susceptibility to volumetric changes.

The study by Chen et al. (2019) investigates the impact of drying on the shear strength of xanthan gum biopolymer-treated sandy soil. Biopolymers, recognized for their environmental friendliness, have gained prominence in civil engineering. The research highlights the significance of drying in the behaviour of biopolymer-treated soil, specifically focusing on xanthan gum biopolymer and sand interaction during drying processes. At high water content levels, xanthan gum biopolymer initially exhibits limited effects on the sandy soil. However, as the water gradually evaporates, the bonding properties of the biopolymer become apparent, leading to an increase in soil shear strength when dried at 40°C. Conversely, samples dried at 20°C show an outer surface cemented and crystallized by the biopolymer while the inner part remains moist and weakly cross-linked, resulting in weak shear strength. Complete water evaporation under both drying conditions significantly boosts shear strength, but inconsistencies arise due to biopolymer shrinkage and brittleness. The study employs direct shear tests on more than a hundred samples prepared with varying concentrations of xanthan gum biopolymer. The results demonstrate that the biopolymer-treated soil's shear strength is influenced by drying conditions, with enhanced strength observed after water evaporation. Scanning electron microscope images reveal the interaction between biopolymer and soil particles, forming aggregates that contribute to increased strength. The bonding property of xanthan gum biopolymer is examined, showing a substantial increase in adhesive stress after drying. In conclusion, the research provides valuable insights into the drying effects on xanthan gum biopolymer-treated sandy soil shear strength, elucidating the intricate

interplay between drying conditions, biopolymer concentration, and soil behaviour. The findings contribute to the understanding of the potential applications and limitations of biopolymers in soil stabilization, particularly in the context of varying moisture levels.

In the realm of geotechnical engineering, the research conducted by Lee et al. (2017) presents a substantial contribution to the understanding of soil behaviour, particularly focusing on the influence of xanthan gum biopolymer treatment on sand. The comprehensive study, documented in *Geomechanics and Engineering*, unfolds in four distinct sections, each meticulously exploring different aspects of the geotechnical shear behaviour of xanthan gum-treated sand. The authors delve into the unique characteristics exhibited by sand in the presence of xanthan gum across various hydrogel phases—initial, dried, and re-submerged conditions. Of significant note is the detailed examination of the impact of xanthan gum on shear strength properties, revealing distinctive behaviours such as heightened peak shear strength in the dried state and the consequences of gradual swelling during re-submersion. This research elucidates the intricate interplay between xanthan gum hydrogels and sand particles, shedding light on the mechanisms governing soil improvement. The findings of Lee et al. offer valuable insights into environmentally friendly soil improvement materials, positioning xanthan gum as a noteworthy player in altering shear strength properties. The study's relevance extends to practical applications in geotechnical engineering, providing a nuanced understanding of the factors influencing soil behaviour and offering a foundation for the development of sustainable soil improvement techniques. Through their meticulous exploration of xanthan gum-treated sand, Lee et al. contribute significantly to the existing knowledge base, paving the way for further advancements in the field and emphasizing the potential of biopolymers in geotechnical engineering practices.

The study conducted by Lee et al. (2017) delves into the geotechnical shear behaviour of Xanthan Gum biopolymer-treated sands, primarily scrutinizing its performance under varying confining stress conditions. This investigation builds upon earlier studies that validated the strengthening effects of biopolymer-treated sands through direct shear tests and uniaxial compression tests. Notably, the novelty of Lee et al.'s (2017) work lies in its exploration of shear behaviour under different confining stress

conditions, a facet largely unexplored in prior research. The study conducted triaxial testing with representative confining pressures, unravelling the impact of biopolymer content on shear resistance. The findings, which demonstrated a substantial increase in cohesion and friction angle, underscored the effectiveness of the biopolymer treatment, particularly when the biopolymer film matrix was comprehensively developed. Furthermore, Lee et al. (2019) contributed to this body of knowledge by investigating the laboratory triaxial test behaviour of xanthan gum biopolymer-treated sands. This subsequent study added depth to the understanding of biopolymer-treated soils, offering insights into their elastic-plastic behaviour and strain-softening characteristics under different hydraulic conditions. The choice of Sydney sand as the testing material and Xanthan Gum as the biopolymer in these studies provides specific details crucial for replicability. Collectively, these works contribute valuable insights into the geotechnical applications of biopolymers, suggesting their feasibility for soil stabilization purposes, especially in scenarios involving varying confining pressures. The nuanced exploration of the interplay between biopolymer content, hydraulic conditions, and shear behaviour in these studies enriches the existing literature and provides a solid foundation for further research in the domain of environmentally sustainable soil improvement methodologies.

Wang et al.'s (2021) comprehensive exploration of red clay stabilization with xanthan gum presents a significant advancement in geotechnical engineering. The study meticulously investigates the mechanical properties of treated red clay, providing insights crucial for soil stabilization applications. The investigation begins by assessing the porosity ratio, revealing a substantial alteration with varying xanthan gum content and curing ages. Notably, a distinct threshold at 1.5% xanthan gum content is identified, showcasing a remarkable increase in anti-compression effects by 59.83%-76.05%. Moving to compression properties, the study highlights that, after 28 days of curing, the 1.5% xanthan gum-treated soil exhibits a maximum compression modulus of 33.14 MPa and a minimum compression coefficient of 0.03 MPa<sup>-1</sup>. The direct shear test results demonstrate a substantial enhancement in shear strength parameters. Under various vertical loads, the shear strength of the treated soil, particularly with 1.5% xanthan gum content, surpasses that of untreated red clay. The cohesion of the 2.0% treated soil increases by an impressive 69.79% compared to red clay, emphasizing the significant influence of xanthan gum content on cohesive

strength. Microscopic analysis using scanning electron microscope images further elucidates the microstructural changes induced by xanthan gum, showcasing the formation of gels and biopolymer matrices. This multiscale examination of red clay stabilization contributes foundational knowledge for optimizing xanthan gum dosages, enhancing our understanding of the intricate interplay between xanthan gum, curing ages, and the mechanical behaviour of red clay. These findings have profound implications for the development of sustainable soil stabilization techniques in geotechnical engineering.

In the seminal work conducted by Hamza et al. (2022), the investigation into the geotechnical implications of integrating Xanthan Gum (XG) as a soil stabilizer in subgrade construction yielded comprehensive insights into diverse aspects of soil behaviour. The study's breadth extended from examining compaction properties to elucidating microstructural alterations, presenting a nuanced understanding of the material's response to XG treatment. Noteworthy findings emerged from the modified compaction curves, revealing the flexible nature of XG-treated soil and its capacity to attain desired density over a wide moisture content range. The reduction in Maximum Dry Density (MDD) by 9.1%, coupled with a 20.3% increase in Optimum Moisture Content (OMC) at 5% XG content, showcased a balance in achieving field-appropriate densities. Crucially, the treated samples adhered to the permissible dry density requirements for subgrade construction, highlighting the pragmatic application of XG in optimizing soil compaction. Moving beyond compaction, the study delved into shear strength properties, demonstrating a substantial enhancement with higher XG dosages and prolonged ageing periods. The introduction of predictive models underscored the correlation between XG content, ageing time, and soil strength parameters, establishing 1.5% XG content as optimal for transforming subgrade soil from a medium to hard quality. The substantial improvements in California Bearing Ratio (CBR) values, reaching 6–9 times at optimal XG content, positioned the soil as a hard-quality subgrade, accentuating the material's potential for robust load-bearing capacities. Moreover, the study addressed swell-consolidation properties, revealing a transformative impact on consolidation parameters, swell potential, and swell pressure. Reductions of 83% and 82% in compression and rebound indices, respectively, with optimal 1.5% XG content, signified enhanced soil stiffness over time. The microstructural studies, employing Scanning Electron Microscopy (SEM),

visually validated the development of hydrogels and crosslinked elements within the soil matrix, elucidating the mechanisms behind the observed improvements in strength, compressibility, and swelling behaviour. In conclusion, Hamza et al.'s comprehensive study positions XG as a highly effective soil stabilizer, offering sustainable and cost-effective solutions for subgrade construction challenges, with implications reaching beyond numerical results to encompass predictive models and microstructural elucidation, contributing significantly to the evolving field of geotechnical engineering.

The paper under consideration provides a comprehensive literature review on the utilization of Xanthan Gum (XG) biopolymer in road pavement subgrade construction, as investigated by Cabalar et al. (2023). This study contributes to the broader field of soil stabilization, aligning with previous research endeavours aimed at enhancing the mechanical properties of weak subgrade soils. The authors acknowledge the foundational work conducted by Cabalar et al. (2023), wherein the geotechnical implications of incorporating XG as a soil stabilizer were thoroughly explored. Building upon this seminal research, the paper systematically reviews various facets of soil behaviour, ranging from compaction properties to microstructural changes induced by XG. The alteration of compaction curves highlights the flexible nature of XG-treated soil, ensuring optimal density across diverse moisture content levels. Noteworthy numerical results include a 9.1% reduction in Maximum Dry Density (MDD) and a 20.3% increase in Optimum Moisture Content (OMC) with a 5% XG content. The examination of shear strength properties reveals a significant enhancement, even at lower XG dosages, with the introduction of predictive models demonstrating correlations between XG content, ageing time, and soil behaviour. The application of 1.5% XG content transforms the subgrade soil into a hard quality, surpassing minimum requirements. Further analyses showcase substantial improvements in California Bearing Ratio (CBR) values, underscoring the cost-effectiveness and sustainability of XG-treated soil in subgrade construction. Swell-consolidation properties are also scrutinized, indicating notable reductions with optimal XG content. Microstructural studies through Scanning Electron Microscopy (SEM) visually validate the development of hydrogels and crosslinked elements within the soil matrix. In conclusion, this literature review emphasizes the efficacy of XG as a soil stabilizer, offering valuable insights into sustainable and cost-effective subgrade

construction. The inclusion of numerical results, predictive models, and microstructural observations enhances the understanding and implementation of XG to address challenges associated with weak subgrade soils. Recommendations for future studies include exploring XG's performance under additional environmental vulnerabilities, coupled with field studies and cost analyses for practical applications in the construction industry.

The study conducted by Dehghan et al. (2019) explores the application of xanthan gum and guar gum, two types of biopolymers, as environmentally friendly additives for the stabilization of collapsible soils. The investigation encompasses a comprehensive set of laboratory experiments, including compaction, consolidation, permeability, and unconsolidated-undrained triaxial tests, aiming to quantify the impact of these biopolymers on various engineering properties. In terms of compaction, the results reveal that the addition of xanthan gum and guar gum leads to a reduction in the maximum dry density, with values decreasing from 18.83 kN/m<sup>3</sup> to 17.55 kN/m<sup>3</sup> for 2% xanthan gum and 17.65 kN/m<sup>3</sup> for 2% guar gum. The optimum moisture content increases from 13.2% to 17.2% for 2% xanthan gum and 16.1% for 2% for guar gum. Permeability tests illustrate a significant reduction in permeability due to the addition of biopolymers, with a decrease of 18.6% for 0.5% xanthan gum and 88% for 0.5% guar gum. The study also explores the stress–strain behaviour, demonstrating a substantial increase in maximum soil strength from 228.7 kPa for natural soil to 550 kPa for soil modified with 2% xanthan gum. Additionally, scanning electron microscopy (SEM) results provide visual evidence of the direct interaction between xanthan gum particles and soil particles, highlighting the bonding mechanisms contributing to improved soil strength. Overall, the findings from Dehghan et al. (2019) underscore the potential of xanthan gum and guar gum as effective additives in enhancing the engineering properties of collapsible soils, offering a sustainable alternative in geotechnical applications.

Numerous investigations have been conducted to explore the utilization of xanthan gum biopolymers in the modification of geotechnical properties across various soil types, encompassing sand, clays with varying plasticity levels, silty clays, silts, and silty sands. In the subsequent sections, the studies in question have been duly referenced, signifying their inclusion in the scholarly discourse. However, it is

imperative to note that a comprehensive examination of each study has been intentionally deferred within the confines of this section. The purpose of this deferment is to prioritize a nuanced and in-depth analysis of pertinent themes and findings, ensuring a more detailed exploration in subsequent sections of the discourse (Ayeldeen et al., 2017; Biju & Arnepalli, 2020; Cabalar & Canakci, 2011; Sojeong Lee et al., 2019; Soldo et al., 2020).



## **CHAPTER 3**

### **MATERIALS AND EXPERIMENTAL METHODOLOGY**

#### **3.1 Introduction**

This section provides a detailed exploration of the mechanical and physical characteristics of the materials incorporated in all mixtures, emphasizing a comprehensive analysis through laboratory experiments. The preparation of specimens strictly adheres to the standards set by the American Society Testing and Materials (ASTM) and the British Standards (BS). Specifically, reclaimed asphalt pavement (RAP) is utilized as an aggregate, while xanthan gum assumes a dual role as a binder and stabilizer for clay soil within the examined mixtures. The experimental phase encompasses a suite of laboratory tests meticulously conducted in accordance with both ASTM and BS standards. These tests include the Atterberg limit test, fall cone penetration test, compaction test, specific gravity test, vane shear test, unconfined compression test, one-dimensional consolidation test, California bearing capacity test, and direct shear test. Each test contributes to a comprehensive understanding of the mechanical and physical attributes of the mixtures, as delineated in Table 3.1. The decision to utilize 10% reclaimed asphalt pavement (RAP) in the study was influenced by the findings of Al Yahya Bag's (2018) doctoral dissertation, which identified this concentration as optimal for enhancing geotechnical properties. Concurrently, studies by Chang (2015), Latifi (2016), and Cabalar (2018) underscored the effectiveness of xanthan gum (XG) within the concentration range of 1% to 3%. In order to harness the benefits of both materials while minimizing their proportions, we opted for the lower end of the effective range for XG, employing concentrations of 0.5%, 1%, and 3%. This strategic selection aligns with the goal of maximizing the impact of RAP at its identified optimal concentration while ensuring the efficacy of XG within a range that balances effectiveness and economy. The commitment to precision is underscored by the rigorous adherence to established standards, ensuring the robustness and reliability of the research methodology. The inclusion of diverse experiments offers a nuanced perspective on the materials under investigation, enhancing the scholarly rigour and clarity of the study.

**Table 3.1** Description of samples

Materials	Silty Sand (SM) (%)	Reclaimed Asphalt Pavement (RAP) (%)	Xanthan Gum (XG) (%)
Control Soil	100	0	0
90% SM+10% RAP	90	10	0
89.5% SM+10% RAP+0.5% XG	89.5	10	0.5
89% SM+10% RAP+1% XG	89	10	1
87% SM+10% RAP+3% XG	87	10	3

## 3.2 Materials

In this part of the thesis, materials used during the experimental program—the soil and two additives—were examined, and certain physical and chemical properties of these materials were detailed.

### 3.2.1 Soil

Natural soil obtained from the Gaziantep University campus in Gaziantep province will be used in the experiment. The collected sample contains a large amount of brown to red soil, which seems like cotton soil that is very fertile for agricultural use in the southeast of Turkey, but it is quite unsuitable for construction purposes since it has low bearing capacity and high compressibility (Mohammed & Alhassan, 2018; Wang et al., 2021). The light brown soil was gathered with its natural water content as shown in Figure 3.1 below and the scanning electron microscope (SEM) images presented in Fig. 3.6(a). The liquid limit (LL) and plastic limit of soil were determined as 31.36 and 23.25, respectively, as listed in Table 3.2 by performing the Atterberg limit test according to ASTM D4318 (2017), and the soil material was classified by the sieve analysis test by following ASTM D2487 (2017), as the gradation curve of soil is shown in Figure 3.2, Silty Sand (SM), according to the Unified Soil Classification System (USCS).



**Figure 3.1.** The soil material used in experiments

**Table 3.2** Several characteristics of the soil utilized in the experiments

Parameter	Unit	Value
Natural water content, $w_n$	%	16.4
The plastic limit, PL	%	23.25
Liquid limit, LL	%	31.36
Specific gravity, $G_s$		2.68

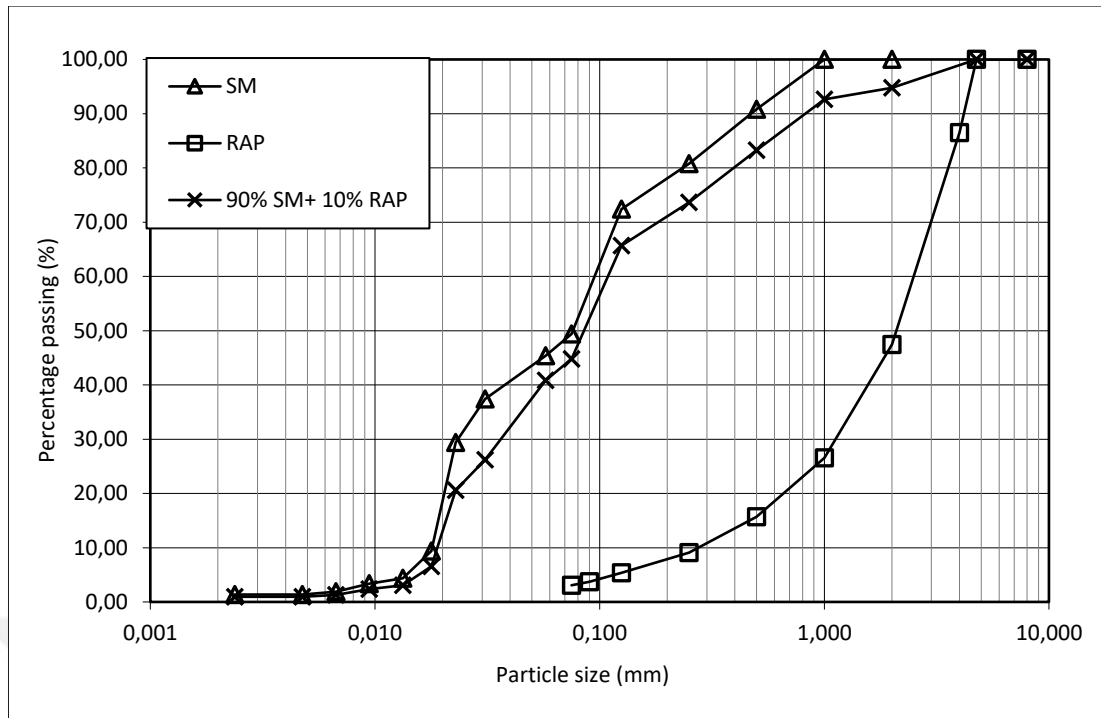


**Figure 3.2.** Particle size distribution of the silty sand, reclaimed asphalt pavement and 90% silty sand-10% reclaimed asphalt pavement

### 3.2.2 Reclaimed Asphalt Pavement

A recycled well-graded sand with gravel (SW) according to ASTM D2487 (2017) was used during laboratory experiments. The reclaimed asphalt pavement (RAP) is a disposal material for an out-of-service road, and it was provided by the municipality. The RAP contains aggregates covered with bitumen and has various shapes that, as shown in Fig. 3.3, provide different properties like strength, porosity, and durability against dragging, freezing, and thawing, and Fig. 3.5(b) shows the SEM images of the RAP.



**Figure 3.3.** The reclaimed asphalt pavement (RAP) used during experiments

### **3.2.3 Xanthan Gum**

In the context of this study, a polymer derived from *Xanthomonas campestris*, specifically xanthan gum (C107H158O90K5), is utilized in its powdered form throughout the experimental program. The visual representation of Xanthan gum is elucidated in Fig. 3.4, with a corresponding scanning electron microscope (SEM) image provided in Fig. 3.5(c). Xanthan gum, a versatile polymer, serves multiple functions within various industries. Primarily, it functions as an emulsion stabilizer and a heat stabilizer. Additionally, it assumes the role of a water-based suspension thickener, functions as a hydrophilic colloid, and contributes to viscosity stabilization, particularly within the food industry. The dual presentation of Xanthan gum through a graphical depiction and a microscopic image enhances the clarity and visual understanding of the material's appearance, a key aspect in comprehending its potential applications and contributions within the experimental framework. (Garcia-Ochoa et al., 2000; Bouazza et al., 2009).

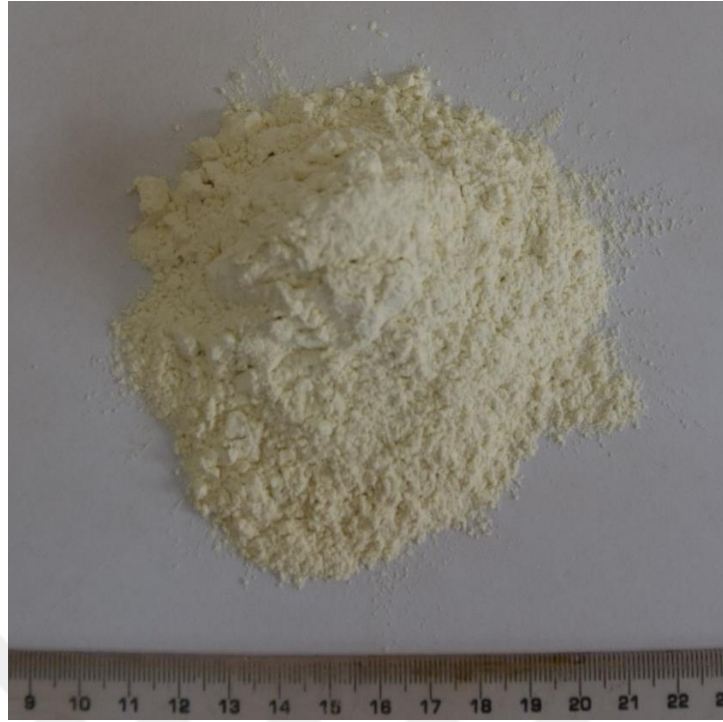
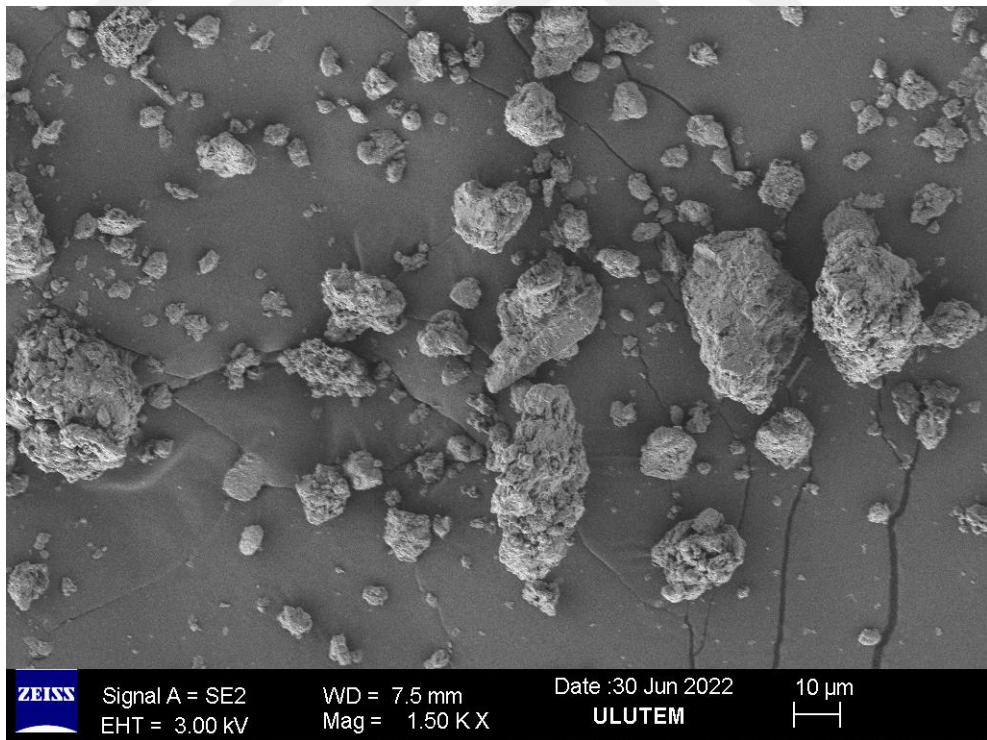
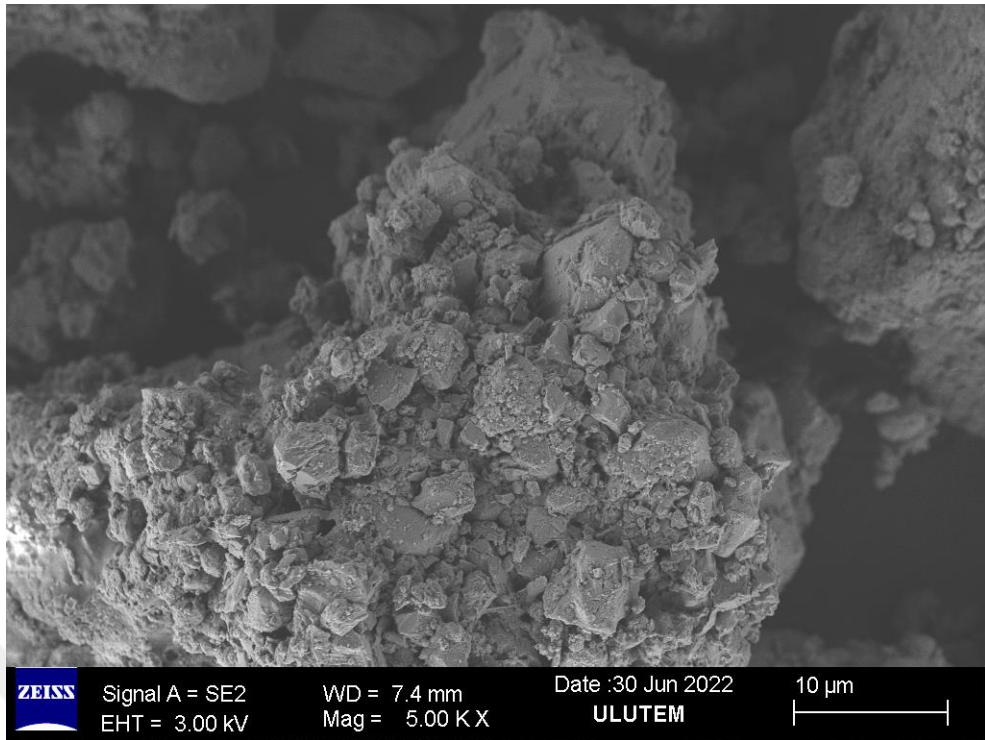


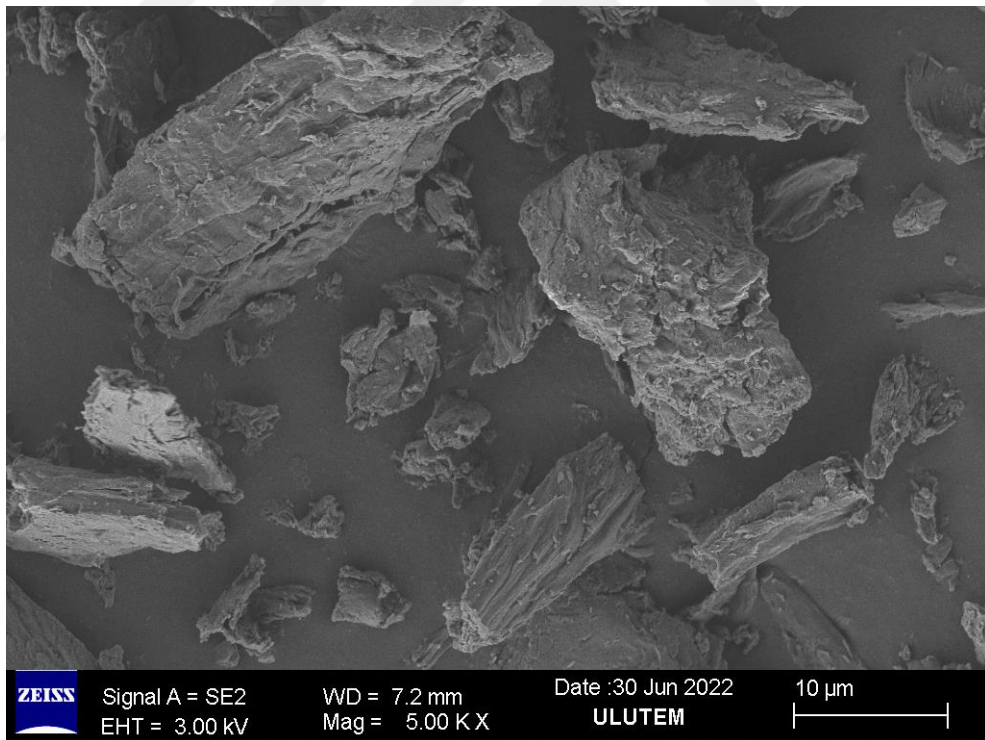
**Figure 3.4.** Xanthan gum utilized in the experiments



(a)



(b)



(c)

**Figure 3.5.** Scanning Electron Microscope images of (a) SM, (b) RAP, and (c) XG

### **3.3 Sample Preparation**

During the experimental program, each test has its own preparation process according to related standards (ASTM, BS, and TS). The soil is sieved from sieve No. 18 (1 mm) (sieved from a smaller sieve for some tests like the fall cone test, which will be detailed in the 3.4 Experimental Methodology section) to ensure homogeneity and prevent the entrance of extraneous materials. The sieved soil was left in the laboratory for 24 hours to be able to obtain 100% dry soil, each time used for a test, and it was mixed with RAP, which was sieved from No. 4 (4.76 mm) and dried xanthan gum in specific proportions as shown in Table 3.1. Following the blending of ingredients, the resultant mixtures are placed in isolated bags or containers to ensure uniform moisture distribution in the samples.

### **3.4 Experimental Methodology**

The process for each test, including some specific arrangements by following related standards, will be presented in this section.

#### **3.4.1 Atterberg' Limit tests**

The testing program began with the Atterberg limit test to determine the consistency properties of untreated and treated soil, such as the liquid limit and plastic limit. A Casagrande apparatus, as shown in Figure 3.6, was used for the liquid limit test, and the thread rolling method was used for the plastic limit according to ASTM standards (ASTM-D4318, 2017). The material used during the test is sieved from sieve No. 40 (0.425 mm). The dried sample (24 hours at 105°) is mixed with a pre-determined water content until it forms a homogenous mixture, and then the prepared sample is placed into a half-globe-shaped cup of apparatus. The top of the cup is trimmed, and the sample is splinted with a grooving tool into two equal parts. The space between the two parts must be 13 mm, which is called the groove. After that, start rotating the handle at a constant speed of 2 revolutions per second until the groove is closed. At that point, the number of revolutions is recorded. The same process is repeated for various water contents, and the water content for which 25 exact rotations are obtained is the liquid limit, but if 25 rotations cannot be hit, the liquid limit can be calculated from the plotted number of blows versus the water content graph.

For the plastic limit, the thread rolling method is simply rolling the sample on a clean, smooth surface until it has a thickness of 3 mm. Generally, it is not easy to match the 3 mm thickness. For that reason, to be able to plot a curve of thickness versus water content, the test is repeated five times for each specimen.



**Figure 3.6.** Casagrande Device

### **3.4.2 Standard Compaction Test**

A laboratory compaction test is conducted to obtain information on the soil's compressibility characteristics. Mainly, the soil is pressed with a specific amount of energy to evacuate air from the soil at different water contents, which gives the maximum compressibility of the soil according to the water content to be applied in the real case (Proctor, 1933). By following the related ASTM standard (ASTM-D698, 2012), a 4 in. (101.60 mm) diameter mold with a 4.584 in. (116.43 mm) and 5.50 lbf (2.495 kg) hammer, as shown in Figure 3.7, was used in the experiment. The prepared moisturized sample is filled into the mold, which corresponds to one-third of the mold. The hammer is released from a 12-inch (304.8 mm) height as free-fall, and after 4 strokes are made to the cardinal points, other strokes are made in a clockwise or opposite direction. A total of 25 strokes are made for each layer to achieve the suggested (12 400 ft-lbf/ft<sup>3</sup> or 600 kN-m/m<sup>3</sup>) energy level by a related standard, and

the process is repeated three times for each specimen to minimize the error margin. Later, the top of the mold is trimmed, the mass is measured, and since the initial mass and volume of the mold are known, the mass of the compacted wet specimen can be determined. A small sample is taken from a compacted wet specimen to measure the exact water content of the specimen. After completing all testing processes, the dry unit weight of the sample can be calculated using the formula below.

$$\gamma_d * \frac{\gamma_m}{1 + \left(\frac{WC}{100}\right)} \quad (3.1)$$



**Figure 3.7.** Standard Compaction Test Apparatus

### 3.4.3 Fall Cone Test

The falling cone test, as is evident from its name, is an experiment developed to determine the undrained shear strength,  $S_u$  value, of the sample by releasing a cone to fall freely from a certain height to the sample. This experiment was performed by following the British standard (BSI, 1990). The device used during the experiment is presented in Fig. 3.8. The sample prepared with a soil sieve from No. 40 (0.475 mm) is carefully placed into a container with a 50 mm diameter and a 40 mm height without applying any compression, ensuring that there is no major space in the container as

well. The edge of a 0.785 N weight cone with a 30° angle is placed on top of the container, barely touching the surface of the sample. After all the adjustments are done, the cone is released, and after counting for 5 seconds, the difference in the gauge is recorded. This process is repeated three times for each water content, and the average of the gauge reading is taken as the final displacement in the height. The test is carried out for each sample for different water contents, and by applying the formula that was given below, the undrained shear strength ( $S_u$ ) of specimens at each water content is calculated.

$$S_u = k * \frac{m * g}{d^2} \quad (3.2)$$



**Figure 3.8.** Fall Cone Test Device

#### **3.4.4 Vane Shear Test**

A laboratory vane shear test is carried out in this study to evaluate the undrained shear strength ( $S_u$ ) of specimens, to compare them with the fall cone test, and to increase their accuracy. In this test, like the fall cone test, a container with a 50-mm diameter

and 50-mm height is filled with a moisture sample and placed into the device shown in Fig. 3.9. Then, the vane blade that has an H=2D ratio of 0.5 in (12.7 mm) is submerged into the sample by 1.5 times the height of the vane blade as recommended by ASTM standard (ASTM-D4648/D4648M, 2016) without disturbing the specimen. The reading gauge is set to zero, and the vane is started to rotate at a rotation rate of 60°/min. After a while, the reading at the gauge stops changing, which means the expected failure happened. Again, this is repeated three times for the same sample, and the average reading is taken as the final gauge reading. The required formula to calculate the undrained shear strength from the vane shear test is shown below:

$$\tau = \frac{K}{T} \quad (3.3)$$



**Figure 3.9.** Device used in the Laboratory Vane Shear Test

### 3.4.5 Unconfined Compressive Strength Test

Compressive strength is a very essential parameter of the ground that describes the resistance potential of soils against axial loading in geotechnical applications. Therefore, a series of unconfined compression tests (UCS) were performed on all specimens at various curing periods (0, 7, 28, and 56 days) according to ASTM standards (ASTM-D2166, 2017). The sample preparation method is critical for UCS because, in this process, preparing the sample slightly drier or wetter and compacting it with a little more energy than necessary will seriously affect the test results. The fully dried SM, RAP, and XG are mixed together at predetermined amounts according to the standard compaction test, and then the process continues with adding water and mixing until they become homogenous. For compacting, the modified compaction apparatus shown in Figure 3.10 is used. This modification was made by Cabalar et al. (2014) by regulating the weight of the hammer, volume of the mould, strike number, and number of layers to match the standard compaction energy when preparing UCS specimens. For 5 layers, with 31 strikes at each layer, the mixture is compacted into a cylindrical mould with a 45 mm diameter and 90 mm height. After compaction, the specimens were placed in a room for different air-open curing periods (7, 28, and 56 days), like in Figure 3.11, or tested immediately.



**Figure 3.10.** Modified Compaction Apparatus of UCS



**Figure 3.11.** Cured Specimens of UCS

The testing procedure begins with placing the specimen between the compression plates of the device. In this study, a fully automated triaxial device is used, as shown in Figure 3.12. After completing the measurement, settings of the device, and placements, the specimen is subjected to compression stress at a constant speed, which was determined to be 0.25 mm/sec for this study, and the change in strength and displacement is recorded concurrently. In general, if the specimen is brittle after reaching the peak, cracking occurs (see Figure 3.13(a)), and after the breaking point, the strength starts to reduce. However, if the material is ductile, the peak point of the strength is not seen clearly (Figure 3.13(b)). At this stage, it is recommended to continue the test until the displacement reaches 10 mm according to the related

standard. The test is finished after taking data like axial force and axial displacement from the software of the testing device.



**Figure 3.12.** The unconfined compression testing device



(a)



(b)

**Figure 3.13.** (a) brittle specimen (b) ductile specimen after the test

### 3.4.6 Consolidation Test

Fine-grained soils are susceptible to consolidation behaviour, and adding xanthan gum has been proven to increase their compressibility in past studies (Kwon et al., 2019). Therefore, performing a consolidation test was decided to be necessary in this study. One-dimensional oedometer tests were conducted on mixtures of silty soil (SM), reclaimed asphalt pavement (RAP), and different percentages (0.5, 1, and 3%) of xanthan gum (XG) by using a manual oedometer testing device shown in Figure 3.14. The sample preparation and testing procedures were based on related ASTM standards (ASTM-D2435, 2011). The day before, the amount of dry material was calculated according to the maximum dry density obtained from the standard compression test and mixed with the optimum water content. With the help of a compression machine, the mixture was compacted homogeneously into a cylindrical piece with a diameter of 50 mm and a height of 20 mm called a ring (Figure 3.15). A piece of filter paper and a porous material that will allow the passage of water but prevent the passage of the material is placed on both sides of the ring, and then this prepared structure is placed in the consolidation cell, and to distribute the load equally, a load pad is placed on it.

Next, the consolidation cell is placed into the oedometer device, and water is added until the cell is fully saturated. To measure the displacement, the manual gauge is set, and the test process is started. First of all, the sample is kept in water for 24 hours in order to remove small-scale swellings that may cause errors in the calculations, and then the gauge is reset and loading is started. Initially, loadings are started to correspond to 25 kPa pressure, and readings are made at regular intervals after loading. The same process is continued by doubling the load every 24 hours, and the cell is kept saturated. When it reaches 800 kPa, the device is unloaded in the same way, each time half of the previous one, and the readings are recorded. After the experiment is over, the weight of the parts inside the cell is measured again to find the final water content.



**Figure 3.14.** Oedometer device



**Figure 3.15.** One-dimensional consolidation testing apparatus

### **3.4.7 California Bearing Ratio (CBR) Test**

Soil stabilization has many applications, and in geotechnical projects, road construction is one of the first things that comes to mind. Bearing capacity is a key parameter in road construction, so to determine the effect of RAP and XG on SM on bearing capacity, a California bearing ratio test was conducted in this presented study. The ASTM standard (ASTM-D1883, 2010) is used as a guideline during the testing program, which starts with preparing the specimen. Recommended compaction by the standard is applying energy advised (56000 ft-lbf/ft<sup>3</sup> (2700 kN-m/m<sup>3</sup>) in ASTM-D1557 (2012) on mixtures prepared with optimum water content and maximum dry density to compact the mixture into a mould with a 6 in. (152.4 mm) diameter and a height of 7 in. (177.8 mm) by a 10.0 lbf (44.48 kN) rammer dropped from a height of 18 in. (457.2 mm) 56 times for 5 layers (Figure 3.16). The first step of the compaction process is measuring the initial width of the mould with an extension collar, then placing a spacer disk with a 150.8 mm outside diameter and 61.37 mm height, and the mixture is compacted as explained before. After compaction, the extension collar is removed, and the surface of the sample is trimmed to obtain a smooth surface area. Then, the spacer disk is removed, and a filter paper with the shape of compacted material is placed on both the bottom and top of the sample since the material has a consistent amount of fine-grained particles. An adjustable stem plate is placed at the very bottom of the mould and the top of the filter paper. Lastly, two metal weights

with a mass of 4.54 kg each are placed on top of the sample, and a dial gauge is placed to measure the expansion or compaction. Generally, after all the preparation process is done, the sample is placed into a soaking tank and kept there for 96 hours, but for this particular study, an unsoaked version of the California bearing ratio (CBR) is decided to be conducted. The reason behind this idea is that soil like SM does not show significant durability against water. especially with XG, it is highly likely to over-expand and overflow out of weights, and additionally, it shows immeasurably low values based on my own experiences.



**Figure 3.16.** Compaction and sample preparation equipment for CBR test

The specimen is kept for 96 hours at constant room temperature, as shown in Figure 3.17. After the curing, the stem plate is removed, and the specimen is placed into an automated loading machine, as shown in Figure 3.18. After that, the sample is started to be loaded at a constant speed of 1.27 mm/min by a 1.954 in. (49.63 mm) diameter penetrant piston until the displacement passes 12.5 mm. Finally, the data collected by

the software is checked during and after the test for accuracy, and a sample is taken from the prepared specimen for the final water content.



**Figure 3.17.** The cured CBR specimen



**Figure 3.18.** CBR loading machine

### **3.4.8 Direct Shear Test**

Last but not least, the direct shear test, was conducted to understand the effect of RAP and XG on the shear behaviour of SM. This test is generally conducted by applying increasing lateral and constant perpendicular stress to a square sample to measure its resistance against shear. In this study, consolidated-drained (CC) direct shear tests were conducted by following ASTM standards (ASTM-D3080, 2012). The specimens for the direct shear test are prepared by compacting a certain amount of mixture of SM, RAP, and XG and specific water that was determined in the compaction test (ASTM-D698, 2012) into a 60- to 60-mm square frame. Then, the frame is placed in the shear box after placing solid plates and porous stones, and the shear box itself is placed into the shear device shown in Figure 3.19. The next step is completing all the required adjustments, such as controlling that the machine does not get stuck during

lateral movement, placing the horizontal load frame, and checking all the values in the software. Afterwards, the horizontal load is applied to consolidate the specimens; the period is determined by the machine to be 60 seconds. After short-term consolidation is completed, the horizontal loading starts at a displacement rate of 0.25 mm/min. At 10 mm displacement, the device stopped the tests automatically, and this process is repeated at 50, 100, and 150 kPa normal pressure for the same specimen. The displacement-shear strength is recorded automatically by the software at frequent intervals. Besides, shear strength at any instant can also be calculated manually using the formula below.

$$\tau = \frac{F}{A} \quad (3.4)$$

The main objective of the direct shear test is to evaluate the change in cohesion ( $c$ ) and internal friction angle with the addition of RAP and XG, or variation of curing time (0, 7, 28, and 56 days). These parameters can be determined by using the formula:

$$\tau = c + \sigma \tan (\phi) \quad (3.5)$$



**Figure 3.19.** Direct shear test device

## **CHAPTER 4 RESULTS AND DISCUSSION**

### **4.1 Introduction**

This chapter of the study presents the results of the experimental program conducted on reclaimed asphalt pavement and xanthan gum-added silty sand at different concentrations and various curing periods. This section also presents a comparison and discussion of the test results of this study and those of similar approved studies.

### **4.2 Atterberg' Limits**

The determination of basic physical properties like the liquid limit (LL) and plastic limit (PL) of SM is a priority at the beginning of the testing program. Therefore, a Casagrande device is used to conduct limit tests on clean SM and SM mixed with 10% RAP and various XG contents (0.5, 1, and 3%). However, it was observed that after adding RAP or XG, performing the test became difficult and began to affect the accuracy of the result since the bitumen-coated RAP particles disturbed the sample, and the addition of XG caused the sample to be too sticky to be grooved. For these reasons, the test was able to be conducted only on clean SM. The test was conducted on different water contents, and for each water content, the number of blows was recorded as shown in Figure 4.1. The equation of intersection points of the water content and number of blows is extracted, and the liquid limit was determined to be 31%, which is equal to the water content that corresponds to 20 blows. On the other hand, the plastic limit was determined to be 22% from the thread rolling test. It is obvious that these results alone do not make much sense, but they were added to this study to make a comparison with the fall cone test results in the next stage.

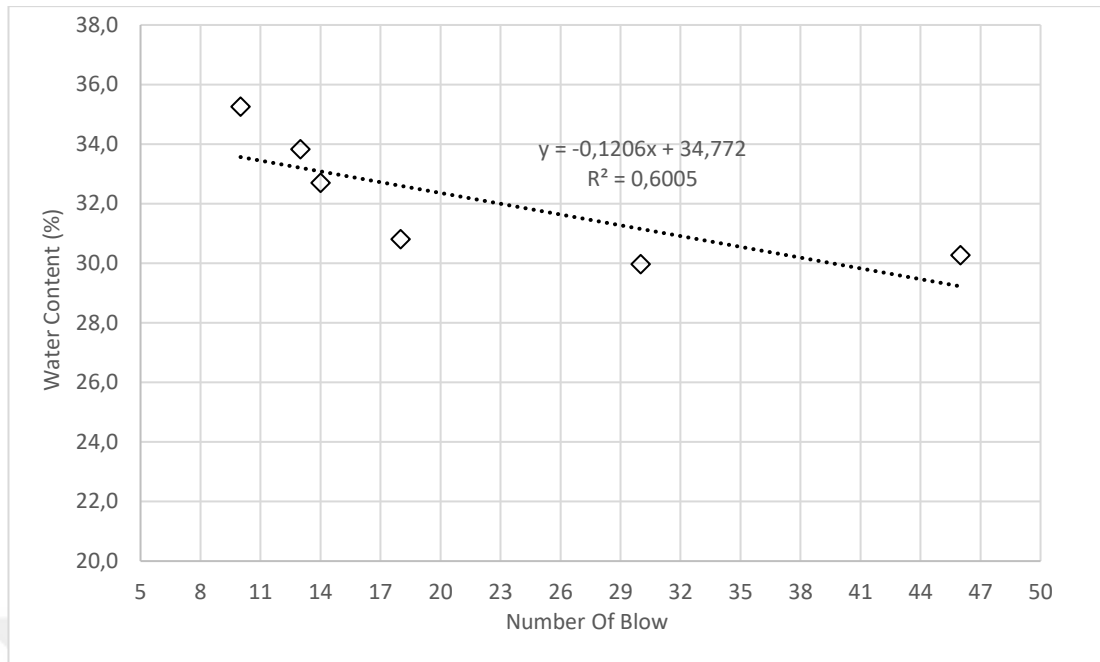


**Figure 4.1.** Liquid Limit (LL) of silty sand from Casagrande Test

### 4.3 Standard Compaction Test

As part of this study, silty sand, reclaimed asphalt pavement, and xanthan gum mixtures with varying content ratios were tested for their compressibility properties according to the ASTM-D698 (2012) standard. The summary of the maximum dry density (MDD) and optimum water content (OMC) for all the mixtures is presented in Table 4.1. The optimum water content decreased slightly with the addition of 10% RAP, and in what follows, the OMC increased more significantly with increasing XG content. The addition of 10% RAP reduced the OMC from 18.5% to 18%; afterwards, the existence of XG increased the OMC to 20%, 21.5%, and 23.5% for 0.5%, 1%, and 3% of XG, respectively. The fact that the linear increase in optimal water content was parallel to the amount of xanthan gum offered the idea that the reason for the increase was simply the water absorption of XG rather than chemical reactions. As it was found similarly in previous studies, the OMC increases and MDD decreases were attributed to several parameters of XG, such as low specific gravity and susceptibility to form high viscosity solutions that fill the pores of the soil, which causes a reduction in the weight of the compacted soil where the volume stays constant or increases, which

eventually decreases the MDD and increases the OMC by absorbing water (Chang et al., 2015; Dehghan et al., 2019; M. Hamza et al., 2022).

In the exact opposite case (except the RAP case) of OMC, a decrease was observed in the maximum dry density of the treated sample compared to non-treated silty sand. The maximum dry density decreased with the addition of both RAP and XG. The MDD of silty sand drops from 17.2 kN/m<sup>3</sup> to 16.4, 15.6, 15.1, and 14.2 kN/m<sup>3</sup> at 10% RAP, 0.5%, 1%, and 3% of XG, respectively. Considering its behaviour at optimal water content, it was expected that the maximum dry density would increase when RAP was added, but on the contrary, an increase was observed. The reason for this is that although RAP is sieved through a NO-4 sieve, it is still a coarse material compared to silty sand, so adding 10% relatively incompressible RAP changes the deformation characteristics of the soil as it reduces the amount of fine particles in the soil (M. Hamza et al., 2022). As shown in Figure 4.2, the standard compaction curve is obtained at the maximum dry density versus the optimum water content graph. The main function of water addition in compaction is that it reduces soil suction, resulting in an increase in dry density up to the optimum water content. As soon as the soil exceeds the water content that is optimum, excessive water causes pore air pressure by filling intergranular spaces and preventing air discharge. Therefore, it reduces the efficiency of the applied compaction energy and reduces the maximum dry density (Hilf, 1956). It has been observed that when xanthan gum is added, the clogging effect is increased since XG absorbs water and forms hydrogels that prevent the escape of air. Moreover, when looking at the graph, the first thing you might observe is that as the XG increases, the curve shifts to the right and down, while it shifts right and down at RAP. In addition, the wings of the curve were widened even further by the increased XG content. This refers to the water sensitivity of the soil, which means the soil becomes less sensitive to changes in water content.

**Table 4.1** Optimum water content and maximum dry density

Mix	OMC (%)	MDD (kN/m <sup>3</sup> )
100% SM	18,5	17,2
90% SM+10% RAP	18	16,4
89.5% SM+10% RAP+0.5% XG	20	15,6
89% SM+10% RAP+1% XG	21,5	15,1
87% SM+10% RAP+3% XG	23,5	14,2

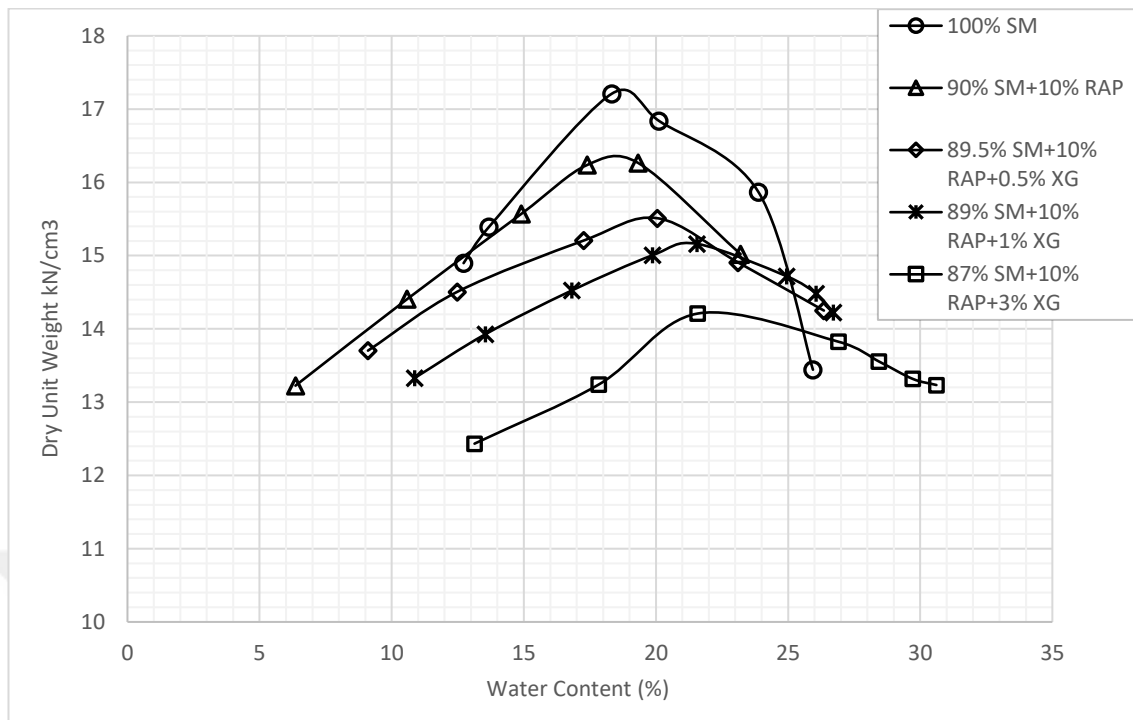


**Figure 4.2.** Compaction curve from the standard compaction test

#### 4.4 Fall Cone Test

The aim of the fall cone test is mainly to evaluate the undrained shear strength ( $s_u$ ) of the samples at various water contents. Besides that, the liquid limit and plastic limit can also be determined with this test. The liquid limit corresponds to a 20 mm penetration with a  $30^\circ$  - 80g cone (Wroth & Wood, 1978). Several studies have explored the determination of the plastic limit using the fall cone test, suggesting an average penetration corresponding to the plastic limit between 2-4 mm (Wasti & Bezirci, 1986; Campbell, 2006; Towner, 2006). In this study, the plastic limit was determined to be 2.5 mm, as within this range, no significant changes were observed (O'Kelly et al., 2017). Numerous studies have been conducted on or involving this test in the past (Kumar & Wood, 1999; Feng, 2000; Cabalar & Mustafa, 2015; Cabalar et al., 2020). Many tests have been conducted on mixtures of silty sand (SM), reclaimed asphalt pavement (RAP) (0, 10%), and xanthan gum (0, 0.5, 1, and 3%). And, when looking at the results shown in Figure 4.3, both the liquid limit and the plastic limit dropped significantly when 10% RAP was added to clean silty sand. The liquid limit decreased by 18% (31.4 to 25.5) and the plastic limit decreased by 66.7% (23.3 to 7.7)

compared to SM when 10% RAP was added. It was not so hard to explain this behaviour since adding non-plastic material at that percentage will reduce the water absorption of soil and cause a reduction in the plastic limit and liquid limit. It has been previously seen that adding a material with a coarse grain structure similar to sand to fine-grained soil reduces the liquid limit and the plastic limit (Cabalar et al., 2020). On the contrary, with the addition of fine-grained, high-absorption plastic, the biological material xanthan gum improved the liquid limit and plastic limit of soil. The liquid limit of the SM+RAP mixture increased from 25.5% to 37.3%, 45.5%, and 57.4% for 0.5%, 1%, and 3% XG, respectively. Additionally, the plastic limit increased from 7.7% to 8.8%, 12.5%, and 19.9% with the addition of 0.5%, 1%, and 3% XG, respectively. The increase in the liquid and plastic limits can be seen as the xanthan gum absorbing excess water and forming new intergranular forms (Kwon et al., 2019).

Moreover, the fall cone test results gave opinions on the change in the undrained shear strength of the soil before and after treatment. Substances such as xanthan gum generally reduce or increase the electrical attraction between the clay particles by changing the water flow between the pores, which indirectly affects the undrained shear strength (Chang et al., 2021). In this study, the effectiveness of RAP and XG at different percentages on the shear behaviour of the SM is evaluated by conducting a fall cone test several times. According to the Su-water content graph presented in Figure 4.4, the RAP addition worsened the Su of the SM; conversely, the XG gum enhanced the Su of the SM heavily. The Su values were determined as 0.881, 0.436, 3.822, 5.284, and 7.442 kPa for SM with 10% RAP, 0.5%, 1%, and 3% XG at a constant water content of 35%. The Su values increased from 0.436 to 7.442, which is more than 16 times with the addition of 3% of XG, and they reduced from 0.881 to 0.436 kPa by half when 10% RAP is added. This proves that the XG increases the favorable water content range for SM and enables it to achieve the same or higher shear strength at high water content, which is the worst case in applications. One of the reasons for this situation is that xanthan gum reacts with water to form hydrogel structures, and these structures fill the spaces between the soil particles and reduce the permeability. Another factor is that the forms play a binding role between the particles (Mendonca et al., 2021). However, unlike xanthan gum, RAP could not play either a binder or filler role in that it reduced the finer-high plasticity material content in the soil, which adversely affected the undrained shear strength of the soil.

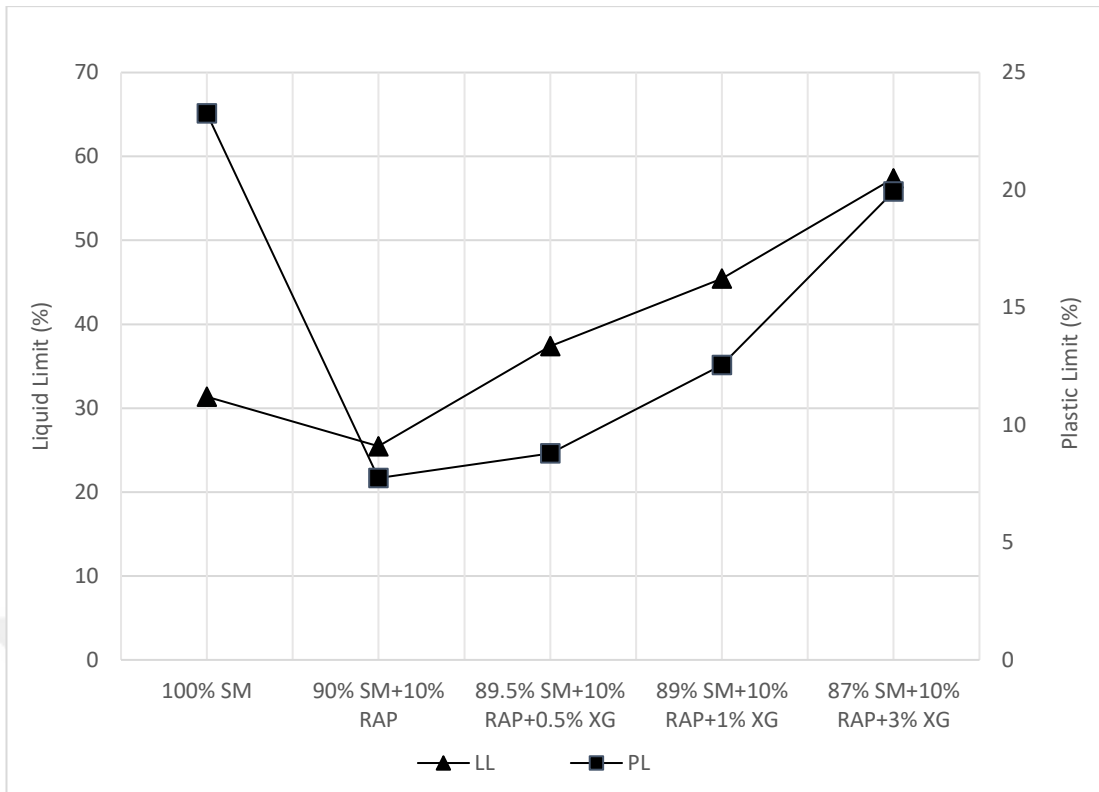


**Figure 4.3.** Liquid Limit (LL) and Plastic Limit (PL) from the fall cone test

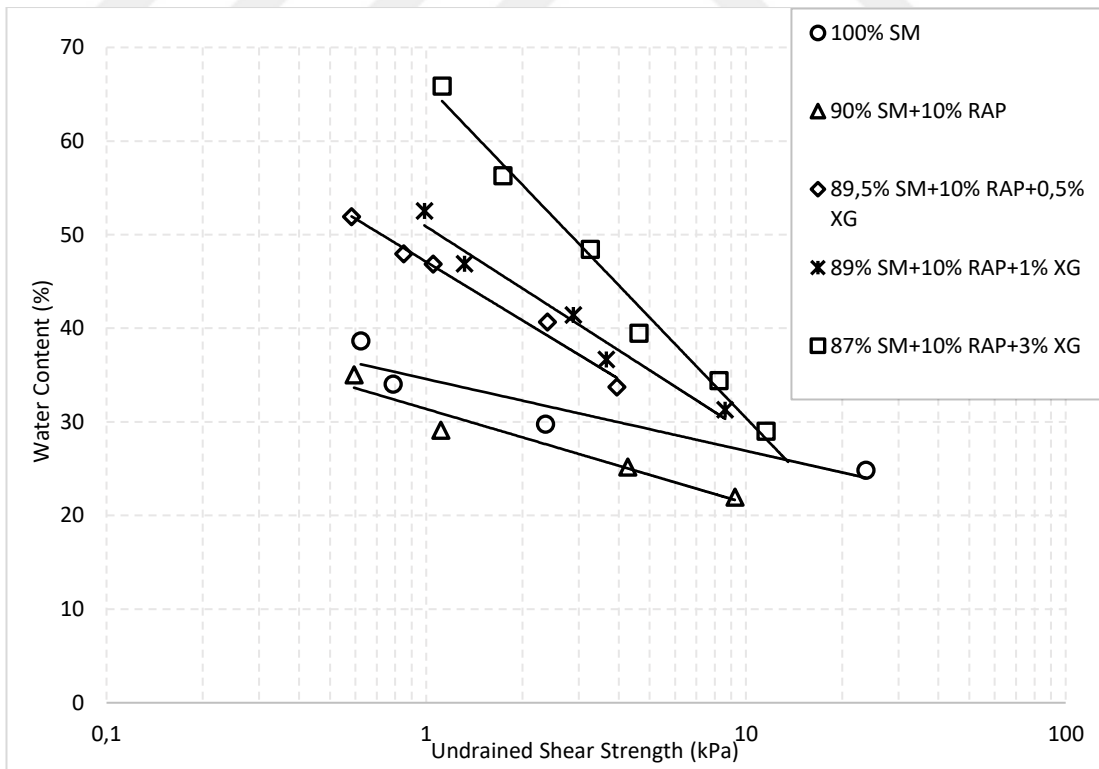


**Figure 4.4.** The water content versus undrained shear strength ( $S_u$ ) graph of the fall cone test

#### 4.5 Vane Shear Test

The undrained shear strength of the silty sand treated with RAP and XG and the silty sand without any treatment was evaluated by performing several vane shear tests in the laboratory. The  $S_u$  values were shown in Figure 4.5 depending on changing water content around the liquid limit for clean silty sand (SM), SM with RAP, SM + 10% RAP, and different XG concentrations (0.5, 1, and 3%). The first thing that catches the eye in the graph is the change in the water content corresponding to the same undrained shear strength for different additives and percentages; in other words, the undrained shear strength has changed significantly for different additives and percentages at the same water content. For example, if the 35% water content were taken as a comparison point, the undrained shear strength values would be respectively 3.538, 1.125, 10.428, 14.483, and 17.494 kPa for SM, SM and RAP, SM+RAP, and 0.5%, 1%, and 3% XG. Similarly, to the fall cone test results, the  $S_u$  value got worse with the addition of 10% RAP, and it showed improvement with increasing XG content. The fact that RAP reduces the shear strength of the soil by almost three times can be simply explained as the material has no shear strength and no plasticity (Hamidi et al., 2009). A noticeable improvement was achieved with the addition of XG biopolymer after the decrease in shear strength caused by RAP, due to the fact that XG interacts with water and forms a solution with high viscosity (Chang et al., 2021). XG solution fills the pores between the grains of the soil, acts as a binder, and increases the undrained shear strength of the silty sand, which has low viscosity and shear strength in interaction with water (Milas et al., 1985).

Furthermore, it can be seen from the graph that the line connecting the intersection points of water content and undrained shear strength becomes more horizontal when RAP is added, while it becomes more vertical as the amount of XG in the mixture increases compared to silty sand. This is another finding that demonstrates the effect of RAP and XG on the water susceptibility of silty sand. Moreover, in Figure 4.6, the comparison of undrained shear strength values gathered from the fall cone test and the

vane shear test was visualized with undrained shear strength versus water content. Contrary to the findings of Cabalar et al. (2018), despite the fact that the  $S_u$  from the vane shear test was higher than the  $S_u$  from the fall cone test, there is not a significant difference between the two. The correlation between  $S_u$  from the fall cone and vane shear test is presented in Figure 4.7 with the equations.

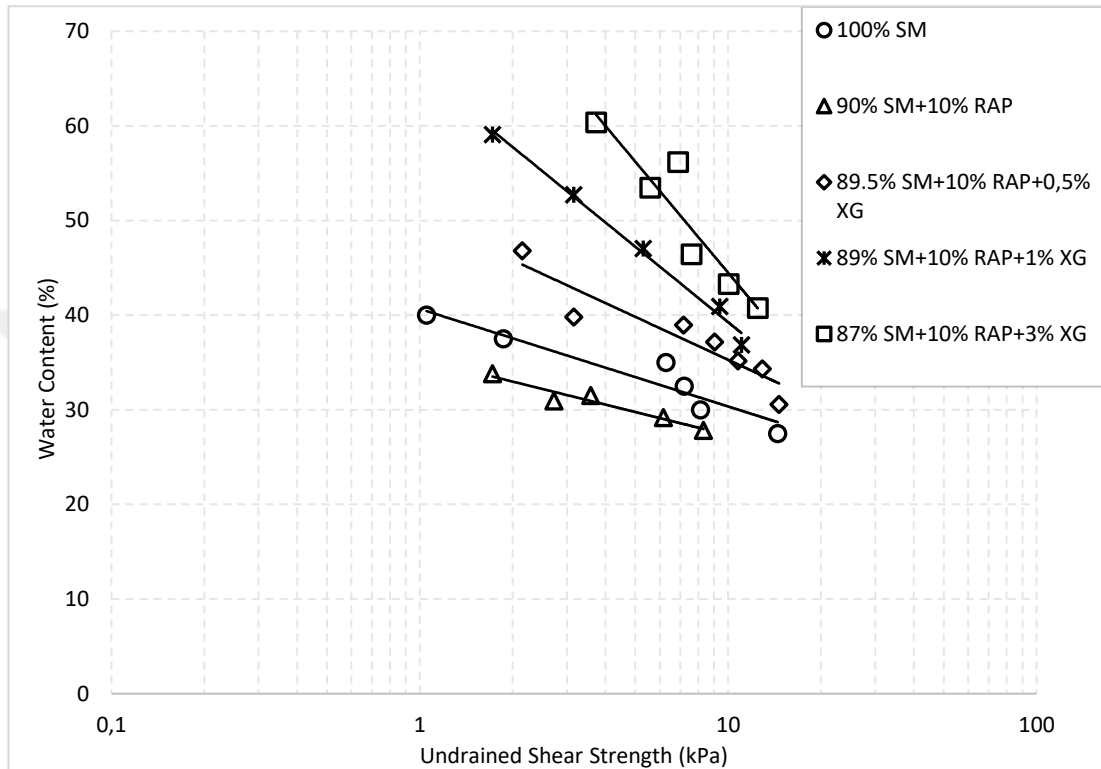


**Figure 4.5.** The water content versus  $S_u$  graph of the vane shear test

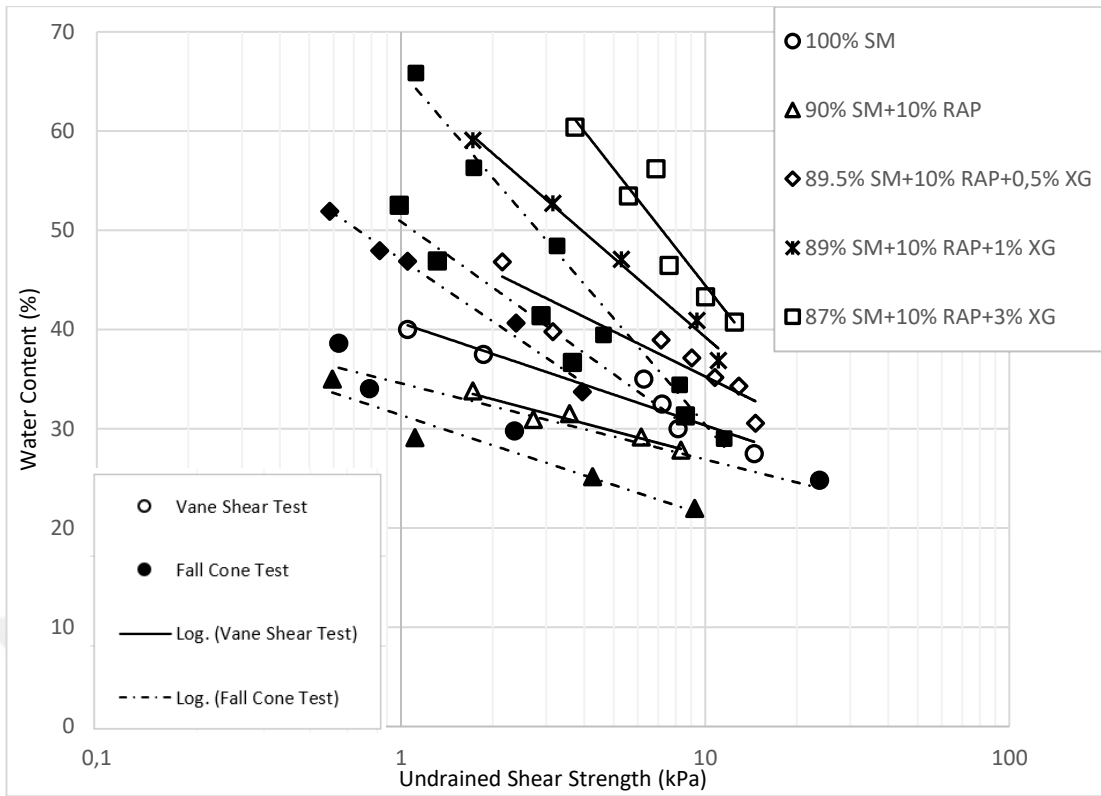


**Figure 4.6.** Comparison of the undrained shear strength of the fall cone and vane shear

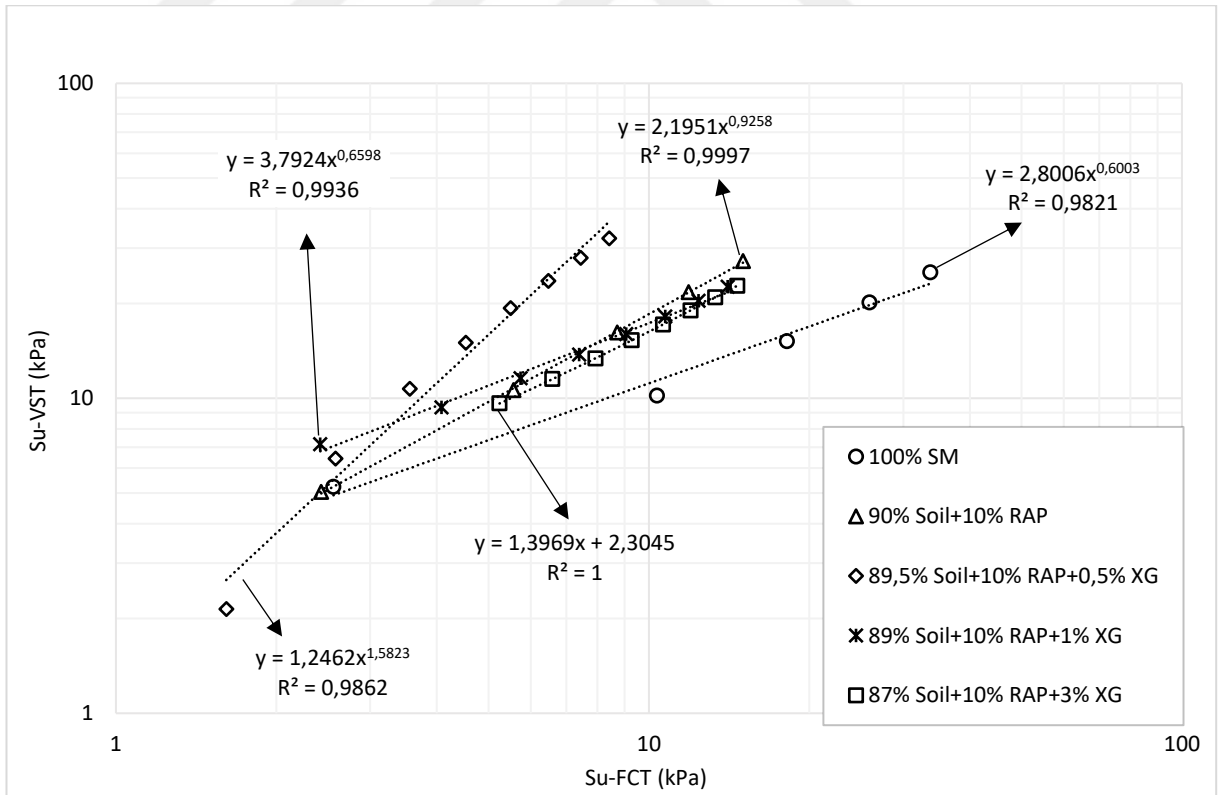
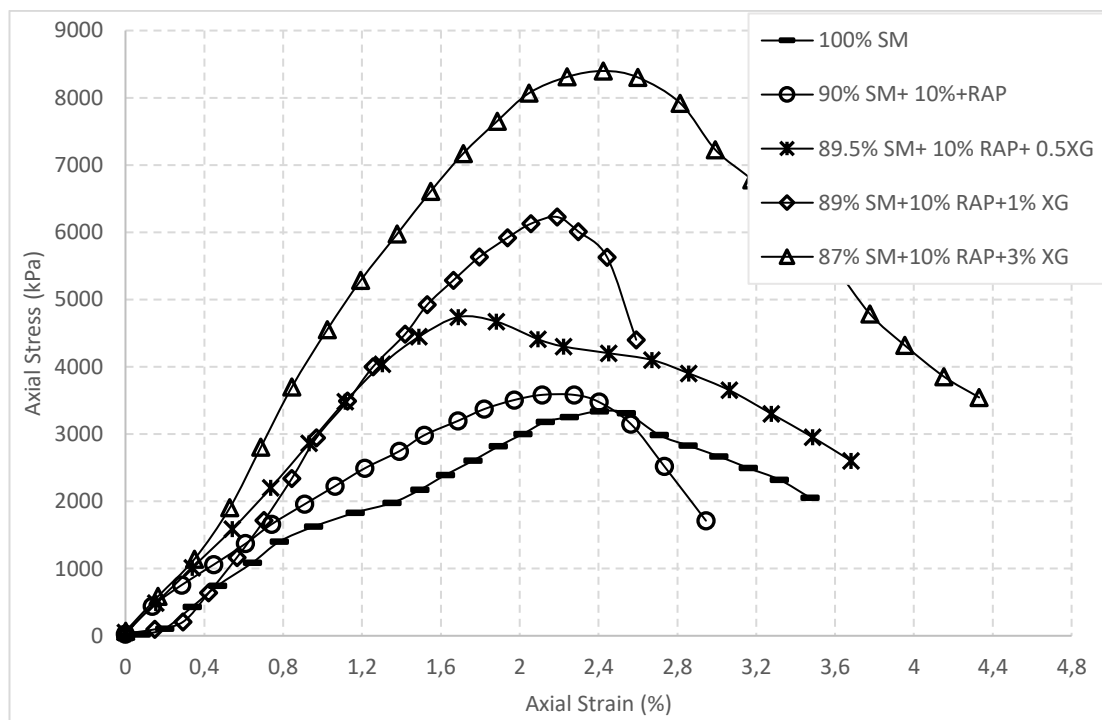


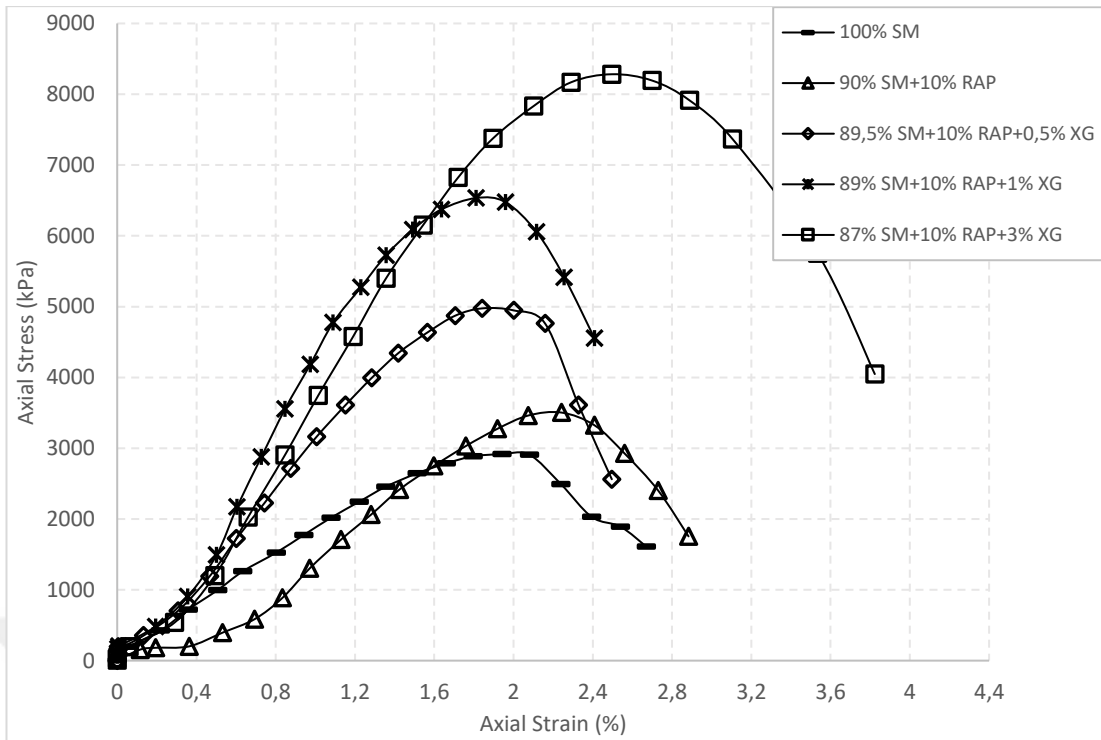
**Figure 4.7.** Correlation between undrained shear strength ( $S_u$ ) from Fall Cone Test (FCT) and Vane Shear Test (VST)

#### 4.6 Unconfined Compressive Strength Test

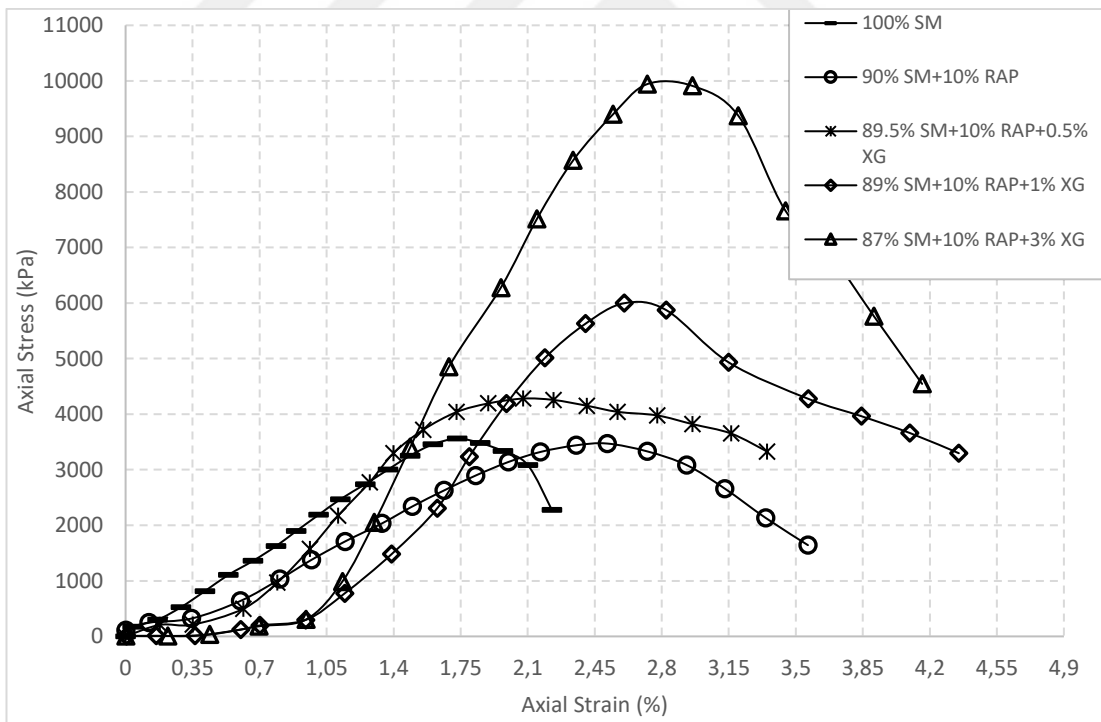
It was possible to determine the effect of reclaimed asphalt pavement and xanthan gum on the compressive strength behaviour of silty sand by performing unconfined compressive strength tests on all mixtures prepared at optimum water content and maximum dry density and exposed to various curing periods (0, 7, 28, and 56 days). Figure 4.8 illustrates a typical stress-strain graph of 7, 28 and 56-days-cured UCS specimens, the main observation being that strength against axial loading increases with the addition of RAP and with increasing XG concentrations. The addition of RAP caused a slight increment in compressive strength in cured specimens (7, 28, and 56 days), which is mainly due to the incompressible characteristic of RAP aggregates that have less void compared to untreated silty sand. When XG was added, the increase in axial stress compared to axial strain was even more noticeable. The axial stress values were increased gradually with increasing XG content in xanthan gum compared to non-treated soil and soil with RAP.



(a)



(b)



(c)

**Figure 4.8.** Stress-strain graph at (a) 7 days, (b) 28 days and (c) 56 days curing

Moreover, while the peak on the curves represents the maximum stress reached, most of the increment in peak stress was observed in the sample with 3% XG. The curing effect on soil strengthening is examined by conducting UCS tests on specimens cured at different time periods, and the results for 1% XG treated at 0, 7, 28, and 56-day curing times shown in Figure 4.9 demonstrate that the variable curing time can be very efficacious on the strength of the samples. The axial stress increased significantly up to 28 days of curing but decreased at 56 days. The compressive stress is measured at 181.7 and 6189.6 kPa for 0 and 7 days of curing, respectively, which shows a great increment nearly thirty-three times. The improvement in strength when the curing time increased was attributed to several reactions of fine particles of soil, xanthan gum, and water, such as cementitious products, hydrogen bonding between the carboxyl group (-COOH) and the hydroxyl (-OH) groups of xanthan, and fine-grained particles of silty sand (Latifi et al., 2016). At 28-day-cured specimens, the peak stress was measured at 6544.5 kPa, which is considered a minor increment compared to the 7-day-cured samples. This basically means that most of the strengthening process is completed in the first 7 days of curing. Additionally, besides the effect of the initial water content on strengthening, as studied by Ni et al. (2020), the presentation of the water during the testing process can be very effective. As a result, the stress values were reduced from 6544.5 kPa to 6040.7 kPa at 28 and 56 days, respectively, proves this claim and shows the 56-day open-air-cured specimens have less water content, which leads to a more brittle behaviour during loading.

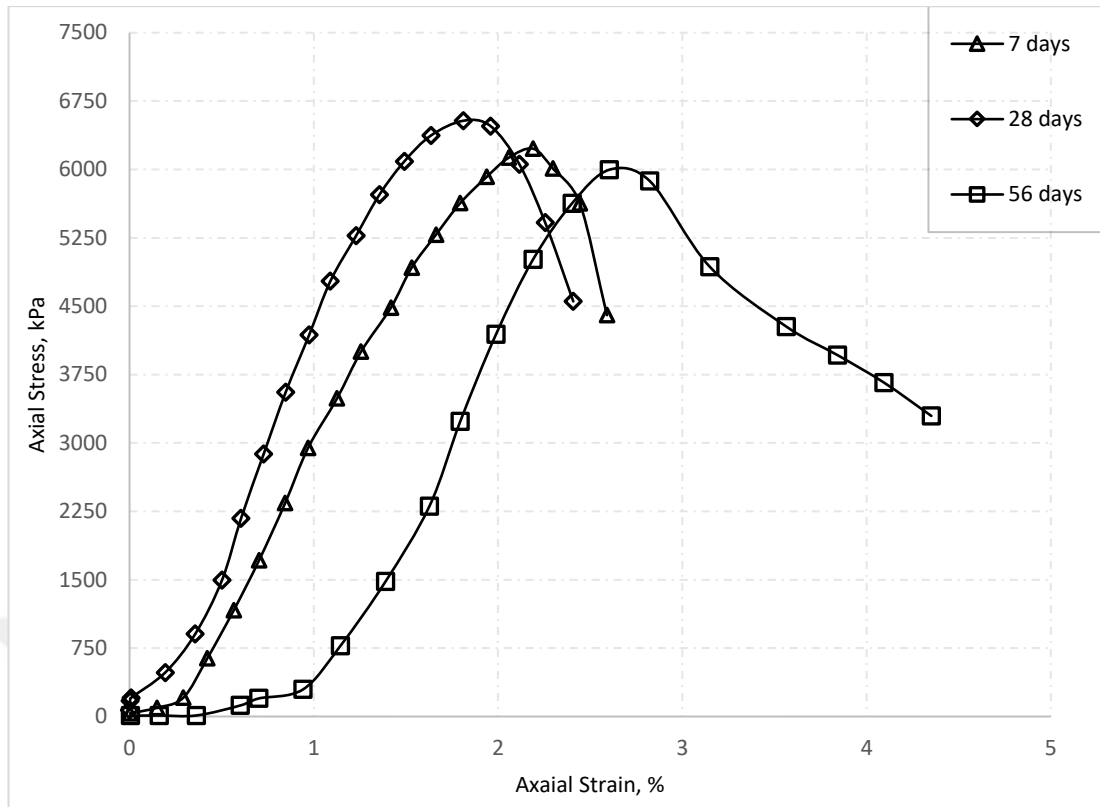


**Figure 4.9.** Stress-strain graph of a 1% XG-cured UCS sample at variable curing periods

Moreover, a summary of compressive strength outcomes concerning the influence of reclaimed asphalt pavement (RAP), variations in Xanthan gum (XG) concentration, and diverse curing periods is presented in Figure 4.10. In alignment with the findings of Chang et al. (2015), it is observed that an elevated XG ratio leads to a gradual augmentation in strength. Furthermore, the strength values exhibit a general increase with prolonged curing time. Additionally, the formation of hydrogels that coat coarse components such as sand particles and RAP particles is believed to be extremely effective in strengthening. Furthermore, electrostatic bonds between fine clay particles and XG monomers also contribute to the increase in strength. Based on Figure 4.11, the energy absorption levels are provided in kPa to demonstrate the energy transfer capability of a material, which is measured by taking the integral of the area below the loading-displacement curve until the peak occurs. The energy absorption values of the non-cured (0-day) sample increased for any substance (i.e., 10% RAP or XG in any ratio) compared to the non-treated soil (100% SM), but for each curing period (7, 28, and 56 days), 10% RAP showed no significant effect on the energy absorption of SM.

The maximum energy absorption was reached in samples with 3% XG when the curing periods were kept constant. In addition to this, the energy absorption levels increased when the samples were subjected to 7-day curing and decreased at higher curing periods (28 and 56 days). Maximum absorption of energy was observed 7 days after curing the sample, as the sample displays optimal rigidity, which is able to resist maximum stress and demonstrate maximum ductility at the same time (Cabalar et al., 2018).

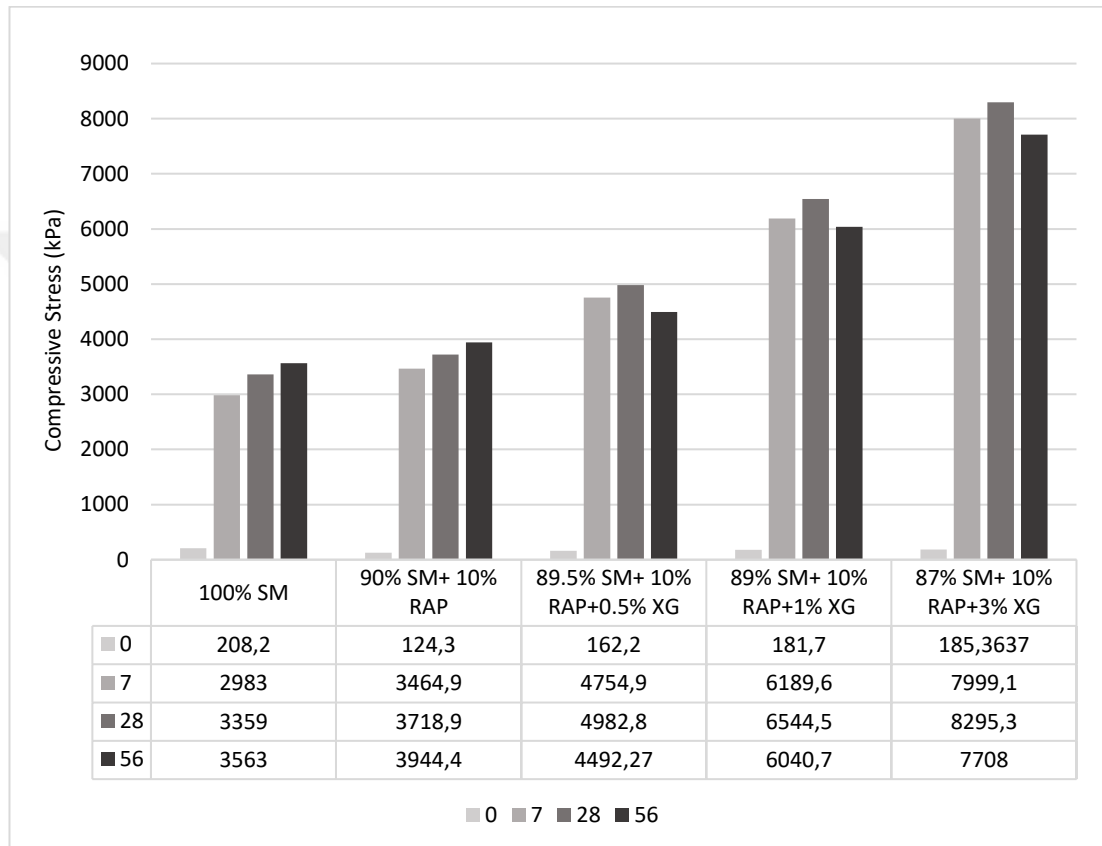


**Figure 4.10.** Maximum compressive stresses for all the mixtures at different curing periods

Figure 4.12 shows the modulus of elasticity derived from the stress-strain graph by dividing the stress by the strain corresponding to the tangent of the linear line to the peak. According to the results, specimens that had been cured for 56 days had the maximum modulus of elasticity.

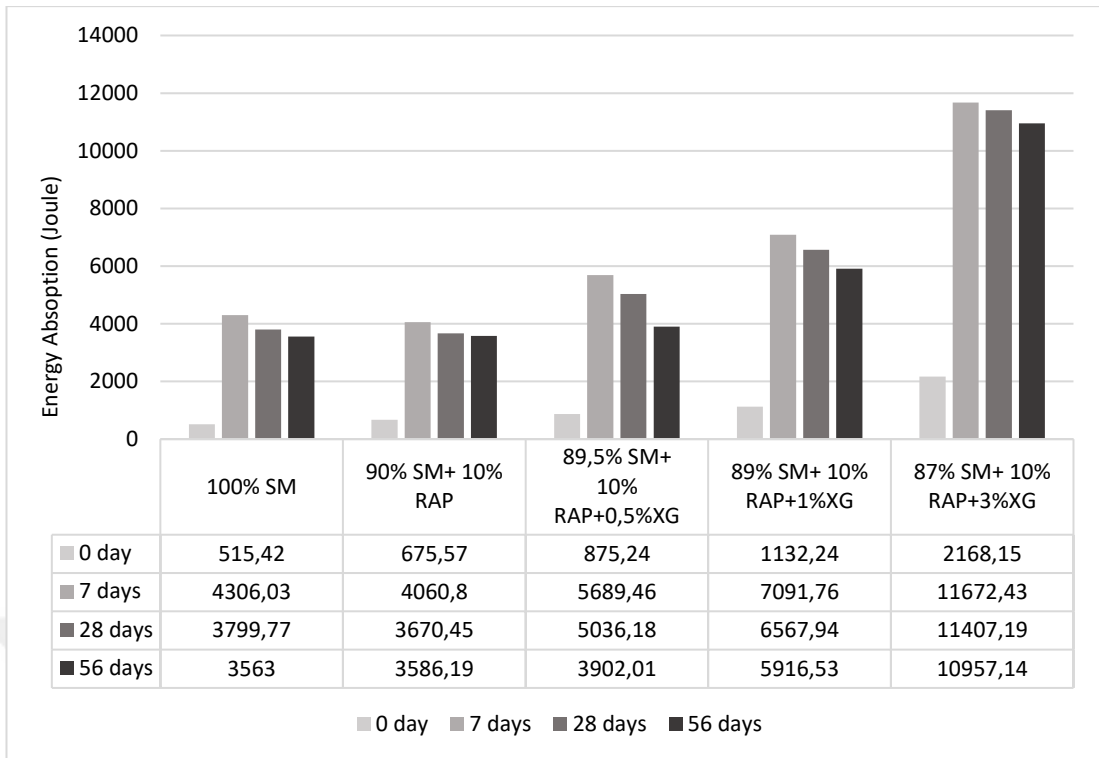


**Figure 4.11.** Energy absorption levels of all the mixtures at different curing periods

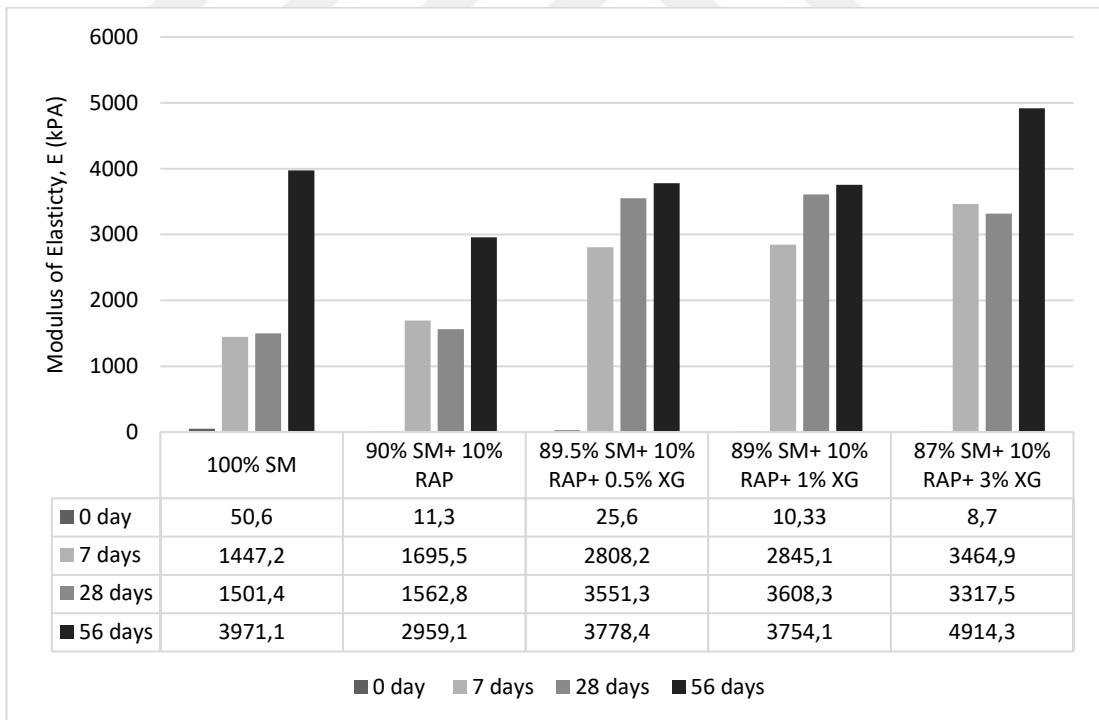


**Figure 4.12.** Modulus of Elasticity

#### 4.7 Consolidation Test

One-dimensional oedometer tests were conducted to examine the general consolidation behaviour of the silty sand treated with 10% RAP and XG at different concentrations (0, 0.5, 1, and 3%). Figure 4.13 presents the void ratio ( $e$ ) versus logarithmic stress ( $\log \sigma$ ) for all the combinations, and the initial void ratio of the soil increased with the addition of RAP and XG. The  $e_0$  increased in specimens with 3% XG by nearly 44% compared to non-treated soil. The increment in the void ratio of the soil with XG can be referred to as the swelling caused by the interaction of XG with water (M. Hamza et al., 2022). The recompression index ( $C_r$ ) is a measure of the compression characteristics of soil and is determined from the slope of the void ratio versus the logarithm of the pressure plot during recompression testing (ASTM-D1883, 2010). Compression index ( $C_c$ ) and  $C_r$  both decreased with the addition of RAP and increased with the addition of XG, as shown in Figure 4.14. The  $C_c$  of the clean soil drops to 0.06 from 0.077 by 28% at 10% RAP and increases linearly to 0.253 at 3% XG. The  $C_r$  of clean soil decreased from 0.141 to 0.128 by nearly 17% at 10% RAP and then increased to 0.25 at 3% XG, where the increment mainly occurred at 0.5% XG. After that, the increment was slightly. The decrease or increase of compression and recompression indices indicates that specimens compress less or expand more in a given pressure range, respectively. In this case, both  $C_c$  and  $C_r$  decreased at specimens that contained 10%, which means that the RAP reduced the compressibility and swelling of the soil. Moreover,  $C_c$  and  $C_r$  both increased with increasing XG content, indicating the effect of XG on increasing soil compressibility and swelling (Cabalar et al., 2017).

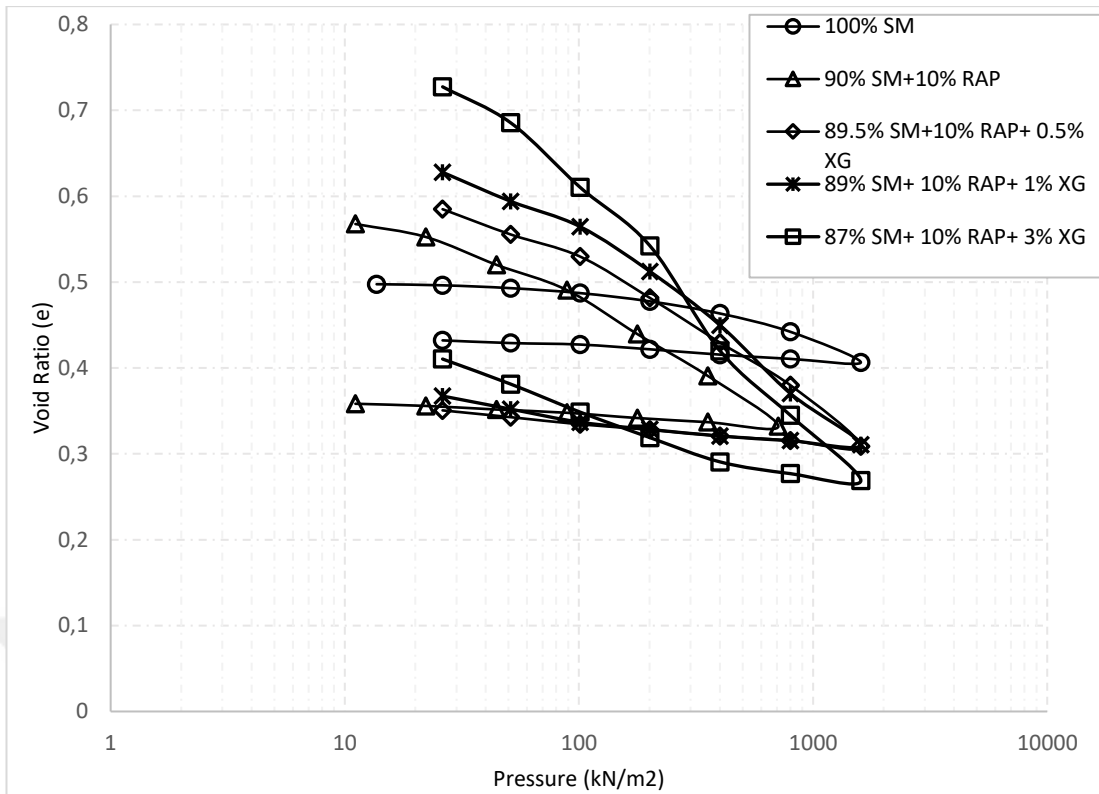


**Figure 4.13.** Void Ratio-Log Graphic

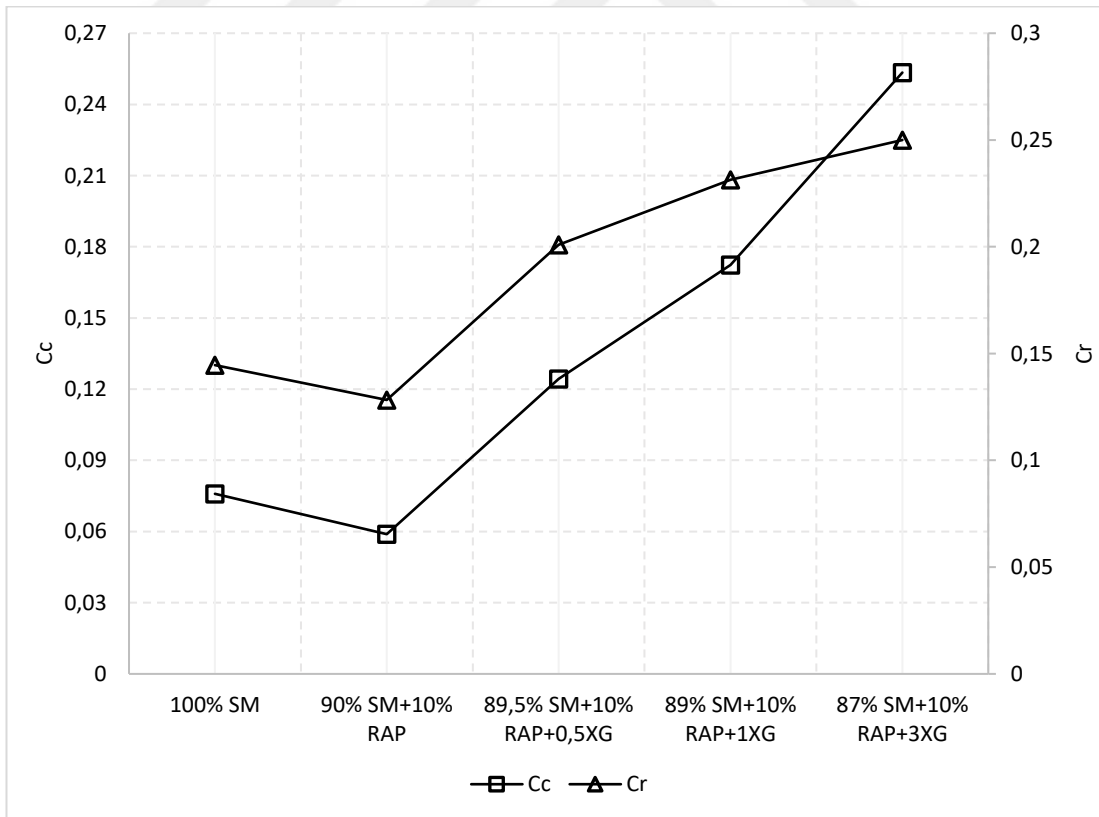


**Figure 4.14.** Compression index (Cc) and recompression index (Cr) of all the mixtures

Figure 4.15 presents the consolidation ratio,  $C_v$  (cm<sup>2</sup>/sec) which is calculated by comparing the change in height of a soil specimen during consolidation by using the formula suggested by ASTM-D2435 (2021). All of the specimens were subjected to the oedometer test immediately after being prepared. According to the curve, similar to previous findings, the only exception was the specimens with 10% RAP. The addition of the RAP caused an increase in  $C_v$  values from 0.585 to 0.734 by 25%. At 3% XG, the  $C_v$  decreased linearly to 0.309, indicating that XG decelerated consolidation and that it took a longer time for settlement to occur. The RAP, on the other hand, accelerates the process of consolidation. Wang et al. (2021) found that in the study of the XG-treated red clay soil,  $C_v$  decreased to 1.5% XG content and increased remarkably with higher XG concentrations. The outcomes from the permeability graph submitted in Fig. 4.16 supported the  $C_v$  results from the consolidation test. The permeability coefficient,  $k$ , rose from  $3.93 \times 10^{-7}$  cm/sec to  $4.18 \times 10^{-7}$  cm/sec when 10% RAP was added. After adding the XG additive, there was a noticeable decrease in the  $k$  value, with the highest decrease occurring in the specimen with 3% XG, and its value decreased by approximately three times to  $8.82 \times 10^{-8}$  cm/sec. There have been similar findings in previous studies, and it is this behaviour that illustrates the parallel between consolidation and permeability (Cabalar et al., 2018; Kwon et al., 2019; Dehghan et al., 2019; Singh & Das, 2020; Kwon et al., 2023).

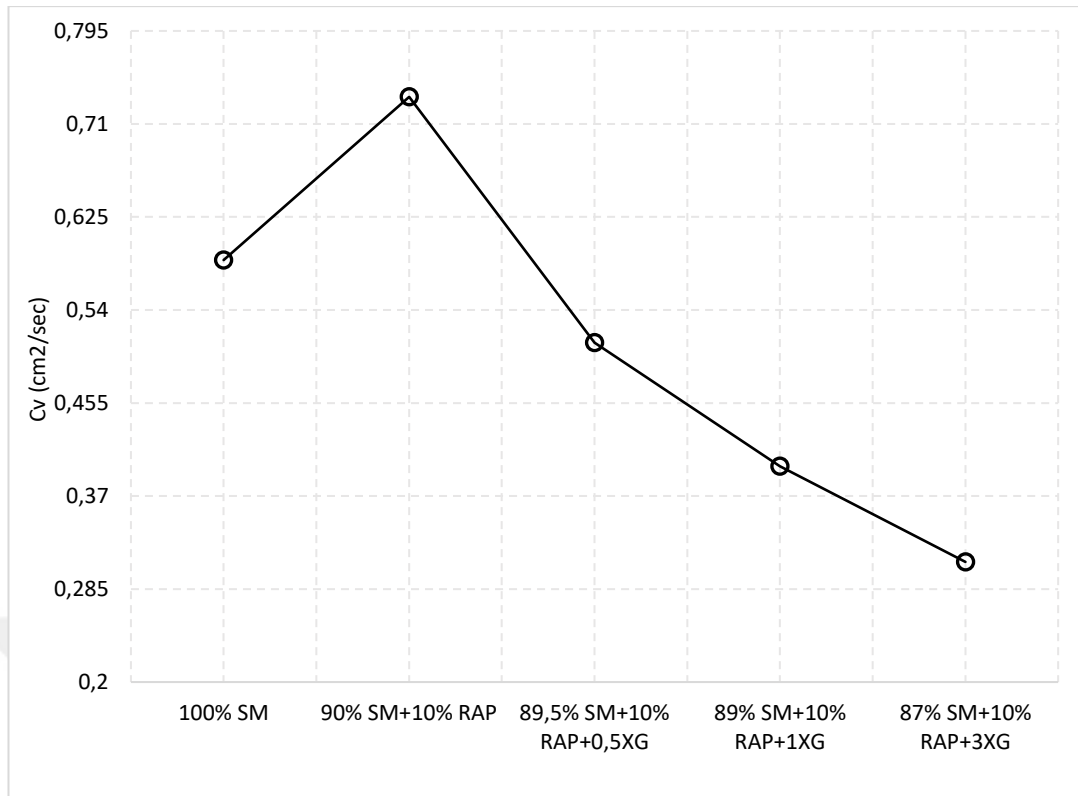


**Figure 4.15.** Variation of the consolidation ratio

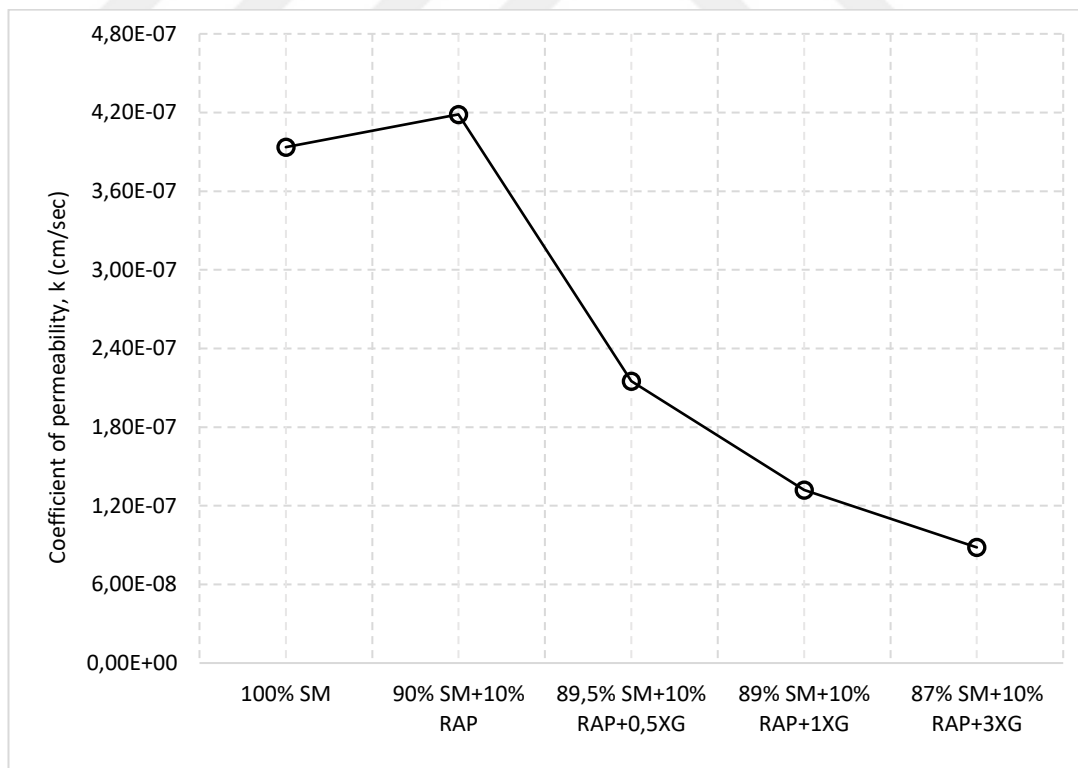


**Figure 4.16.** The coefficient of permeability for all the mixtures

#### 4.8 California Bearing Ratio (CBR) Test

In this section of the study, the California bearing capacity (CBR) test, which is widely used before construction projects, especially in pavement design, is presented. The general aim of the test is to calculate the strength and resistance to penetration of the soil under vertical loading. Different materials, mainly recycled construction materials such as crushed brick (CB), recycled concrete aggregate (RCA), reclaimed asphalt pavement (RAP), waste rock (WR), etc., are used to improve the bearing ratio of weak soil (Arulrajah et al., 2011; Arulrajah et al., 2013; Rahman et al., 2015).

In this presented study, CBR tests were performed on silty sand treated with RAP and XG under unsoaked conditions in accordance with ASTM D 1883. The process of the tests was given under Chapter 3, and the stress versus displacement of the specimens is presented in Fig. 4.17. In specimens with 10% RAP, the stress values were very close to those of the SM, and at the point of 5 mm penetration, the stress of the SM began to exceed the stress of the RAP. On the other hand, the addition of XG resulted in a substantial reduction in stress levels. The measured stress value of 527.2 kPa in the sample with 10% RAP decreased to 175 kPa when 0.5% XG was added, while this value decreased to 125.9 kPa in the sample with 3% XG.

The CBR values of all specimens at 2.5, 5, and 10 mm penetration are presented in Figure 4.18. The first observation was that the CBR is higher at 2.5 mm, then at 5 mm, and highest at 10 mm penetration. Furthermore, 10% RAP added to specimens resulted in a slight increase in CBR, and all CBR values were lower with XG compared to specimens that did not contain XG. As shown in Figure 4.19, the CBR (%) increased 7.57 from 6.98 by nearly 10% and decreased nearly with increasing XG content up to 1.81 by nearly 3 times at 3% XG. Studies have been conducted with similar materials, and the findings indicate that CBR values increase with increasing XG content under unsoaked conditions after a 0-day curing period (Muhammad Hamza et al., 2022; Hamza et al., 2023). CBR was found to be reduced in this study due to the swelling potential of the XG materials since an increase in the volume of the specimens as well as a loose form were observed just before testing. As can be seen from this situation, the XG has absorbed water and become expanded, resulting in an alteration to the compaction of the specimens.

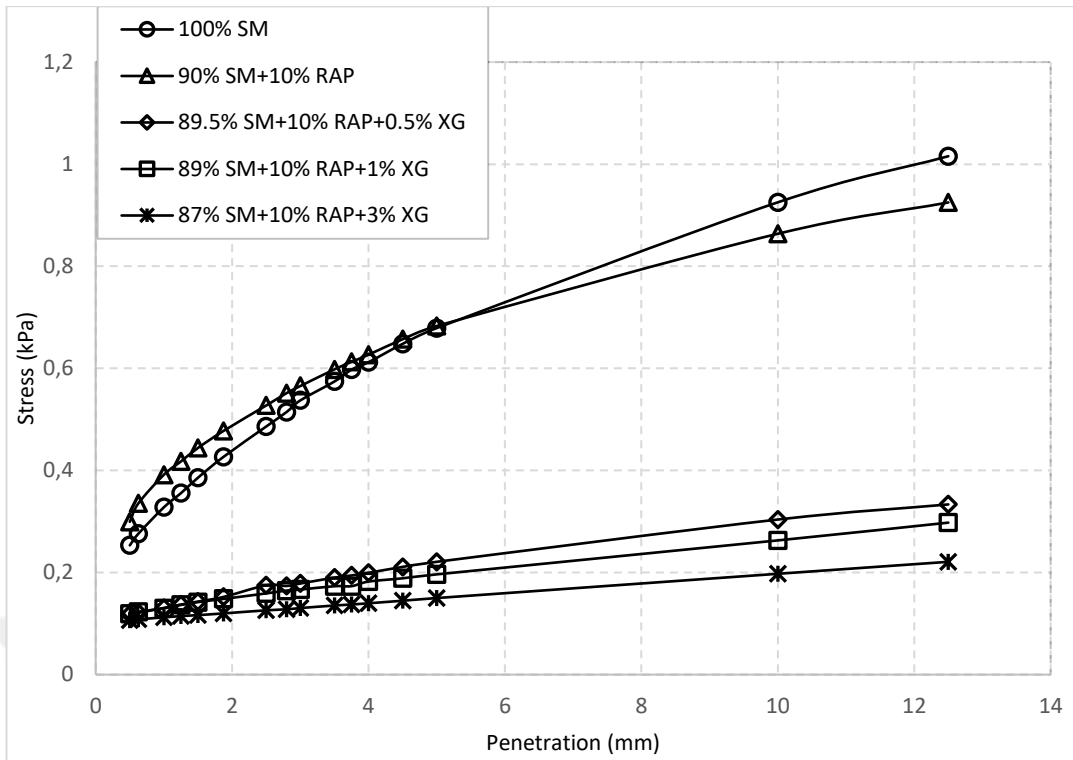


Figure 4.17. Load-penetration of all the mixtures

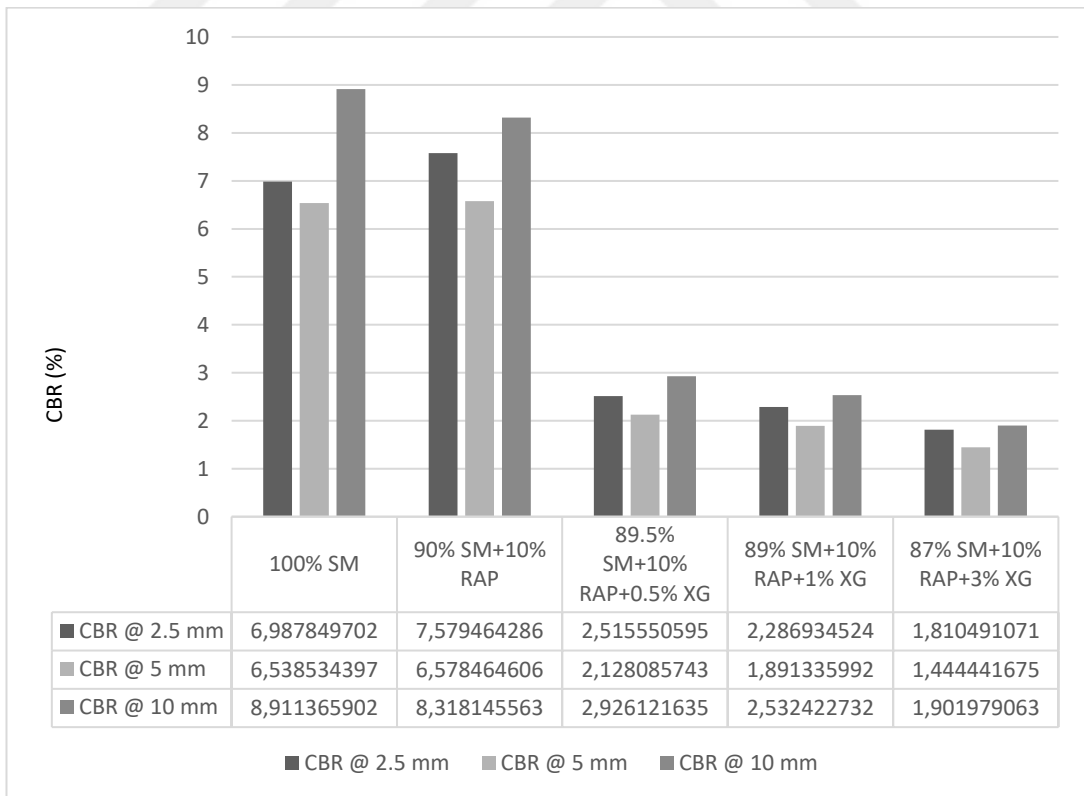
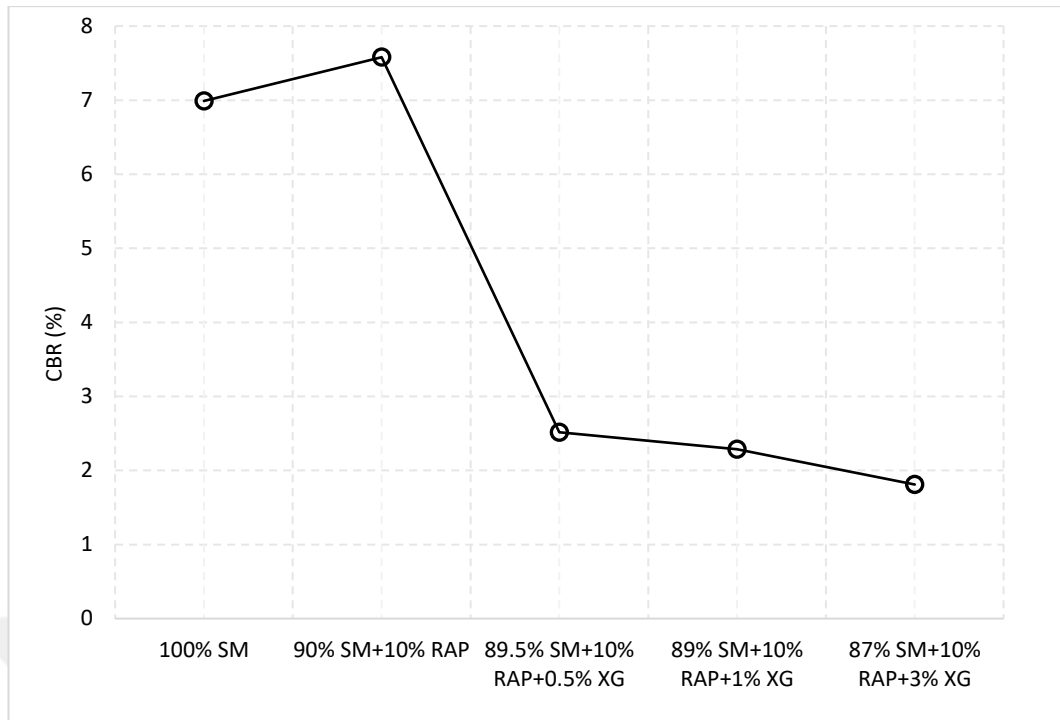


Figure 4.18 CBR values at different penetrations



**Figure 4.19:** CBR values at 2.5 mm

#### 4.9 Direct Shear Test

In order to establish the shear strength parameter, which indicates the resistance of a material to horizontal force as a geotechnical aspect, a number of direct shear tests were conducted in accordance with ASTM-D4318 (2017), which is the recognized standard for determining shear strength parameters. A direct shear test was conducted on specimens with different mixtures just after preparation in order to determine how RAP and XG content affect the shear strength of silty sand soil. It was also intended to investigate the curing effect by testing specimens aged 0, 7, and 28 days; however, the testing apparatus's limit (1000 kPa) was insufficient to permit the test to be conducted properly on specimens aged 7 and 28 days. The stress-strain diagram of all the mixtures under 150 kPa normal pressure is given in Fig. 4.20. According to the graphic, a noticeable reduction in shear stress occurred due to the addition of RAP. The peak stress of SM decreased from 124.6 kPa to 99.2 kPa, and after that, the 0.5% XG showed nearly the same trend as specimens with 10% RAP. Increasing XG content caused a reduction in shear stress; at 3% XG, the peak shear stress decreased to 80.8 kPa by nearly 54% compared to clean soil. The bar graphic presented in Fig. 4.21 reveals the general effect of RAP and XG on cohesion (c) and internal friction angle

( $\phi$ ). It is noted that the cohesion values initially decreased with the addition of 10% RAP but showed a linear increase with an increase in XG content. In a similar manner to cohesion, the internal friction angle also decreased at specimens with a 10% RAP. Later, XG increased the internal friction angle to some degree, but not to a significant extent. The cohesion values were measured as 35.15, 33.01, 35.60, 56.62, and 66.76 kPa for 100% SM, SM with 10% RAP, and XG of 0.5, 1, and 3%, respectively. On the other side, the internal friction angle remains within the range of 29.85° to 31.25°. The reduction in both cohesion and internal friction angle with the addition of 10% RAP can be basically connected to the shear characteristics of the RAP, which means that sands and graves are accepted to be cohesionless materials in the literature (Fannin et al., 2005), so it can be seen normally to reduce the shear parameters of the SM. However, the rising trend of cohesion with increasing XG content in the mixtures was attributed to the viscosity of the hydrogel form of the XG (Lee et al., 2017). As similar findings were observed in past research, the XG showed no or a minor effect on internal friction angle, which increased the internal friction angle slightly in this presented study compared to decreased internal friction angle in related studies (Cabalar et al., 2018; Lee et al., 2019), and this behaviour can be explained by the material used in this study, which has less clay and is coarser.

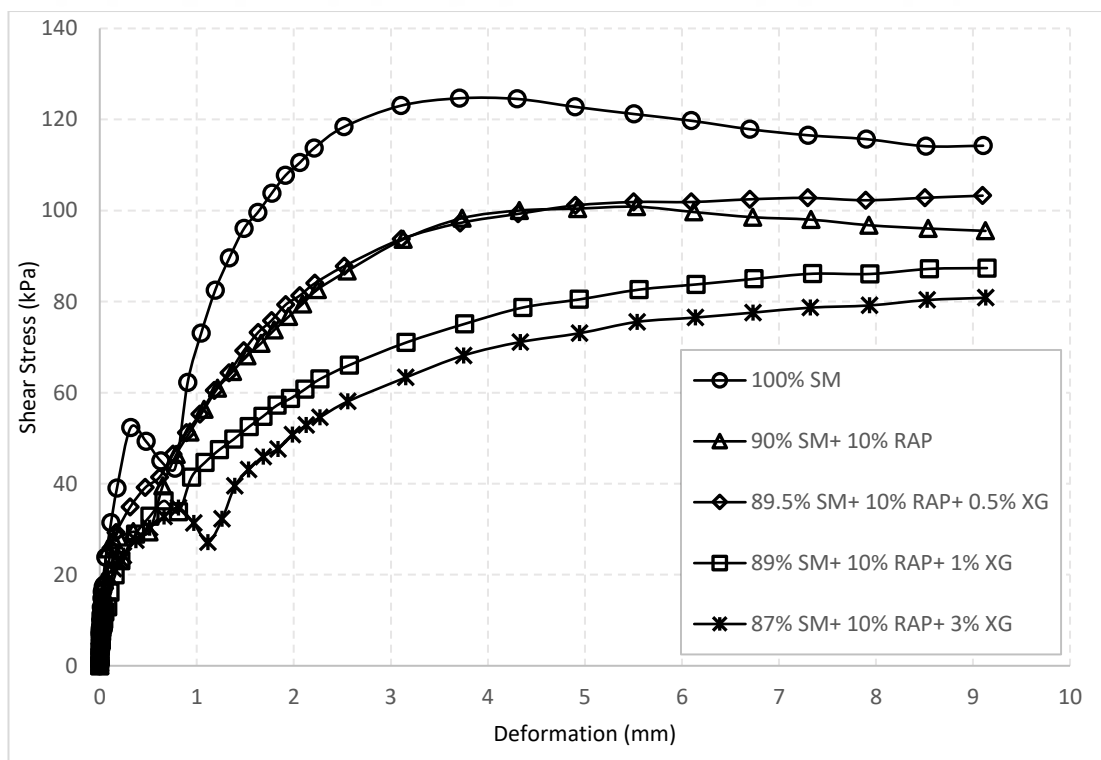


**Figure 4.20.** Stress-strain from the direct shear test at 150 kPa normal pressure

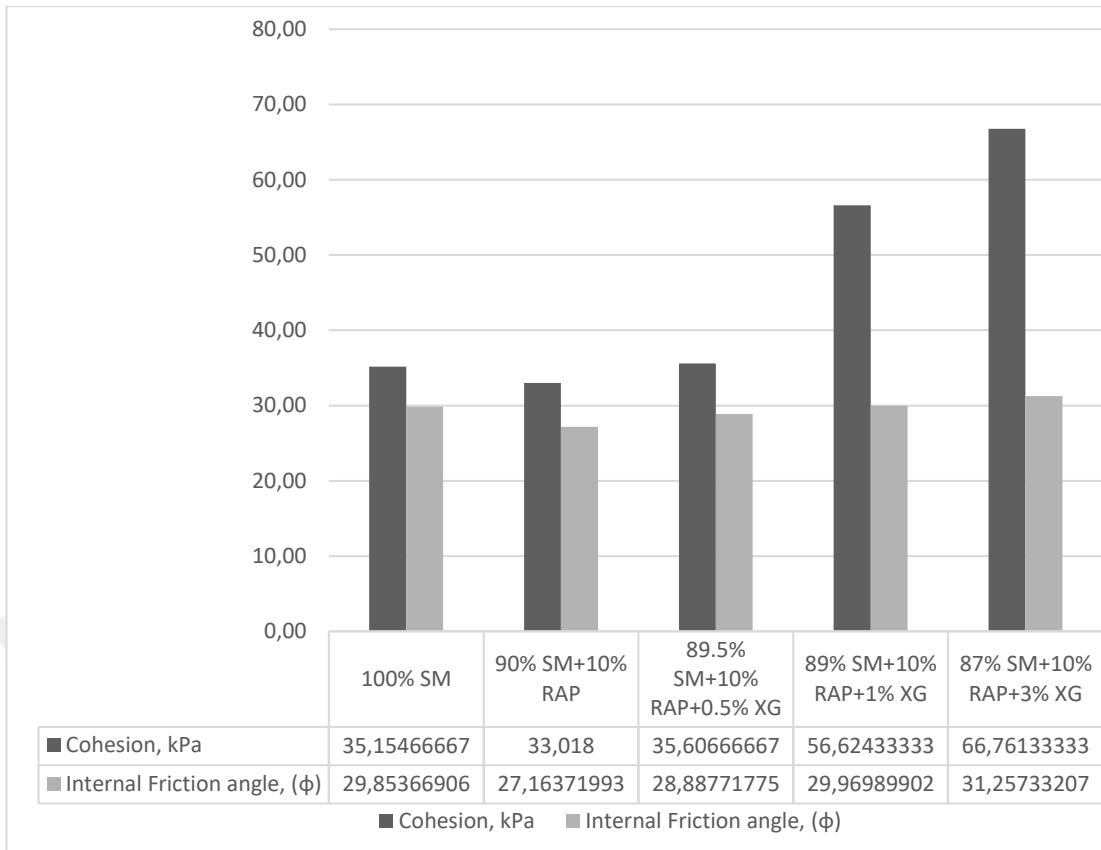


**Figure 4.21:** Cohesion and internal friction angle bar graph

## **CHAPTER 5 CONCLUSIONS AND RECOMMENDATIONS**

### **5.1 General**

A sequence of experiments was conducted within a laboratory setting to examine the impact of reclaimed asphalt pavement (RAP) and the environmentally friendly biopolymer Xanthan gum (XG) on silty sand (SM) natural soil. Various specimens were prepared, incorporating different combinations of SM, RAP, and XG at distinct curing times. These specimens underwent a battery of tests, and the results of these assessments are comprehensively presented in this section.

### **5.2 Conclusion**

- 1.** The liquid limit (LL) and plastic limit (PL) were measured using the fall cone test. Basically, the RAP reduced both LL and PL, and XG increased both LL and PL in the soil. The LL decreased remarkably with the addition of 10% RAP, from 31.36% to 25.46%, where it increased to 37.37, 45.45, and 57.39% for 0.5, 1, and 3% of XG, respectively. The PL dropped sharply from 23.25% to 7.7% when the 10% RAP was added and increased with XG content, reaching its peak point at 3% XG with 19.93% still lower than the PL of the clean soil.
- 2.** The optimum water content (OMC) of the soil first decreased with 10% RAP and then increased with XG concentration. The OMC values were measured as 18.5, 18, 20, 21.5, and 23.5% for SM, SM with 10% RAP, and XG by 0.5, 1, and 3% by weight. The maximum dry density decreased gradually with the addition of 10% RAP and XG content, where the lowest point was measured at 14.2% at 3% XG.
- 3.** The undrained shear strength of the soil was investigated by conducting the fall cone test (FCT) and the vane shear test (VST). Similar findings were observed for specimens with 10% RAP from FCT and VST, where in both tests the undrained shear strength values decreased with the addition of RAP. Contrarily, at both tests, the XG increased the undrained shear strength of the soil perceptibly. The  $S_u$  values were determined as 0.881, 0.436, 3.822, 5.284, and 7.442 kPa at FCT and 3.538, 1.125,

10.428, 14.483, and 17.494 kPa at VST for SM, SM with 10% RAP, 0.5%, 1%, and 3% XG at a constant water content of 35%.

4. There have been several tests of unconfined compressive strength on specimens prepared in different mixtures and subjected to different curing conditions. With respect to the UCS results of the noncured specimens, they show a similar trend to those of the undrained shear strength tests (FCT and VST), where the addition of RAP led to a reduction, and with the addition of XG content, the UCS values rose. Upon subjecting the specimens to a curing period of 28 days, it was observed that the strength values exhibited an increase with both reclaimed asphalt pavement (RAP) and xanthan gum (XG). The peak, noted at 8295 kPa, representing the highest value attained among all specimens, occurred at a 3% XG concentration. The curing effect on the strengthening was examined, and the peak UCS results of the specimens with 1% XG measured 181.7, 6189.6, 6544.5, and 6040.7 kPa for 0, 7, 28, and 56-day curing periods, respectively. According to the test results of the cured specimens (7, 28, and 56 days), the compression strength of the soil was always found to be maximum at 28 days for the cured specimens, regardless of the mixtures except the one with SM+10%. Moreover, the energy absorption of all the mixtures was obtained from UCS results. For the non-cured specimens, the energy absorption capacity increased with 10% RAP and XG content, but for the cured specimens, the capacity decreased with RAP and increased with increasing XG content. The energy absorption capacity of the soil increased with curing time and reached its maximum at the 7-day curing period, slightly decreasing with higher curing times (28 and 56 days).

5. The consolidation behaviour of the soil treated with RAP and XG was investigated under several parameters, such as void ratio ( $e$ ), compression ( $C_c$ ) and recompression ( $C_r$ ) indices, consolidation ratio ( $C_v$ ), and coefficient of permeability ( $k$ ). As shown in the void ratio versus log pressure graphic, the interstitial space between the initial void ratio ( $e_0$ ) and the final void ratio ( $e_f$ ) widened with the addition of RAP and XG. Both  $C_c$  and  $C_r$  were reduced with the addition of 10% RAP and increased with XG content. The  $C_c$  was dropped from 0.075 to 0.058 and rose up to 0.25 at 3% XG, while the  $C_r$  was reduced to 0.12 from 0.14 and increased to 0.25 at 3% XG. The  $C_v$  of the soil showed the expected results, where the  $C_v$  increased with RAP and decreased with XG content. The  $C_v$  was calculated as 0.58 cm<sup>2</sup>/sec for clean soil and 0.73, 0.51, 0.39, and 0.30 cm<sup>2</sup>/sec for 10% RAP and 0.5, 1, and 3% XG, respectively. Parallel to  $C_v$ , the permeability showed similar results. The  $k$  of the clean soil was measured as 3.93E-

07 cm/sec and increased to 4.18E-07 cm/sec with 10% RAP and 2.15E-07, 1.32E-07, and 8.82E-08 cm/sec for 0.5, 1, and 3% of XG.

6. California bearing capacity (CBR) tests were conducted on specimens under unsoaked conditions, and the results indicated that adding 10% RAP to silty sand soil had no sufficient effect on improving or reducing its bearing capacity, whereas adding even a small amount of XG significantly reduced the bearing capacity. Based on the CBR values at 2.5 mm penetration, the CBR increased from 6.98% to 7.57%, and it is calculated as 2.51, 2.28, and 1.81% for 0.5, 1, and 3% of XG, respectively.

7. Shear stress ( $\tau$ ), cohesion ( $c$ ), and internal friction angle ( $\phi$ ) of the soil were obtained by performing a direct shear test. The peak shear stress reached in non-cured specimens was decreased with RAP and XG. The cohesion of the soil first decreased with RAP, then increased with increasing XG content. The maximum cohesion was reached at 3% XG with 66.7°, which increased by nearly 90% compared to SM. However, not only the RAP but also the XG show no great effect on the internal friction angle. The internal friction angle decreased to 27.1° from 29.8° when 10% RAP was added and increased slightly to 28.8°, 29.9°, and 31.25° for 0.5, 1, and 3% of XG.

### **5.3 Recommendations**

In light of the results of this intensive laboratory testing program, the following recommendations can be made for further research:

1. The soil that was classified as silty sand (SM) in the presented study can be replaced with finer soil such as silty clays (ML) or low- or high-plasticity clays (CL, CH) to better observe the interaction of XG material with fine-grained structures.
2. A more focused test program can be used by reducing the test variety and changing the percentiles of the RAP (15% or 20%) and XG (1.5, 2, and 2.5%) materials in this program. This allows for a much more detailed examination of how the bituminous material affects the effectiveness of XG, as well as a more precise determination of the optimum XG percentage.
3. The durability of a possible improvement can be investigated by applying a longer curing time. In addition, especially for consolidation and CBR experiments, samples can be prepared with less density than MDD or more water content than OMC to be able to test worse scenarios.

4. It is also possible to conduct detailed analyses on cost calculations, environmental impacts, and applicability in the field.



## REFERENCES

- Acharya, R., Pedarla, A., Bheemasetti, T. V., & Puppala, A. J. (2017). Assessment of Guar Gum Biopolymer Treatment toward Mitigation of Desiccation Cracking on Slopes Built with Expansive Soils. *Transportation Research Record*, 2657(1), 78-88. <https://doi.org/10.3141/2657-09>
- Adhikari, S., Khattak, M. J., & Adhikari, B. (2020). Mechanical characteristics of Soil-RAP-Geopolymer mixtures for road base and subbase layers. *International Journal of Pavement Engineering*, 21(4), 483-496. <https://doi.org/10.1080/10298436.2018.1492131>
- Al Yahya Bag, M. D. A. (2018). Use of construction and demolition materials to improve geotechnical properties of a clay, PhD Thesis, Gaziantep University, Gaziantep.
- Alizadeh, A., & Modarres, A. (2019). Mechanical and Microstructural Study of RAP&#x2013;Clay Composites Containing Bitumen Emulsion and Lime. *Journal of Materials in Civil Engineering*, 31(2), 04018383. [https://doi.org/doi:10.1061/\(ASCE\)MT.1943-5533.0002583](https://doi.org/doi:10.1061/(ASCE)MT.1943-5533.0002583)
- Arulrajah, A., Piratheepan, J., Aatheesan, T., & Bo, M. W. (2011). Geotechnical Properties of Recycled Crushed Brick in Pavement Applications. *Journal of Materials in Civil Engineering*, 23(10), 1444-1452. [https://doi.org/10.1061/\(asce\)mt.1943-5533.0000319](https://doi.org/10.1061/(asce)mt.1943-5533.0000319)
- Arulrajah, A., Piratheepan, J., Disfani, M. M., & Bo, M. W. (2013). Geotechnical and Geoenvironmental Properties of Recycled Construction and Demolition Materials in Pavement Subbase Applications. *Journal of Materials in Civil Engineering*, 25(8), 1077-1088. [https://doi.org/10.1061/\(asce\)mt.1943-5533.0000652](https://doi.org/10.1061/(asce)mt.1943-5533.0000652)
- ASTM-D698. (2012). Standard Test Methods for Laboratory Compaction Characteristics of Soil Using Standard Effort (12,400 ft-lbf/ft<sup>3</sup> (600 kN-m/m<sup>3</sup>

- ASTM-D1557-12. (2021). Standard Test Methods for Laboratory Compaction Characteristics of Soil Using Modified Effort (56,000 ft-lbf/ft<sup>3</sup> (2,700 kN-m/m<sup>3

ASTM-D1883. (2010). Standard Test Method for CBR (California Bearing Ratio) of Laboratory-Compacted Soils. In. West Conshohocken, PA: ASTM International.

ASTM-D2166. (2017). Standard Test Method for Unconfined Compressive Strength of Cohesive Soil. In. West Conshohocken, PA: ASTM International.

ASTM-D2435. (2011). Standard Test Methods for One-Dimensional Consolidation Properties of Soils Using Incremental Loading. In. West Conshohocken, PA: ASTM International.

ASTM-D3080. (2012). Standard Test Method for Direct Shear Test of Soils Under Consolidated Drained Conditions. In. West Conshohocken, PA: ASTM International.

ASTM-D4318. (2017). Standard Test Methods for Liquid Limit, Plastic Limit, and Plasticity Index of Soils. In. West Conshohocken, PA: ASTM International.

ASTM-D4648/D4648M. (2016). Standard Test Methods for Laboratory Miniature Vane Shear Test for Saturated Fine-Grained Clayey Soil. In. West Conshohocken, PA: ASTM International.

Ayeldeen, M., Negm, A., El-Sawwaf, M., & Kitazume, M. (2017). Enhancing mechanical behaviors of collapsible soil using two biopolymers. *Journal of Rock Mechanics and Geotechnical Engineering*, 9(2), 329-339. <https://doi.org/https://doi.org/10.1016/j.jrmge.2016.11.007>

Biju, M. S., & Arnepalli, D. N. (2020). Effect of biopolymers on permeability of sand-bentonite mixtures. *Journal of Rock Mechanics and Geotechnical Engineering*, 12(5), 1093-1102. <https://doi.org/https://doi.org/10.1016/j.jrmge.2020.02.004>

Bouazza, A., Gates, W. P., & Ranjith, P. G. (2009). Hydraulic conductivity of biopolymer-treated silty sand. 59(1), 71-72. <https://doi.org/10.1680/geot.2007.00137>

BSI, B. (1990). Methods of Test for Soils for Civil Engineering Purposes, British Standards Institution, Milton Keynes, UK, Classification tests.

Butler, L., West, J. S., & Tighe, S. L. (2011). The effect of recycled concrete aggregate properties on the bond strength between RCA concrete and steel reinforcement.</sup>

- Cement and Concrete Research*, 41(10), 1037-1049.  
<https://doi.org/10.1016/j.cemconres.2011.06.004>
- Cabalar, A. F., & Alosman, S. O. (2021). Influence of rock powder on the behaviour of an organic soil. *Bulletin of Engineering Geology and the Environment*, 80(11), 8665-8676. <https://doi.org/10.1007/s10064-021-02457-2>
- Cabalar, A. F., Awraheem, M. H., & Khalaf, M. M. (2018). Geotechnical Properties of a Low-Plasticity Clay with Biopolymer. 30(8), 04018170. [https://doi.org/doi:10.1061/\(ASCE\)MT.1943-5533.0002380](https://doi.org/doi:10.1061/(ASCE)MT.1943-5533.0002380)
- Cabalar, A. F., & Canakci, H. (2011). Direct shear tests on sand treated with xanthan gum. *Proceedings of the Institution of Civil Engineers-Ground Improvement*, 164(2), 57-64. <https://doi.org/10.1680/grim.800041>
- Cabalar, A. F., Karabash, Z., & Mustafa, W. S. (2014). Stabilising a clay using tyre buffings and lime. *Road Materials and Pavement Design*, 15(4), 872-891. <https://doi.org/10.1080/14680629.2014.939697>
- Cabalar, A. F., Khalaf, M. M., & Isik, H. (2020). A comparative study on the undrained shear strength results of fall cone and vane shear tests in sand–clay mixtures. *Arabian Journal of Geosciences*, 13(11), 395. <https://doi.org/10.1007/s12517-020-05351-5>
- Cabalar, A. F., & Mustafa, W. S. J. E. G. (2015). Fall cone tests on clay–sand mixtures. 192, 154-165.
- Cabalar, A. F., Wiszniewski, M., & Skutnik, Z. (2017). Effects of Xanthan Gum Biopolymer on the Permeability, Odometer, Unconfined Compressive and Triaxial Shear Behavior of a Sand. *Soil Mechanics and Foundation Engineering*, 54(5), 356-361. <https://doi.org/10.1007/s11204-017-9481-1>
- Cabalar, A. F., Akbulut, N., Demir, S., & Yildiz, O. (2023). Use of a Biopolymer for Road Pavement Subgrade. *Sustainability*, 15(10), 8231. <https://doi.org/10.3390/su15108231>
- Chang, I., Im, J., Prasadhi, A. K., & Cho, G.-C. (2015). Effects of Xanthan gum biopolymer on soil strengthening. *Construction and Building Materials*, 74, 65-72. <https://doi.org/https://doi.org/10.1016/j.conbuildmat.2014.10.026>
- Chang, I., Kwon, Y. M., & Cho, G. C. (2021). Effect of Pore-Fluid Chemistry on the Undrained Shear Strength of Xanthan Gum Biopolymer-Treated Clays. *Journal of Geotechnical and Geoenvironmental Engineering*, 147(11), Article 06021013. [https://doi.org/10.1061/\(asce\)gt.1943-5606.0002652](https://doi.org/10.1061/(asce)gt.1943-5606.0002652)

- Chang, I., Prasadhi, A. K., Im, J., & Cho, G.-C. (2015). Soil strengthening using thermo-gelation biopolymers. *Construction and Building Materials*, 77, 430-438. <https://doi.org/10.1016/j.conbuildmat.2014.12.116>
- Chen, C. H., Wu, L., Perdjon, M., Huang, X. Y., & Peng, Y. X. (2019). The drying effect on xanthan gum biopolymer treated sandy soil shear strength. *Construction and Building Materials*, 197, 271-279. <https://doi.org/10.1016/j.conbuildmat.2018.11.120>
- Corinaldesi, V. (2010). Mechanical and elastic behaviour of concretes made of recycled-concrete coarse aggregates. *Construction and Building Materials*, 24(9), 1616-1620. <https://doi.org/10.1016/j.conbuildmat.2010.02.031>
- Dehghan, H., Tabarsa, A., Latifi, N., & Bagheri, Y. (2019). Use of xanthan and guar gums in soil strengthening. *Clean Technologies and Environmental Policy*, 21(1), 155-165. <https://doi.org/10.1007/s10098-018-1625-0>
- Edeh, J., Eberemu, A. O., & Agnes, O. (2012). Lateritic Soil Stabilization of Reclaimed Asphalt Pavement as Flexible Highway Pavement Materials. *Advanced Materials Research*, Vol. 367, pp 3-11. <https://doi.org/10.4028/www.scientific.net/AMR.367.3>
- Elkafoury, A., & Azzam, W. (2020). Utilize Xanthan gum for enhancing CBR value of used cooking oil-contaminated fine sand subgrade soil for pavement structures. *Innovative Infrastructure Solutions*, 6(1), Article 25. <https://doi.org/10.1007/s41062-020-00389-6>
- Eltwati, A., Elkaseh, A., & Tarhuni, F. (2020). Engineering Properties of Clayey Soil Stabilized with Waste Granite Dust. *International Journal of Advanced Science and Technology*, 29, 750-757.
- Fannin, R. J., Eliadorani, A., & Wilkinson, J. M. T. (2005). Shear strength of cohesionless soils at low stress. *Géotechnique*, 55(6), 467-478. <https://doi.org/10.1680/geot.2005.55.6.467>
- Fattah, M. Y., al-Musawi, H. H. M., & Salman, F. A. (2012). Treatment of Collapsibility of Gypseous Soils by Dynamic Compaction. *Geotechnical and Geological Engineering*, 30(6), 1369-1387. <https://doi.org/10.1007/s10706-012-9552-z>
- Feng, T.-W. J. G. (2000). Fall-cone penetration and water content relationship of clays. *50(2)*, 181-187.

- García-Ochoa, F., Santos, V. E., Casas, J. A., & Gómez, E. (2000). Xanthan gum: production, recovery, and properties. *Biotechnology Advances*, *18*(7), 549-579. [https://doi.org/10.1016/S0734-9750\(00\)00050-1](https://doi.org/10.1016/S0734-9750(00)00050-1)
- Hamidi, A., Yazdanjou, V., & Salimi, N. (2009). Shear strength characteristics of sand-gravel mixtures. *International Journal of Geotechnical Engineering*, *3*(1), 29-38. <https://doi.org/10.3328/IJGE.2009.03.01.29-38>
- Hamza, M., Nie, Z., Aziz, M., Ijaz, N., Ijaz, Z., & Rehman, Z. u. (2022). Strengthening potential of xanthan gum biopolymer in stabilizing weak subgrade soil. *Clean Technologies and Environmental Policy*, *24*(9), 2719-2738. <https://doi.org/10.1007/s10098-022-02347-5>
- Hamza, M., Zhihong, N., Aziz, M., Ijaz, N., Ameer, M., & Ijaz, Z. (2023). Geotechnical properties of problematic expansive subgrade stabilized with xanthan gum biopolymer. *Road Materials and Pavement Design*, *24*, 1869-1883. <https://doi.org/10.1080/14680629.2022.2092027>
- Hidalgo, C., Carvajal, G., & Munoz, F. (2019). Laboratory Evaluation of Finely Milled Brick Debris as a Soil Stabilizer. *Sustainability*, *11*(4), Article 967. <https://doi.org/10.3390/su11040967>
- Hilf, J. J. P. D., US Bureau of Reclamation, Denver. (1956). An investigation of pore pressure in compacted cohesive soils.
- Jang, J. (2020). A Review of the Application of Biopolymers on Geotechnical Engineering and the Strengthening Mechanisms between Typical Biopolymers and Soils. *Advances in Materials Science and Engineering*, *2020*, 1465709. <https://doi.org/10.1155/2020/1465709>
- Khatami, H. R., & O'Kelly, B. C. (2013). Improving Mechanical Properties of Sand Using Biopolymers. *139*(8), 1402-1406. [https://doi.org/doi:10.1061/\(ASCE\)GT.1943-5606.0000861](https://doi.org/doi:10.1061/(ASCE)GT.1943-5606.0000861)
- Khay, S. E. E., Said, S. E. E. B., Loulizi, A., & Neji, J. (2015). Laboratory Investigation of Cement-Treated Reclaimed Asphalt Pavement Material. *27*(6), 04014192. [https://doi.org/doi:10.1061/\(ASCE\)MT.1943-5533.0001158](https://doi.org/doi:10.1061/(ASCE)MT.1943-5533.0001158)
- Kianimehr, M., Shourijeh, P. T., Binesh, S. M., Mohammadinia, A., & Arulrajah, A. (2019). Utilization of recycled concrete aggregates for light-stabilization of clay soils. *Construction and Building Materials*, *227*, Article 116792. <https://doi.org/10.1016/j.conbuildmat.2019.116792>

- Kota, P. B. V. S., Hazlett, D., & Perrin, L. (1996). Sulfate-Bearing Soils: Problems with Calcium-Based Stabilizers. *1546*(1), 62-69. <https://doi.org/10.1177/0361198196154600107>
- Kumar, G., & Wood, D. M. J. G. (1999). Fall cone and compression tests on clay±gravel mixtures. *49*(6), 727-739.
- Kwon, Y.-M., Chang, I., & Cho, G.-C. (2023). Consolidation and swelling behavior of kaolinite clay containing xanthan gum biopolymer. *Acta Geotechnica*. <https://doi.org/10.1007/s11440-023-01794-8>
- Kwon, Y., Chang, I., Lee, M., & Cho, G.-C. (2019). Geotechnical engineering behavior of biopolymer-treated soft marine soil. *Geomechanics and Engineering*, *17*, 453-464. <https://doi.org/10.12989/gae.2019.17.5.453>
- Latifi, N., Meehan, C., Abd Majid, M. Z., Tahir, M., & Mohamad, E. (2016). Improvement of Problematic Soils with Biopolymer—An Environmentally Friendly Soil Stabilizer. *Journal of Materials in Civil Engineering*, *29*. [https://doi.org/10.1061/\(ASCE\)MT.1943-5533.0001706](https://doi.org/10.1061/(ASCE)MT.1943-5533.0001706)
- Lee, S., Chang, I., Chung, M., Kim, Y., & Kee, J. (2017). Geotechnical shear behavior of Xanthan Gum biopolymer treated sand from direct shear testing. *Geomechanics and Engineering*, *12*, 831-847. <https://doi.org/10.12989/gae.2017.12.5.831>
- Lee, S., Chung, M., Park, H. M., Song, K. I., & Chang, I. (2019). Xanthan Gum Biopolymer as Soil-Stabilization Binder for Road Construction Using Local Soil in Sri Lanka. *Journal of Materials in Civil Engineering*, *31*(11), Article 06019012. [https://doi.org/10.1061/\(asce\)mt.1943-5533.0002909](https://doi.org/10.1061/(asce)mt.1943-5533.0002909)
- Lee, S., Im, J., Cho, G.-C., & Chang, I. (2019). Laboratory triaxial test behavior of xanthan gum biopolymer-treated sands. *Geomechanics and Engineering*, *17*, 445-452. <https://doi.org/10.12989/gae.2019.17.5.445>
- Mendonca, A., Morais, P. V., Pires, A. C., Chung, A. P., & Oliveira, P. J. V. (2021). Reducing Soil Permeability Using Bacteria-Produced Biopolymer. *Applied Sciences-Basel*, *11*(16), Article 7278. <https://doi.org/10.3390/app11167278>
- Milas, M., Rinaudo, M., & Tinland, B. (1985). The viscosity dependence on concentration, molecular weight and shear rate of xanthan solutions. *Polymer Bulletin*, *14*(2), 157-164. <https://doi.org/10.1007/BF00708475>
- Mohammadinia, A., Arulrajah, A., Horpibulsuk, S., & Chinkulkijniwat, A. (2017). Effect of fly ash on properties of crushed brick and reclaimed asphalt in

- pavement base/subbase applications. *Journal of Hazardous Materials*, 321, 547-556. <https://doi.org/10.1016/j.jhazmat.2016.09.039>
- Mohammed, M., & Alhassan, M. (2018). Effect of Reclaimed Asphalt Pavement Stabilization on the Microstructure and Strength of Black Cotton Soil. *International Journal of Technology*, 9, 722. <https://doi.org/10.14716/ijtech.v9i4.435>
- Muguda, S., Booth, S., Hughes, P., Augarde, C., Perlot, C., Bruno, A. W., & Gallipoli, D. (2017). Mechanical Properties of Biopolymer-Stabilised Soil-Based Construction Materials. *Géotechnique Letters*, 7, 1-18. <https://doi.org/10.1680/jgele.17.00081>
- Naeini, S., & Masoud, G. (2010). Effect of Wet and Dry Conditions on Strength of Silty Sand Soils Stabilized with Epoxy Resin Polymer. *Journal of Applied Sciences*, 10. <https://doi.org/10.3923/jas.2010.2839.2846>
- Ni, J., Li, S. S., Ma, L., & Geng, X. Y. (2020). Performance of soils enhanced with eco-friendly biopolymers in unconfined compression strength tests and fatigue loading tests. *Construction and Building Materials*, 263, Article 120039. <https://doi.org/10.1061/j.conbuildmat.2020.120039>
- Nugent, R. A., Zhang, G. P., & Gambrell, R. P. (2009). Effect of Exopolymers on the Liquid Limit of Clays and Its Engineering Implications. *Transportation Research Record*(2101), 34-43. <https://doi.org/10.3141/2101-05>
- O'Kelly, B. C., Vardanega, P. J., & Haigh, S. K. (2017). Use of fall cones to determine Atterberg limits: a review. *Géotechnique*, 68(10), 843-856. <https://doi.org/10.1680/jgeot.17.R.039>
- Pappu, A., Saxena, M., & Asolekar, S. R. (2007). Solid wastes generation in India and their recycling potential in building materials. *Building and Environment*, 42(6), 2311-2320. <https://doi.org/https://doi.org/10.1016/j.buildenv.2006.04.015>
- Pastor, J. L., Tomas, R., Cano, M., Riquelme, A., & Gutierrez, E. (2019). Evaluation of the Improvement Effect of Limestone Powder Waste in the Stabilization of Swelling Clayey Soil. *Sustainability*, 11(3), Article 679. <https://doi.org/10.3390/su11030679>
- Plati, C., & Cliatt, B. (2019). A Sustainability Perspective for Unbound Reclaimed Asphalt Pavement (RAP) as a Pavement Base Material. *11*(1), 78. <https://www.mdpi.com/2071-1050/11/1/78>

- Proctor, R. R. (1993). Fundamental principles of soil compaction. *Engineering News Record*, 111(9), 245–248.
- Rahman, M. A., Imteaz, M. A., Arulrajah, A., Piratheepan, J., & Disfani, M. M. (2015). Recycled construction and demolition materials in permeable pavement systems: geotechnical and hydraulic characteristics. *Journal of Cleaner Production*, 90, 183-194. <https://doi.org/10.1016/j.jclepro.2014.11.042>
- Rajabi, A. M., & Hosseini, A. (2022). Effect of Liquid Polyvinyl Acetate and Micronized Calcium Carbonate on Strength Parameters of Silty Sand Soil. *Iranian Journal of Science and Technology, Transactions of Civil Engineering*, 46(1), 385-395. <https://doi.org/10.1007/s40996-021-00621-y>
- Singh, S. P., & Das, R. (2020). Geo-engineering properties of expansive soil treated with xanthan gum biopolymer. *Geomechanics and Geoengineering*, 15(2), 107-122. <https://doi.org/10.1080/17486025.2019.1632495>
- Soldo, A., Miletic, M., & Auad, M. L. (2020). Biopolymers as a sustainable solution for the enhancement of soil mechanical properties. *Scientific Reports*, 10(1), Article 267. <https://doi.org/10.1038/s41598-019-57135-x>
- Suebsuk, J., Horpibulsuk, S., Suksan, A., Suksiripattanapong, C., Phoo-ngernkham, T., & Arulrajah, A. (2019). Strength prediction of cement-stabilised reclaimed asphalt pavement and lateritic soil blends. *International Journal of Pavement Engineering*, 20(3), 332-338. <https://doi.org/10.1080/10298436.2017.1293265>
- Suebsuk, J., & Suksan, A. (2014). Strength assessment of cement treated soil-reclaimed asphalt pavement (RAP) mixture. *International Journal of GEOMATE*, 6, 878-884. <https://doi.org/10.21660/2014.12.3262>
- Tavakol, M., Kulesza, S., Jones, C., & Hossain, M. (2020). Effect of Low-Quality Recycled Concrete Aggregate on Stabilized Clay Properties. *Journal of Materials in Civil Engineering*, 32(8), Article 04020196. [https://doi.org/10.1061/\(asce\)mt.1943-5533.0003263](https://doi.org/10.1061/(asce)mt.1943-5533.0003263)
- Wang, L., Weng, Z., Liu, Q., Wang, T., Pan, X., Li, G., & Wang, Z. (2021). Improving the Mechanical Properties of Red Clay Using Xanthan Gum Biopolymer. *International Journal of Polymer Science*, 2021, 1535772. <https://doi.org/10.1155/2021/1535772>
- Wasti, Y., & Bezirci, M. J. C. G. J. (1986). Determination of the consistency limits of soils by the fall cone test. 23(2), 241-246.

- Winterkorn, H. F., & Pamukcu, S. (1991). Soil Stabilization and Grouting. In H.-Y. Fang (Ed.), *Foundation Engineering Handbook* (pp. 317-378). Springer US. [https://doi.org/10.1007/978-1-4615-3928-5\\_9](https://doi.org/10.1007/978-1-4615-3928-5_9)
- Worrell, E., Price, L., Martin, N., Hendriks, C., & Ozawa-Meida, L. (2001). Carbon Dioxide Emission from the Global Cement Industry. *Annu. Rev. Energy Environ*, 26, 303-329. <https://doi.org/10.1146/annurev.energy.26.1.303>
- Wroth, C. P., & Wood, D. M. (1978). The correlation of index properties with some basic engineering properties of soils. *Canadian Geotechnical Journal*, 15(2), 137-145.



## CURRICULUM VITAE

### PERSONAL INFORMATION

Name and Surname: Halil BAL

### EDUCATION

Degree	Graduate School	Year
B.Sc.	Gaziantep University	2020
High School	Türkan Ömer Okan Anatolian High School	2015

### PUBLICATIONS

Bal, H., Cabalar, A. F. (2023). Advancing Sustainability in Geotechnical Engineering: Reclaiming Infrastructure Waste for Soil Improvement, The GAP 11th International Summit Scientific Research Congress (2023).